CONTINUOUS FLOW CATALYSIS FOR THE VALORIZATION OF CARBON DIOXIDE

Nicola Zanda

UNIVERSITAT
ROVIRA i VIRGILI

Continuous Flow Catalysis for the Valorization of Carbon Dioxide

---

NICOLA ZANDA

DOCTORAL THESIS
2022

PhD Thesis

Continuous Flow Catalysis for the Valorization of Carbon Dioxide

Nicola Zanda

Supervised by:
Prof. Dr. Miquel À. Pericàs and
Prof. Dr. Arjan W. Kleij

Tarragona
June 2022

UNIVERSITAT ROVIRA i VIRGILI

UNIVERSITAT ROVIRA i VIRGILI

ICIQ Institut Català d'Investigació Química

Prof. Dr. Miquel À. Pericàs, Group Leader at the Institute of Chemical Research of Catalunya (ICIQ) and Research Professor at the Departament of Organic and Inorganic chemistry at the University of Barcelona (UB),

and,

Prof. Dr. Arjan W. Kleij, Group Leader at the Institute of Chemical Research of Catalunya (ICIQ) and Research Professor at the Catalan Institution for research and Advanced Studies (ICREA),

We STATE that the present study, entitled "**Continuous Flow Catalysis for the Valorization of Carbon Dioxide**", presented by Nicola Zanda to receive the degree of Doctor, has been carried out under our supervision at the Department at the Institute of Chemical Research of Catalunya, ICIQ.

Tarragona, June 2022

Doctoral Thesis Supervisor/s

Prof. Dr. Miquel À. Pericàs

Prof. Dr. Arjan W. Kleij

UNIVERSITAT ROVIRA I VIRGILI
CONTINUOUS FLOW CATALYSIS FOR THE VALORIZATION OF CARBON DIOXIDE
Nicola Zanda

Curriculum Vitae

Nicola Zanda was born in Nuoro (Italy) in 1993. In 2017, he obtained a Master Degree in pharmaceutical chemistry and technology from the Cagliari State University (UNICA) with a qualification of 110/110 (cum laude). During his undergraduate studies, he performed his master thesis work in the area of medicinal chemistry at Institute of Medicinal Chemistry (IQM-CSIC), which was funded by an Erasmus+ Traineeship grant. From 2015 till 2016, he studied for one year at the Lithuanian University of Health Sciences as part of an exchange year supported by the Erasmus+ Studies program. From September till December 2017, he did an internship in medicinal chemistry (topic: peptide synthesis and molecular modelling) at IQM under the Erasmus + Traineeship program. He further worked at Janssen-Cilag through the CITIUS postgraduate program of the Autonomous University of Madrid (Spain) from March 2018 till January 2019. Soon after he was awarded a La Caixa funded PhD fellowship (INPhINIT program) and carried out the work described in this thesis (2019–2022) under the supervision of Prof. Miquel Pericàs and Prof. Arjan W. Kleij at the Institute of Chemical Research of Catalonia (ICIQ) in Tarragona (Spain), with a 3-month internship in the group of Prof. C. Oliver Kappe in Graz (Austria).

Part of the work was communicated at the 4th EuCheMS Conference on Green and Sustainable Chemistry (2019).

UNIVERSITAT ROVIRA I VIRGILI
CONTINUOUS FLOW CATALYSIS FOR THE VALORIZATION OF CARBON DIOXIDE
Nicola Zanda

Acknowledgements

This stepstone in my personal growth would not have been possible without the people I spent these three years with and who constantly helped me during this process.

First and foremost, I would like to thank my supervisors. I am deeply proud to have been able to grow as a scientist at the side of two leaders such as Prof. Miquel Pericàs and Prof. Arjan Kleij. Their curiosity and ideas inspired me during these years, I thank you both for your patient guidance throughout the process, which I know meant a ton of work, I truly appreciate it. I think the combined qualities and constant suggestions and dedication of both of you made me a better researcher, our discussions about chemistry and more general life-related topics improved my critical thinking and knowledge. I will make treasure of it in my future endeavors. Also, I thank Prof. Oliver Kappe and Prof. David Cantillo for their kind assistance during my stay abroad in Graz. And of course, all the Electro team and the Kappe group for their warm welcome and generosity.

I also would like to thank Sara Garcia for her amazing work and help to during all the administrative tasks, and to Patri our LabCop or better SuperMum. She helped us and me in immeasurable ways, without saving any energy, and with enormous generosity and care.

I would like to thank all the former and current colleagues of the Pericàs and Kleij Groups. These have been three funny years and I enjoyed my time here at ICIQ and in Tarragona: Prachi, Adrian, Cong, Marco, Laura, Mauro, Lluis, Tamás, Elena, Stefania, Justine, Flore, Gerard, Josefine, Kike, Aijie, Jianing, Àlex, Cristina, Kun, Chang, Alèria, Bart, Alexander, Debasish, Alba, Xuetong, Jixiang, Qian, Arianna, David, Wangyu, Fengyun and Dirk. I would like to acknowledge Esther, Santi, Pedro and Anna for assisting me with patience and fill my gaps of knowledge at the beginning of this journey, which surely helped me to progress during the following years. Junshan and Pari, you have been my ‘forced’ desk-mates and we spent great time together discussing chemistry and much more, I thank you both for all the patience with my black humor jokes and suggestions.

I would like to show my deepest gratitude to Moreshwar for his help in terminating the last experiments and tricks, I am still waiting for a question he does not know the answer. A special THANK YOU for their precious and life-saving help go to Leijie and Ludovica, who collaborated and worked with me during the most intense months of my PhD. I am sure there are many other people who helped me during these years who I forgot to mention. You have my gratitude.

In addition, I would like to thank my family, who always supported me in any decision I ever took and my friends for their constant and joyful distractions. Last and most important, I would like to express my huge gratitude to JESSICA for the colossal support and comprehension during these years. I would not have done it without you!

UNIVERSITAT ROVIRA I VIRGILI
CONTINUOUS FLOW CATALYSIS FOR THE VALORIZATION OF CARBON DIOXIDE
Nicola Zanda

Financial Sources

The project that gave rise to these results received the support of a fellowship from ”la Caixa” Foundation (ID 100010434). Fellowship code LCF/BQ/IN18/11660003.
This project has received funding from the European Union´s Horizon 2020 research and innovation program under the Marie Skłodowska-Curie grant agreement No. 713673.
We thank the CERCA Program/Generalitat de Catalunya, ICREA, MINECO/FEDER (CTQ2017-88920-P, PID2020-112684GB-100 and PID2019-109236RB-I00), MICINN through Severo Ochoa Excellence Accreditation 2020-2023 (CEX2019-000925-S, MIC/AEI), and AGAUR (2017-SGR-232 and 2017-SGR-1139) for support.

List of Publications

The results described in this doctoral thesis are based on the following publications:

- N. Zanda, A. Sobolewska, E. Alza, A. W. Kleij and Miquel À. Pericàs *ACS Sustainable Chem. Eng.* **2021**, *9*, 4391−4397
- N. Zanda, L.Zhou, E. Alza, A. W. Kleij and Miquel À. Pericàs, *Green Chem.* **2022**, *24*, DOI: 10.1039/D2GC00503D.
- N. Zanda, L. Primitivo, M. Chaudari, A. W. Kleij and Miquel À. Pericàs, *Manuscript in preparation*

Other publications:

- Revuelto, A.; López-Martin, I.; de Lucio, H.; Garcia-Soriano, J. C.; Zanda, N.; de Castro, S.; Gago, F.; Jiménez-Ruiz, A.; Velázquez, S.; Camarasa, M.-J. B. *Pharmaceuticals* **2021**, *14*, 689-703.

List of Abbreviations

In this doctoral thesis, the abbreviations and acronyms most commonly used are based on the recommendations of the ACS ‘’Guidelines for authors’’, which can be found and consulted at https://www.cas.org/support/documentation/references/cas-standard-abbreviations#listinga.

UNIVERSITAT ROVIRA I VIRGILI
CONTINUOUS FLOW CATALYSIS FOR THE VALORIZATION OF CARBON DIOXIDE
Nicola Zanda

Table of contents

UNIVERSITAT ROVIRA I VIRGILI
CONTINUOUS FLOW CATALYSIS FOR THE VALORIZATION OF CARBON DIOXIDE
Nicola Zanda

UNIVERSITAT ROVIRA I VIRGILI
CONTINUOUS FLOW CATALYSIS FOR THE VALORIZATION OF CARBON DIOXIDE
Nicola Zanda

Chapter 1: General Introduction

1.1 CO_2 capture and utilization

The amount of CO_2 in the atmosphere is on the rise.[1] This increase is associated to anthropogenic activities and linked with the "greenhouse effect", and more in general, with climate change.[1] Various approaches have been proposed to mitigate CO_2 emissions, ranging from CO_2 capture,[2] its use for commercial purposes[3] and its transformations to access more complex molecules.[4] This last approach is interesting, as it can deliver value-added chemicals and polymers and ideally lead to circular product chains.

Currently, we use crude oil and natural gas as carbon feedstock resulting in CO_2 emissions during their refining, transformation and at the end-of-life disposal of the product that are made from these non-renewable resources. The use of fossil feedstock leads to an increase in CO_2 emission whereas carbon-neutral (or near-neutral) chemical processes are desired to combat the negative effects of this greenhouse gas.

The evolution of CO_2 capture techniques has resulted in a low commercial price of CO_2. As a consequence, it has become attractive to use this carbon feedstock for a wide variety of existing and novel transformations as attested by the recent literature. Though CO_2-based chemical synthesis will not be able to reduce annual CO_2 emissions, the use of a renewable, cheap and accessible carbon feedstock is attractive from a synthetic point of view. Among the C_1 synthons available, CO_2 is the cheapest, safest and most versatile one. As depicted in Figure 1, the utilization of carbon dioxide can be broadly classified in three areas on the basis of the change in oxidation state of its carbon center and the synthetic target.[4d]

First of all, the synthesis of carbonates and carbamates has been greatly advanced over the years representing an example of "non-reductive" transformations of CO_2. In this case, CO_2 functions as a sustainable alternative to phosgene and its derivatives, which are typically toxic and dangerous to use. In order to make these reactions thermodynamically feasible, higher-energy reaction partners such as strained cyclic ethers (epoxides, oxetanes) are required and depending on the catalyst provide access to either polymers or cyclic structures.

A second category of conversions are denoted as "reductive transformations". In these cases, the carbon center of CO_2 is reduced and become "functionalized" such as in the case of carboxylic acids and formamides. This broad category of reactions usually employs high reactive partners[6] or organometallic reagents.

The last category is the reduction of CO_2 providing "energy vectors" such as CO, HCOOH, MeOH and CH_4. These conversions are related to the second category but lack their functionality. Furthermore, they represent a way to store renewable energy into small molecules that can be seen as energy carriers provided that molecular hydrogen can be easily released from them. The reduction of CO_2 can be realized by chemical, photochemical and electrochemical methods and gives relatively simple products.

---

1 a) D. Keith, *Science* **2009**, *325*, 1654-1655; b) M. Cokoja, C. Bruckmeier, B. Rieger, W. A. Herrmann and E. Fritz, *Angew. Chem. Int. Ed.* **2011**, *50*, 8510-8537; c) L. M. Alsarhan, A. S. Alayyar, N. B. Alqahtani and N. H. Khdary, *Sustainability* **2021**, *13*, 11625-11650; d) A. Saravan, P. S. Kumar, D.-V. N. Vo, S. Jeevanantham, V. Bhuvaneswari, V. A. Narayanan, P. R. Yaashikaa, S. Wetha and B. Reshma, *Chem. Eng. Sci.* **2021**, *236*, 116515-116531.

2 a) A. A. Olajire, *J. CO_2 Utiliz.* **2013**, *3*, 74-92 b) T. Wilberforce, A. Olabi,E. T. Sayed, K. Elsaid and M. A. Abdelkareem, *Sci. Total Environ*. **2020**, *761*, 143203-143214.

3 a) Rafiee, K. R. Khalilpour, D. Milani, M. Panahi, *J. Environ. Chem. Engin.* **2018**, *6*, 5771–5794; b) M. Pérez-Fortes, A. Bocin-Dumitriu and E. Tzimas, *Energy Procedia* **2014**, *63*, 7968–7975; A. Goeppert, M. Czaun, J. Jones, G. K. Surya Prakash and A. G. Olah, *Chem. Soc. Rev.* **2014**, *43*, 7995-8048.

4 a) M. Mikkelsen, M. Jorgensen and F. C. Krebs, *Energy Environ. Sci.* **2010**, *3*, 43-81; b) M. Poliakoff, W. Leitner and E. S. Streng, *Faraday Discuss.* **2015**, *183*, 9-17; c) T. Sakakura, J.-C Choi and H. Yasuda, *Chem. Rev.* **2007**, *107,* 2365–2387; d) C. Maeda, Y. Miyazaki and T. Ema, *Catal. Sci. Technol*. **2014**, *4*, 1482-1499.

Aside from safety, toxicity and price another advantage of using CO_2 as a reagent is that can be easily removed from the reaction media and recycled for further use. However, its use has both thermodynamic and kinetic hurdles. The thermodynamic stability requires high-energy reactants (non-reductive conversions),[5] whereas its high kinetic stability makes the use of catalytic methods a necessity. Typically, non-catalytic CO_2 valorization techniques usually employ high temperature, pressure and high reactive partners[6] to overcome challenges associated with CO_2 conversion, and catalysis is key to devise more sustainable approaches to its valorization.

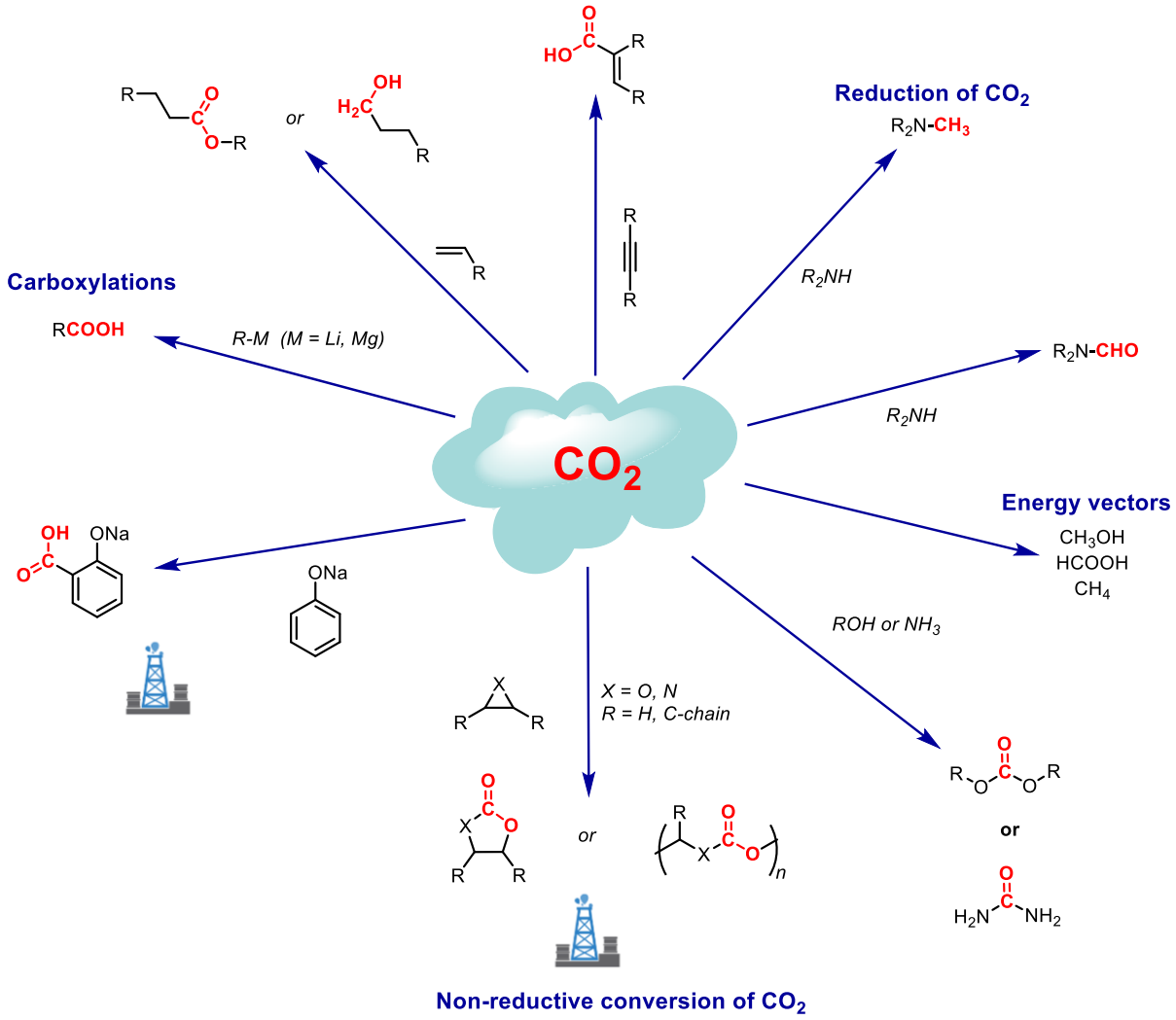

Figure 1. Examples of some of the most important transformations of CO_2.[7]

Despite the high stability of CO_2, its carbon center is electrophilic and can be easily activated by strong nucleophiles. For this reason, several reports are available for the transformation of CO_2 with organometallic species to give carboxylic acids, lactones, esters and related derivatives. However, very few processes have been industrialized, and of particular relevance is the reaction of sodium phenolate with carbon dioxide to give salicylic acid (Kolbe-Schmitt

[5] N. Von der Assen, J. Jung and A. Bardow, *Energy Environ. Sci.* **2013**, *6*, 2721-2734.
[6] a) R. R. Shaick, S. Pornpraprom and V. D'Elia, *ACS Catal.* **2018**, *8*, 419–450; b) A. Polyzos, M. O'Brien, T. P. Petersen, I. R. Baxendale and S. V. Ley, *Angew. Chem.* **2011**, *123*, 1222-1225.
[7] Q. Liu, L. Wu, R. Jackstell and M. Beller, *Nat. Commun.* **2015**, *6,* 5933.

reaction) which is the precursor of Aspirin. Other relevant processes are the production of cyclic carbonates such as glycidol carbonate (prepared using solid KI as catalyst) and (aliphatic) polycarbonates, which are a more environmentally friendly alternative to isocyanate-based polyurethanes.

1.2.1 Cycloaddition of CO_2 to epoxides

One of the most studied transformations in the field of CO_2 valorization is the formal [3+2] cycloaddition of CO_2 to epoxides.[8] The resulting products, cyclic carbonates, are interesting intermediates in various fields such as in polymer science to prepare polycarbonates[9], battery development playing the role of electrolytes,[10] and synthons in organic chemistry being alternatives to epoxides or giving access to more complex structures.[11]

The field is dominated by binary catalytic systems combining a metal complex and halogen-based nucleophile. This type of catalytic system generally operates via a double activation manifold, with the metal center usually acting as a Lewis acid able to activate the epoxide reagent whereas the halogen nucleophile is involved in the ring opening of the epoxide.[12] As a result, a metal-stabilized alkoxide species is formed that can activate CO_2 and advance the reaction to the desired product.

In general, various metals can be employed as long as they have a certain degree of Lewis acidity. In particular, Al, Mg, Cr, Co, Zn and Fe have been rather popular metals over the last decade and were mostly selected in this area. Metal complexes with a wide variety of ligands such as porphyrins, salen/salphens, bimetallic macrocyclic phenolates, aminotriphenolates and related multidentate ligands have been frequently reported.[13]

A direct comparison of the catalyst efficiencies of known catalysts for cyclic carbonate formation remains difficult since these systems have been employed with different combinations of reaction temperature and pressure, different metal/halide loadings, various substrates and different reactor set ups. A seminal report in 2017 showed the importance of proper benchmarking within a selection of 5 known Al-based binary catalysts, and the role of several parameters including the type of epoxide (terminal vs internal), halogen co-catalyst and its relative ratio to the metal complex, temperature, solvent and the scale of the reaction.[14]

However, general trends can be delineated by comparison based on the catalysts turnover frequencies (TOF). In Scheme 1, some of the best catalytic systems derived from earth abundant metals[15] are presented that are able to achieve high TOFs. It has to be noted that this is not an absolute measure since the TOF data is related to different substrates and conditions.[16] Furthermore, the depicted activity is usually a combination of more than one catalytic cycle: the one from the binary catalyst combining a Lewis acid and nucleophile co-catalyst, and the one promoted by the (excess of) nucleophile alone.[17]

---

8 P. P. Pescarmona, *Curr. Opin. Green Sustain. Chem.* **2021**, *29*, 100457-100466.

9 a) A. Brege, B. Grignard, R. Méreau, C. Detrembleur, C. Jerome and T. Tassaing, *Catalysts* **2022**, 12, 124-164; b) V. Bonamigo Moreira, J. Rintjema, F. Bravo, A. W. Kleij, L. Franco, J. Puiggalí, C. Alemán and E. Armelin, *ACS Sustainable Chem. Eng.* **2022**, *10*, 2708–2719.

10 B. Scrosati and J. Garche, *J. Power Sources* **2010**, *195*, 2419–2430.

11 a) S. Xue, A. Cristòfol, B. limburg, Q. Zeng and A. W. Kleij, *ACS Catal.* **2022**, *12*, 3651-3659; b) X. Li, A. Villar-Yanez, C. Ngassam Tounzoua, J. Benet-Buchholz, B. Grignard, C. Bo, C. Detrembleur and A. W. Kleij, *ACS Catal.* **2022**, *12*, 2854–2860; c) K. Guo, W. Zeng, A. Villar-Yanez, C. Bo and A. W. Kleij, *Org. Lett.* **2022**, *24*, 637–641.

12 F. Della Monica and A. W. Kleij, *Catal. Sci. Technol.* **2020**,*10*, 3483-3501.

13 A. J. Kamphuis, F. Picchioni and P. Pescarmona, *Green Chem.* **2019**, *21*, 406-449.

14 J. Rintjema and A. W. Kleij, *ChemSusChem* **2017**, *10*, 1274-1284.

15 Based on Element Scarcity – EuChemS Periodic Table (2021) https://www.euchems.eu/euchems-periodic-table/.

16 C. Martín, G. Fiorani and A. W. Kleij, *ACS Catal.* **2015**, *5*, 1353-1370.

17 V. Campisciano, C. Calabrese, F. Giacalone, C. Aprile, P. Lo Meo and M. Gruttadauria, *J. CO_2 Utiliz.* **2020**, *38*, 132-140.

The best results (in terms of TOF/metal center) have been achieved using Al- and Mg-based catalysts. In 2013, our group showed how a Cl-substituted Al(III) aminotriphenolate complex efficiently converts 1,2-epoxypentane into its corresponding cyclic carbonate at 90 ºC with a TOF up to 36.000 h^{-1}. It should be noted that increasing the catalyst loading allows for this reaction to be performed at nearly ambient temperature (30 ºC) with a TOF of 100 h^{-1}.[18] In this work TBAI (tetrabutylammonium iodide) was used as co-catalyst, though Ema and co-workers reported (multinuclear) Mg- and Zn-based complexes appended with bromide anions that showed high TOF/metal center. In these examples, the halogen co-catalyst was embedded within the structure and are typically denoted as "bifunctional".[19]

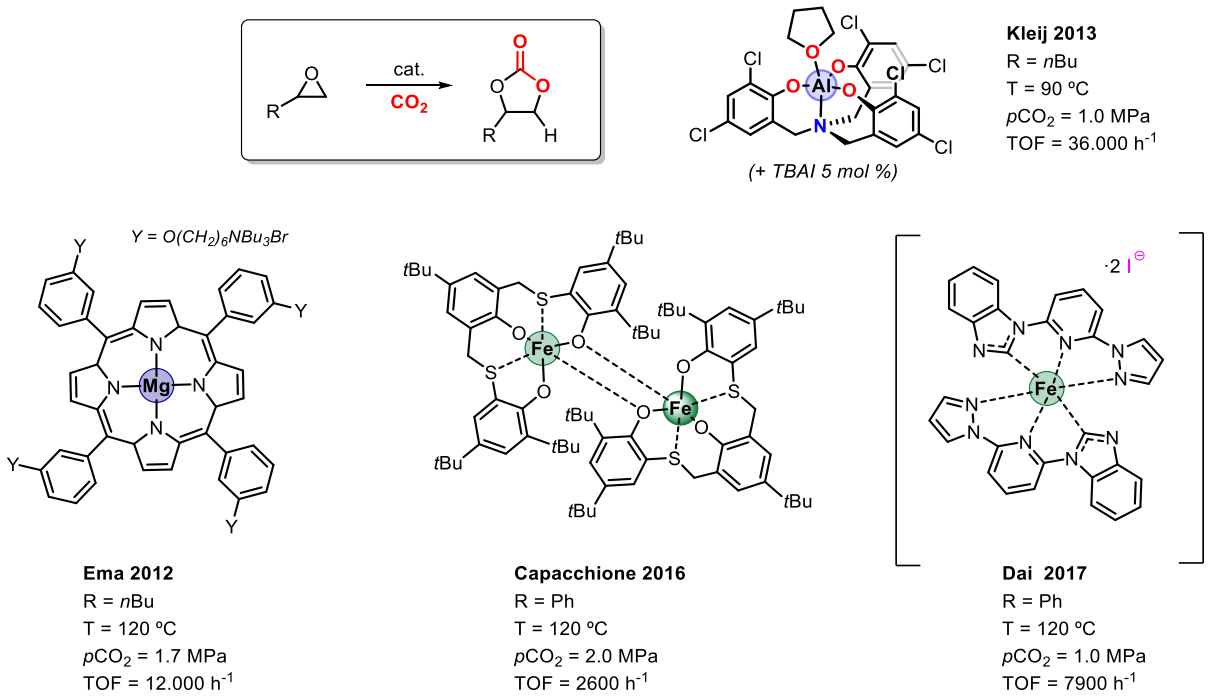

Scheme 1. Structures of successful metal complexes exhibiting high catalytic activity in cyclic carbonate synthesis.

In the last few years, several iron-based complexes have emerged.[20] More specifically, the Dai group reported an Fe(II) bis-CNN-chelating pincer complex that could achieve a TOF of 7900 h^{-1} in the conversion of propylene oxide to propylene carbonate. Notably, the same catalyst could also efficiently convert various other epoxides at r.t.[21] Although this catalyst surpassed the efficiency of previously Fe-catalysts developed by the Capacchione group using terminal

[18] C. J. Whiteoak, N. Kielland V. Laserna, F. Castro-Gómez, E. Martin, E. C. Escudero-Adán, C. Bo and A. W. Kleij, *Chem. Eur. J.* **2014**, *20*, 2264–2275.

[19] a) T. Ema, Y. Miyazaki, S. Koyama, Y. Yano and T. Sakai, *Chem. Commun*. **2012**, *48*, 4489−4491; b) T. Ema, Y. Miyazaki, J. Shimonishi, C. Maeda, and J.-Y. Hasegawa, *J. Am. Chem. Soc*. **2014**, *136*, 15270−15279; c) C. Maeda, T. Taniguchi, K. Ogawa and T. Ema, *Angew. Chem. Int. Ed*. **2015**, *54*, 134−138.

[20] F. Della Monica, A. Buonerba and C. Capacchione, *Adv. Synth. Catal.* **2019**, *361*, 265-282.

[21] F. Chen, N. Liu and B. Dai, *ACS Sustain. Chem. Eng.* **2017**, *5*, 9065–9075.

epoxides, the thioether-triphenolate Fe(III) complexes designed by the latter group also proved to be useful to achieve high TOF/metal center with an internal epoxide (i.e., hexene oxide).[22] An important result in this area of CO_2 catalysis was reported by the North group. They showed that bis-Al(III) complexes (*O*-bridged) can promote the cycloaddition of CO_2 to epoxides without the need of an additional nucleophile. The complex is able to activate the CO_2 by means of insertion into one of the Al–$O_{phenolate}$ bonds. The resulting complex can ring-open the epoxide *en route* to the final carbonate product.[23]

Despite the important results that have been achieved in terms of activity-per-catalyst in the field of the metal-catalyzed cycloaddition of CO_2 to epoxides, this type of (binary/bifunctional) catalyst tends to be air- and moisture-sensitive. Besides, their preparation sometimes is tedious affecting practicality. Furthermore, more complex ligands can increase the price of the CO_2-fixation process in case of an eventual scale up, and it also has to be considered that (with few exceptions)[24] an external nucleophile is necessary that may cause reactor corrosion.

An alternative approach is offered by organocatalysis. Organocatalysts are usually cheaper and less sensitive thus not requiring strictly anhydrous/inert reaction conditions when compared to metal-based systems. Ideally, they are easily prepared, modular and/or based on bio-precursors. However, as recently reviewed by D'Elia and co-workers, there is still much room for improvement with respect to their productivity (i.e., TOF).[25]

1.2.3 Organocatalysis in the cycloaddition of CO_2 to epoxides

Several types of organocatalysts have been used for organic carbonate formation such as *N*-heterocyclic bases, NHCs (i.e., carbenes), FLPs (frustrated Lewis pairs), organic salts, ionic liquids (ILs) and hydrogen-bond donor catalysts. In general, they share some common features including a nucleophilic character and basicity. Depending on the balance of these two properties they either activate the epoxide or the CO_2 molecule (Figure 2, upper part).

As mentioned in the previous paragraph, ILs are among the most widely used organocatalysts in cyclic carbonate formation. Their mode of action involves activation and ring opening of the epoxide.[26] After this step, the in situ generated alkoxy-based nucleophile attacks the carbon atom of CO_2 generating a hemi-carbonate that ring-closes giving the cyclic carbonate product and re-generates the catalyst for additional turnover.

The weak aspect of this approach is the difficult separation of the catalyst from the cyclic organic carbonates that, due their high boiling points, is energy-consuming if distillation is applied. Obviously, the heterogenization of such catalysts will provide a solution to overcome this limitation.[27] However, this type of catalyst also suffers from thermal deactivation by de-

[22] F. Della Monica, S. V. C. Vummaleti, A. Buonerba, A. D. Nisi, M. Monari, S. Milione, A. Grassi, L. Cavallo and C. Capacchione, *Adv. Synth. Catal.* **2016**, *358*, 3231-3243.

[23] a) J. A. Castro-Osma, M. North and X. Wu, *Chem. Eur. J.* **2014**, *20*, 15005-15008; b) J. A. Castro-Osma, M. North, W. K. Offermans, W. Leitner and T. E. Müller, *ChemSusChem* **2016,** *9,* 791-794.

[24] V. Laserna, W. Guo and A. W. Kleij, *Adv. Synth. Catal*. **2015**, *357*, 2849-2854.

[25] R. R. Shaikh, S. Pornpraprom and V. D'Elia, *ACS Catal.* **2018**, *8*, 419−450.

[26] A. Rehman, F. Saleem, F. Javed, A. Ikhlaq, S. W. Ahmad and A. Harvey, *J. Environ. Chem. Eng*. **2021**, *9*, 105113-105141.

[27] a) Y. Zhang, G. Chen, L. Wu, K. Liu, H. Zhong, Z. Long, M. Tong, Z. Yang and S. Dai, *Chem. Commun.* **2020**, *56*, 3309-3312; b) A. H. Jadhav, G. M. Thorat, K. Lee, A. C. Lim, H. Kang and J. G. Seo, *Catal. Today* **2016***, 265*, 56-67.

quaternarization of the nitrogen centers,[28] which is not desired and perhaps difficult to avoid as generally high reaction temperatures are requisite for catalyst efficacy.[29]

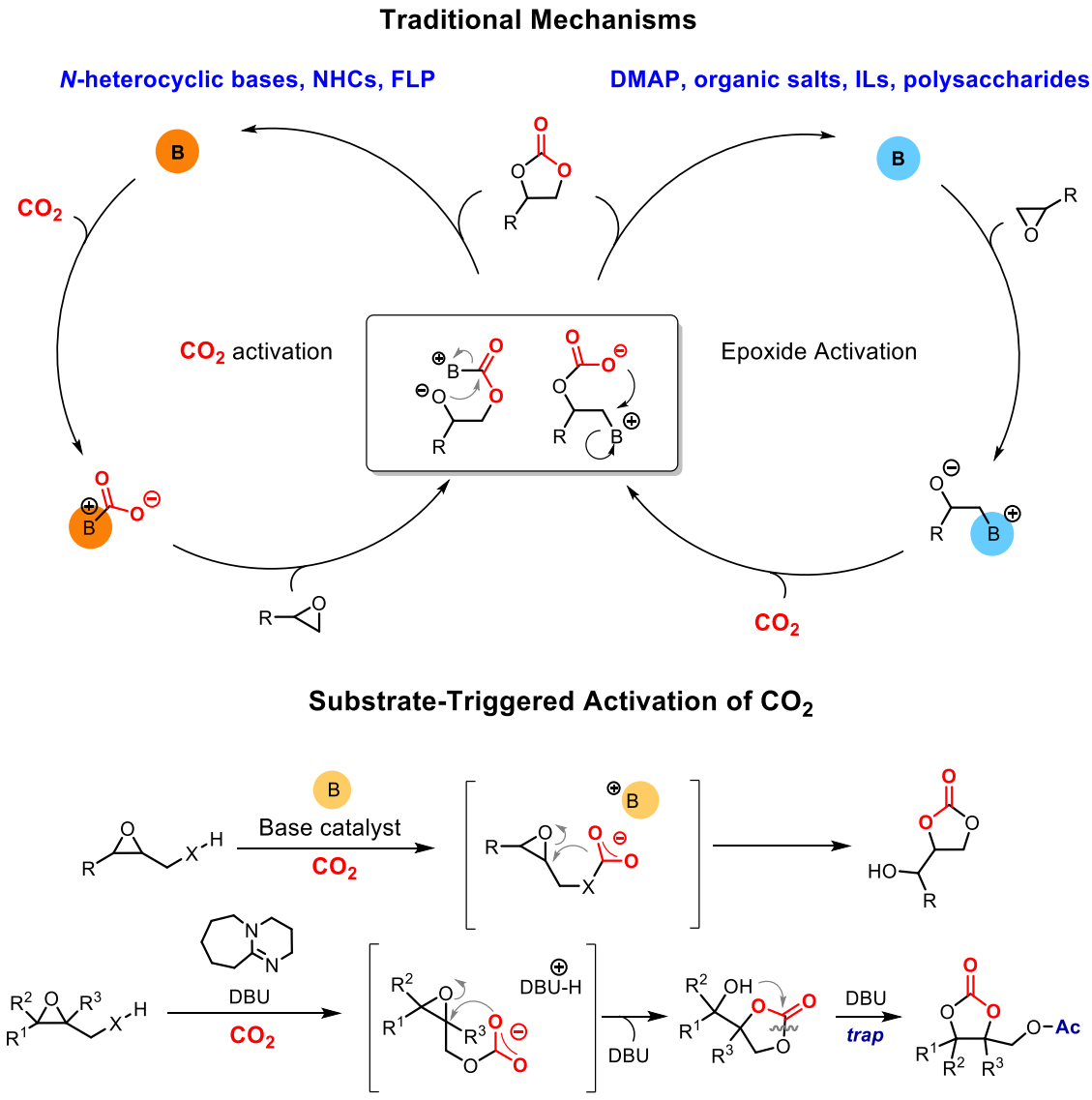

Figure 2. General modes of substrate activation with the most common organocatalysts.[25,30]

Other types of catalysts are (strong) Lewis bases such as DMAP, imidazole and DBU.[31] They operate via a similar mechanism as promoted by ILs in the absence of water, while in the presence of water the process may be mediated by bicarbonate anions.[32]

[28] C. J. Whiteoak, A. Nova, F. Maseras and A. W. Kleij, *ChemSusChem* **2012**, *5*, 2032–2038.
[29] a) P. P. Pescarmona and M. Taherimehr, *Catal. Sci. Technol.* **2012**, *2*, 2169-2187; b) M. North, R. Pascuale and C. Young, *Green Chem.* **2010**, *12*, 1514-1539.
[30] G. Fiorani, W. Guo and A. W. Kleij, *Green Chem.* **2015**, *17*, 1375–1389.
[31] R. A. Shiels and C. W. Jones, *J. Mol. Catal. A*: *Chem.* **2007**, *261*, 160–166.
[32] K. R. Roshan, R. A. Palissery, A. C. Kathalikkattil, R. Babu, G. Mathai, H.-S. Lee and D.-W. Park, *Catal. Sci. Technol.* **2016**, *6*, 3997-4004.

If the epoxide is functionalized with pro-nucleophilic groups and a base catalyst is employed, then proton transfer can be facilitated and converting OH and NHR fragments into strong nucleophiles. This type of activation can generate a different and more complex cyclic carbonate product when coupled with alcohol protection, allowing for equilibration to more substituted carbonate congeners (Figure 2, lower part: DBU as catalyst). Such elusive carbonate structures were recently prepared by our group by using a Payne type rearrangement approach.[33]

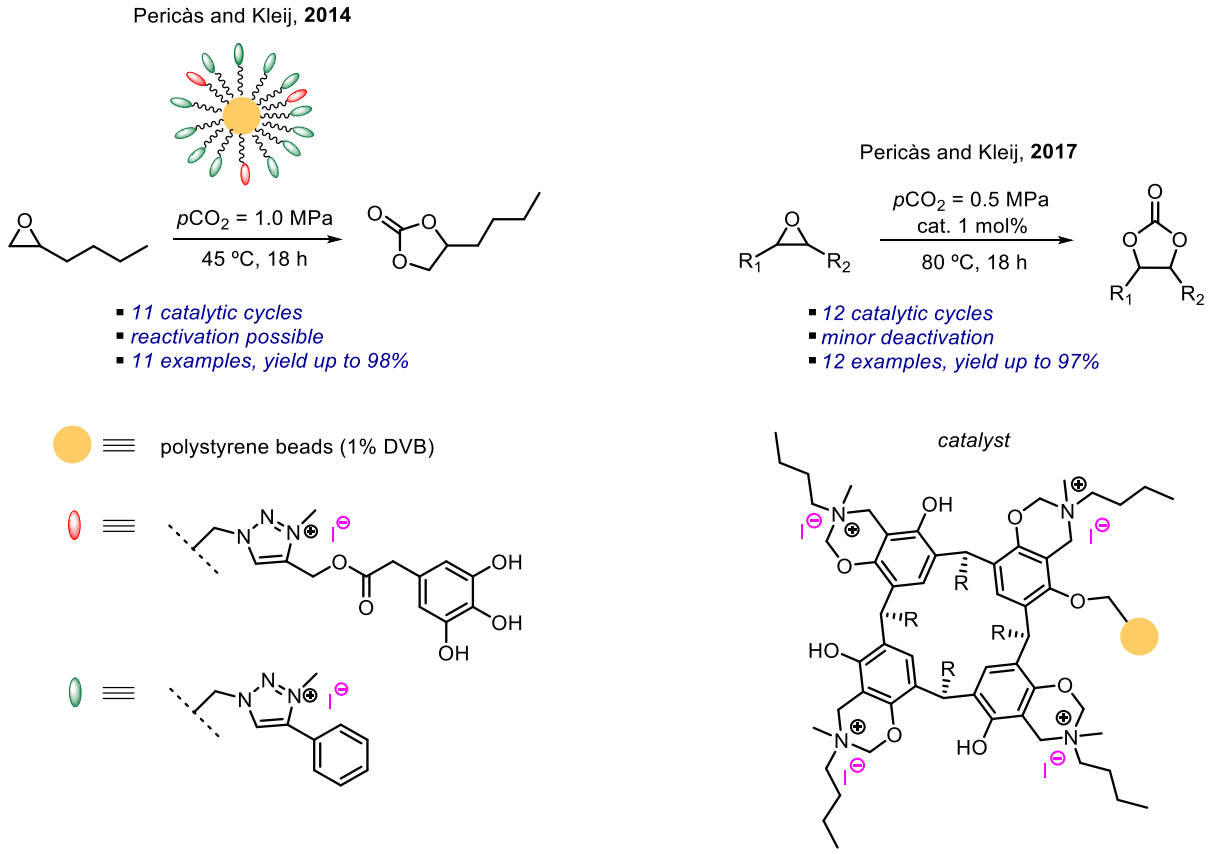

Figure 3. Cycloaddition of CO_2 to epoxides using polystyrene-supported bifunctional organocatalysts reported by Pericàs and Kleij.

Another type of catalyst that was not mentioned so far in this section are hydrogen bond donor (HBD) catalysts.[34] These, usually are combined with a halogen derived co-catalyst and offer a purely organocatalytic approach and immobilization potential. A joint effort of Pericàs and Kleij groups (Figure 3) produced two highly active heterogeneous catalysts[35] that take advantage of their bifunctionality having embedded both HBD groups and halide nucleophiles in their structures. In 2014, a supported binary catalyst based on pyrogallol and TBAI was shown as an effective catalyst for the cycloaddition of CO_2 to epoxides at mild temperature (45 ºC) and, despite minor deactivation due to Hoffman-type elimination resulting in the demethylation of the triazole and loss of halogen nucleophile, it could be reactivated by simply

[33] S. Sopeña, M. Cozzolino, C. Maquilón, E. C. Escudero-Adán, M. Martinez Belmonte and A. W. Kleij, *Angew. Chem. Int. Ed.* **2018**, *130*, 11373-11377.

[34] P. Yingcharoen, C. Kongtes, S. Arayachukiat, K. Suvarnapunya, S. V. C. Vummaleti, S. Wannakao, L. Cavallo, A. Poater and V. D'Elia, *Adv. Synth. Catal.* **2019**, *361*, 366-373.

[35] a) C. J. Whiteoak, A. H. Henseler, C. Ayats, A. W. Kleij and M. A. Pericàs, *Green Chem.* **2014**, *16*, 1552-1559.; b) T. Jose, S. Cañellas, M. A. Pericàs and A. W. Kleij, *Green Chem.* **2017**, *19*, 5488-5493.

adding more CH_3I.[35a] The bifunctional catalyst developed in 2017, which was based on resorcinarenes and TBAI, showed a promising higher degree of activity. The required catalyst loading to achieve full substrate conversion under similar reaction conditions as reported in 2014 was determined to be only 0.80 mmol %. However elemental analysis of the catalyst material showed a loss in N- and I-content, which was caused by a retro-Mentschutkin reaction.[35b]

1.3 Heterogenization of catalysts

The lower reactivity of organocatalysts can be generally overcome by increasing the catalyst loading, however this could be considered as a less efficient approach because the isolation of the product might become an issue. However, the immobilization of the catalyst onto a support (being a nanoparticle or an inorganic or organic macroscopic material) reduces this possible drawback and adds additional benefits such as easier recyclability of the catalyst.[36]

There are many strategies to support an organocatalyst but the most important one is the generation of a covalent bond between the support and the catalyst. This reduces significantly the possibility of catalyst leaching, which is usually a problem with catalyst modules anchored to a support material via electrostatic or coordinative interactions, or chemical absorption.[37]

The final material (support + catalyst) may be soluble in the reaction media, and in this case recyclable through precipitation or by a magnetic separation in the case of magnetic nanoparticles. More conveniently, insoluble catalysts are used which can be separated by simple filtration.[38] Recycling is advantageous but there are some limitations that are typical for heterogeneous but not for homogeneous catalysts. For instance, mass transfer can become an issue, and for a heterogeneous system to work efficiently it is crucial that the reagents are able to reach the active sites. This can be affected by the support in several ways such as direct interactions with the substrate, and additionally the morphology (i.e., channels and pores) can affect the mobility of the substrates inside the matrix. These effects can be mitigated by a proper design of the material, however materials such as silicas, zeolites and carbon-based nanostructures always present some degree of mass transfer limitation inside their macro/microstructures.

An alternative to these materials is the use of organic polymeric supports.[39] These organic polymers have the same versatility in terms of matrix design but they have an important advantage. They swell when put in contact with a suitable solvent and form a gel-like phase. This property allows to massively reduce potential mass transfer and leads to a behavior which is best described between purely homogeneous and heterogeneous. These types of catalysts can be prepared by straightforward polymerization but their synthesis is often difficult to reproduce. Therefore, the use of commercially available functionalized supports greatly reduces reproducibility issues. The most commonly found resins in the literature are polystyrene based ones. These materials are less versatile in terms of channel shape, but high variability is provided by the crosslinking units (Figure 4, in green), in terms of type and ratio to the monomer (blue color) employed and to the anchoring unit (red color), which is used to covalently bind the organocatalyst.

---

[36] a) Z. D. Susam and C. Tanyeli, *Asian J. Org. Chem*. **2021**, *10*, 1251–126; b) A. Franconetti and G. de Gonzalo *ChemCatChem* **2018**, *10*, 5554-5572.

[37] a) J. M. Fraile, J. I. Garcia and J. A. Mayoral, *Chem. Rev.* **2009**, *109*, 360–417; b) L. Zhang, S. Luo and J.-P. Cheng, *Catal. Sci. Technol.* **2011**, *1*, 507-516; c) T. Fulgheri, F. Della Penna, A. Baschieri and A. Carlone, *Curr. Opinion in Green Sustain. Chem.* **2020**, *25*, 100387-100397.

[38] C. Ren, X. Zhu, N. Zhao, S. Fang and Z. Li, *Polymer* **2020**, *204*, 122797-122805.

[39] C. Rodríguez-Escrich and M. A. Pericàs, *Chem. Rec.* **2019**, *19*, 1872 – 1890.

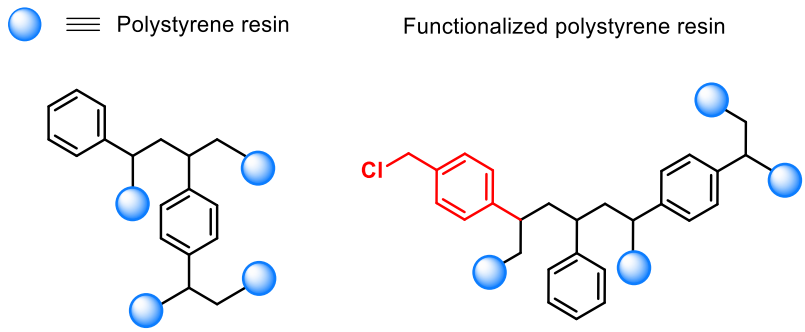

Figure 4. On the left, a representation of a polystyrene polymer (DVB as crosslinker). On the right, representation of a chloromethyl benzene resin (Merrifield: when a low degree of crosslinking is used), with in red functionalizable moieties (chloromethyl benzene), the blue spheres the chains (styrene).

In chapter 2 and 4 of this thesis, the crosslinker unit (about 1% ratio) present in the catalyst structure was in most of the cases divinyl benzene (DVB). These supports swell well in apolar solvents such as DCM, THF and toluene and tend to have lower degrees of swelling in water, DMF and polar solvents. The gels are normally microporous materials with a flexible structure. The polystyrene resin used in chapter 3 is of a microporous nature too, however, the reaction conditions employed do not allow its swelling but with 5.5% of DVB the pores are surely bigger. Figure 5 shows that the pores in a resin with 5.5% DVB are clearly visible at low magnification, whereas the pores in a real microporous system (1% DVB) are not visible even at higher magnification.

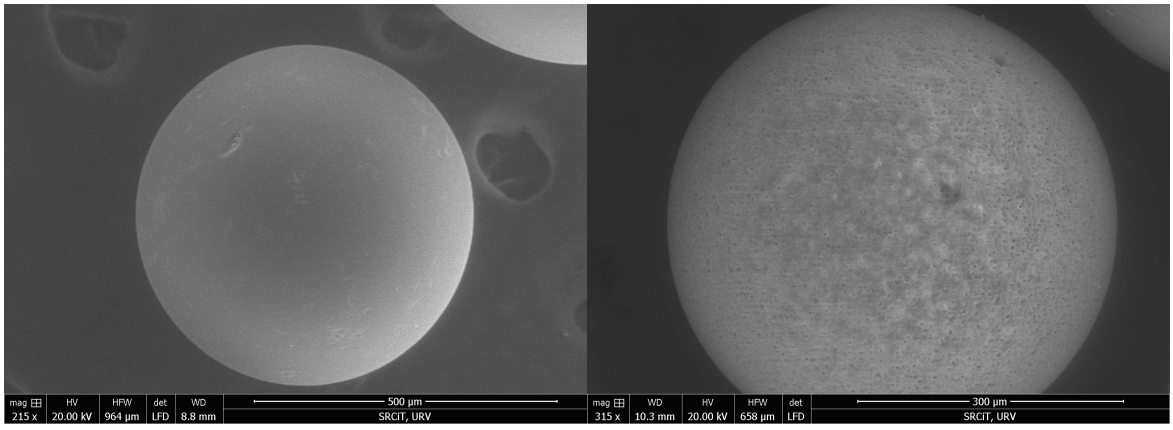

Figure 5. SEM (scanning electron microscopy) pictures of polystyrene beads. On the left, a Merrifield resin (1% DVB), on the right a chloromethyl polystyrene (5.5% DVB).

An attractive feature of heterogeneous catalysts is that they can be charged into a reactor and used in continuous flow mode. This allows to potentially run the reactions infinitively if the catalyst does not deactivate or decompose over time under the given conditions.

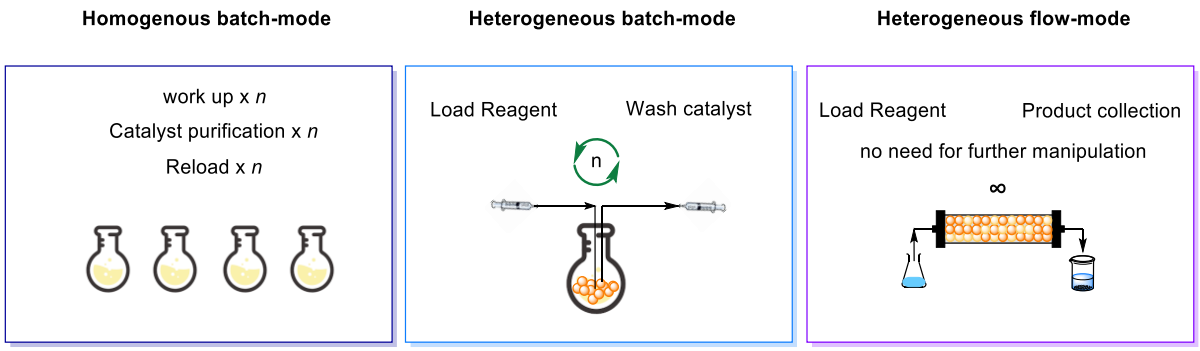

Figure 6. Comparison between different catalyst recycling approaches and process intensification.

The fact that the catalyst is isolated from the environment thereby reduces mechanical damage and that it is in contact only with the stream of the reactant usually results in an increased lifetime.[40] It must be noted that swellable catalysts have a limitation that exclude 'a priori' the possibility of being used forever. In fact, their flexible structure when exposed to a unilateral pressure such as in continuous flow, tends to collapse.[41] This leads to movement of the beads or mechanical damage and pore occlusion, increase of the risk of pressure drops and eventually a decrease of the catalytic activity.[42] This phenomenon tends to be more relevant when high flow-rates and -pressures are employed.

[40] C. I. Herrerías, L. Solà and M. A. Pericàs, *Adv Synth Catal*. **2008**, *350*, 927–932.
[41] X. C. Cambeiro, R. Martín-Rapún, P. O. Miranda, S. Sayalero, E. Alza, P. Llanes and M. A. Pericàs, *Beilstein J Org Chem*. **2011**, *7*, 1486–1493.
[42] G. Jas and A. Kirschning, *Chem. Eur. J.* **2003**, *9,* 5708–5723.

1.4.1 Flow chemistry

In a continuous flow system, the reagents are pushed into channels (tubing) towards a reactor in which they are exposed to the reaction conditions (temperature, light, current, gas, catalyst) and then the product stream is flowed out to be collected.[43] An extension to this is the use of continuous stirred tank reactors in which the reagents are continuously flowed through batch reactors but operated in a continuous manner.

As formulated by Seeberger and co-workers in 2017: "*Is flow the answer to the ultimate question of life, the universe and everything? No.*.".[44] With respect to the current thesis, there are several advantages of running reactions in flow:

- **Gaseous reagent**. It is easier to control the amount of gas employed and easier to charge it into the system when the reaction is run under flow. The control of pressure and mixing of the gas allows to scale up the reaction in a more efficient way due to a better mass and heat transfer.[45]
- **Safety**. The volume of a flow system is usually smaller than the respective batch counterpart. Eventual thermal run-aways are of lower impact.[46]
- **Practicality**. As stated above, once the heterogeneous catalyst is loading into a flow system, it does not need any further manipulation. A continuous flow reactor is ideal for heterogeneous catalysts. Running the reaction means preparing the feed solution and starting the system, the washing operation is as simple as changing the feed for clean solvent and the system will clean itself. Finally, collection happens in pre-selected reservoir and does not need any further operation (*provided that substrate conversion is maintained very high and high chemo-selective synthesis takes place*).[47]
- **Selectivity**. During a continuous flow experiment the time during which the starting materials are in contact with the catalyst, heat and in general under the reaction conditions is reduced when compared to batch operation and this reduces the possibility of side reactions.
- **Process intensification**: the use of immobilized catalysts intrinsically unites the steps of reaction and filtration. This is many cases allows to avoid the work-up, which is the step in which most of the solvent is consumed.
- **Temperature control**: less energy is required to maintain the desired temperature in the reactor. The volume that has to be cool down or heated at a given moment is far smaller than in a batch operation.

Other more general advantages are:[48]

- **Modularity**. Multistep reactions can be run in flow. This allows to reduce the overall waste in terms of solvent and reduces any necessary purification steps. Highly reactive and toxic reagents can be used and quenched without the need to be in contact with them.

---

43 C. A. Hone and C. O. Kappe, *Chem. Meth.* **2021**, *1*, 454-467.
44 M. B. Plutshack, B. Pieber, K. Gilmore and P. H. Seeberger, *Chem. Rev.* **2017**, *117*, 11796−11893.
45 C. J. Mallia and I. Baxendale, *Org. Proc. Res. Dev,* **2016**, *20*, 327-360.
46 D. Dallinger, B. Gutmann and C. O. Kappe, *Acc. Chem. Res,* **2020**, *53*, 1330–1341.
47 a) Y. Saito, K. Nishizawa, B. Laroche, H. Ishitani and S. Kobayashi, *Angew. Chem. Int. Ed.* **2022***, 61,* e202115643; b) S. B. Ötvös, P. Llanes, M. A. Pericàs and C. O. Kappe, *Org. Lett.* **2020**, *22*, 8122–8126.
48 P. D. Morse, R. L. Beingessner and T. F. Jamison, *Isr. J. Chem.* **2017**, *57*, 218-227.

- **Inline monitoring**. The reactions can be monitored instantaneously, and the parameters quickly modified to obtain the best result. This recently resulted in the design of several automatized platforms to perform synthetic organic chemistry with the aid of artificial intelligence (AI).[49]
- **Facile scale-up:** scaling up a reaction might be easier by simple numbering up of the reactors. Since a Flow reactor occupies less space the dimensional factor of the reactors is not as problematic as for batch operations.

[49] a) P. Sagmeister, F. F. Ort, C. E. Jusner, D. Hebrault, T. Tampone, F. G. Buono, J. D. Williams and C. O. Kappe, *Adv. Sci.* **2022***, 12,* 2105547-2105558; b) R. W. Epps, A. A. Volk, M. Y. S. Ibrahim and M. Abolhasani, *Chem* **2021**, *7*, 2541-254; c) N. Heublein, J. S. Moore, C. D. Smith and K. F. Jensen, *RSC Adv.* **2014**, *4*, 63627−63631.

1.4.2 Types of continuous flow systems

It is generally accepted that flow systems can be broadly classified in 4 types. This classification was first introduced by Shu Kobayashi, and considers only the physical state of the reagents and catalysts.[50] Below a brief description is provided on the general types of "flow" and some recent/relevant examples are given for the sake of clarity.

In **Type I** flow, two reagents are flowed into the desired reactor (coil or chip), in which they are exposed to the reaction conditions. All the components are homogeneous and at the end of the system the crude product is collected and purified where necessary. Figure 7 shows an example of a nucleophilic aromatic substitution of 1,2-di-fluoro-4-nitrobenzene by morpholine that was used by Jamison and co-worker as one of the separate 7 steps in the continuous flow synthesis of Linezolid. At the end of the process, they could isolate the target drug with a throughput of 0.816 $g \cdot h^{-1}$.

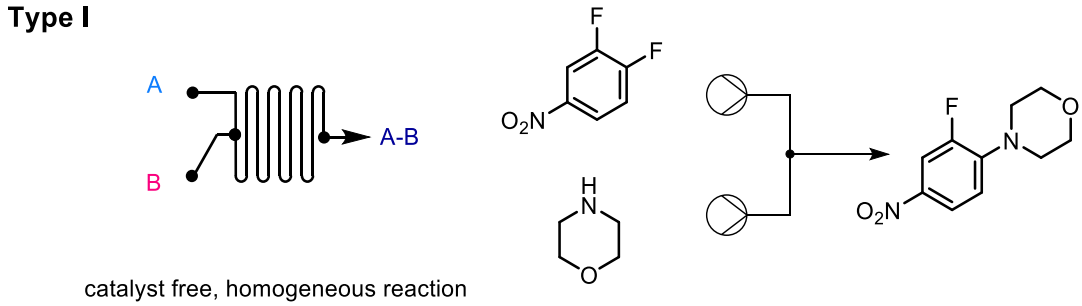

Figure 7. Type I flow reaction and an example of a homogeneous reaction.[51]

In a **Type II** flow process (Figure 8), one of the reagents is a solid and is kept inside a reactor, while the second reagent is flowed through it and the reaction happens by contact of both.

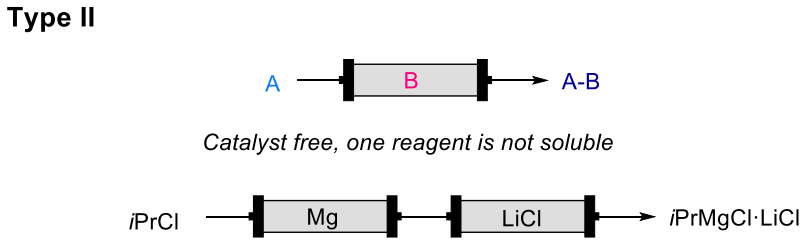

Figure 8. Type II flow reaction and the example of the synthesis of a turbo Grignard.[52]

In the illustrated example, the McQuade group demonstrated the preparation of turbo Grignard reagents by packing the column with solid magnesium and LiCl. An alkyl chloride was flowed through both columns to produce the desired organometallic species. This approach is not

[50] T. Tsubogo, H. Oyamada and S. Kobayashi, *Nature* **2015**, *520*, 329-332.
[51] M. G. Russel and T. F. Jamison, *Angew. Chem. Int. Ed.* **2019**, *131*, 7760-7763.
[52] M. Berton, K. Sheehan, A. Adamo and D. T. McQuade, *Beilstein J. Org. Chem.* **2020**, *16,* 1343–1356.

limited to these reagents. Apart from the latter, the Knochel-Hauser base,[53] common Grignards[54] and organozincates[55] have been prepared with this approach.

In contrast with the previous two types, **Type III** flow (Figure 9) is a catalytic reaction and all reactants and the catalyst are soluble. This type of flow is particularly advantageous when a photocatalytic reaction[56] is performed but is not limited to this. In the example reported in Figure 9, the Noël group developed a rather fast photocatalytic procedure (5 minutes residence time) for the acylation of strong aliphatic C-H bonds.

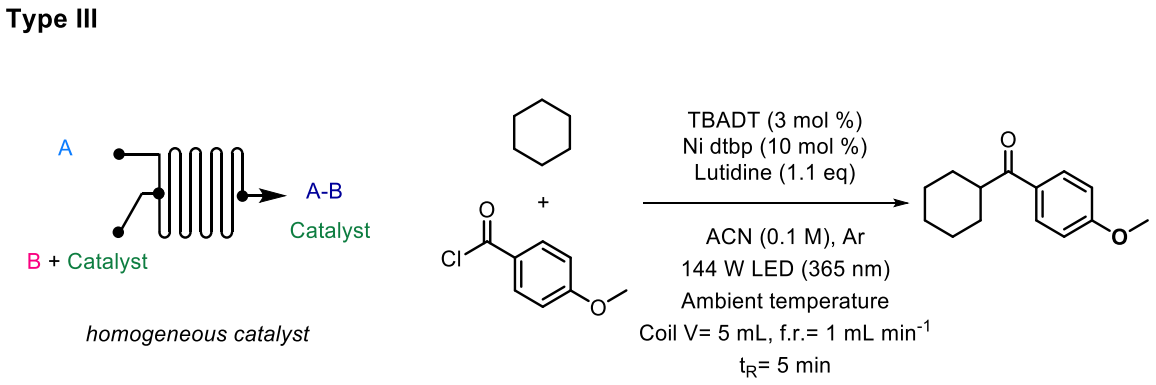

Figure 9. Type III flow process for the photocatalytic C(sp^3)-H acylation/arylation.[57]

Finally, the last type of flow is the one that is most relevant for the current thesis. A solid catalyst is packed in a reactor and the reagents, liquids and gases are passed through the catalytic bed. A common reaction, commonly carried out in flow set ups in many laboratories is a reduction reaction using H_2 as reductant and empowered by a heterogeneous catalyst such as Pd/C.[58]

The main difference and advantage of this type when compared to type III is that under ideal conditions the purification of the products is rather easy. Furthermore, the recycling of the catalyst makes this process ideal for the development of sustainable and efficient processes.[59]

---

53 A. Krasovskiy, V. Krasovskaya and P. Knochel, *Angew. Chem. Int. Ed*. **2006**, *45*, 2958–2961.

54 L. Huck, A. de la Hoz, A. Diaz-Ortiz and J. Alcazar, *Org. Lett.* **2017**, *19*, 3747–3750.

55 a) N. Alonso, L. Z. Miller, J. de M. Muñoz, J. Alcázar and D. T. McQuade, *Adv. Synth. Catal*. **2014**, *356*, 3737-3741 b) M. Berton, L. Huck and J. Alcazar, *Nat. Protoc.,* **2018**, *13*, 324-334.

56 a) L. Buglioni, F. Raymenants, A. Slattery, S. D. A. Zondag and T. Nöel, *Chem. Rev.* **2022**, 122, 2752–2906; b) C. Sambiagio and T. Nöel, *Trends Chem.* **2020**, *2*, 92-106; c) T. Nöel, *J. Flow Chem.* **2017**, *7*, 87–93.

57 D. Mazzarella, A. Pulcinella, L. Bovy, R. Broersma and T. Noël, *Angew. Chem. Int. Ed.* **2021**, *60*, 21277-21282.

58 a) S. Sharma, Y. Das and P. Das, *New J. Chem*. **2019**, *43*, 1764-1769; b) M. Baghbanzadeh, T. N. Glasnov and C. O. Kappe, *J. Flow Chem*. **2013**, *3*, 109–113; c) D. Cantillo, M. Baghbanzadeh and C. O. Kappe, *Angew. Chem. Int. Ed*. **2012**, *51*, 10190–10193; d) M. Irfan, T. N. Glasnov and C. O. Kappe, *ChemSusChem* **2011**, *4*, 300–316 e) T. Ouchi, C. Battilocchio, J. M. Hawkins and S. V. Ley, *Org. Process Res. Dev*. **2014**, *18*, 1560–1566; f) D. L. Riley and N. C. Neyt, *Synthesis* **2018**, *50*, 2707-2720.

59 a) P. T. Anastas, *Green Chemistry Textbook*; Oxford University Press: New York, **2004**; b) R. Porta, M. Benaglia and A. Puglisi, *Org. Process Res. Dev.* **2016**, *20*, 2–25 c) M. Baumann, T. S. Moody, M. Smyth and S. Wharry, *Org. Process Res. Dev.* **2020**, *24*, 1802–1813; d) B. Martin, H. Lehmann, H. Yang, L. Chen, X. Tian, J. Polenk and B. Schenkel, *Curr. Opin. Green Sustain. Chem.* **2018**, *11*, 27– 33.

For this reason, in the Pericàs Group we have been not only interested in developing new organocatalysts,[60] but also their application under continuous flow operation.[61]

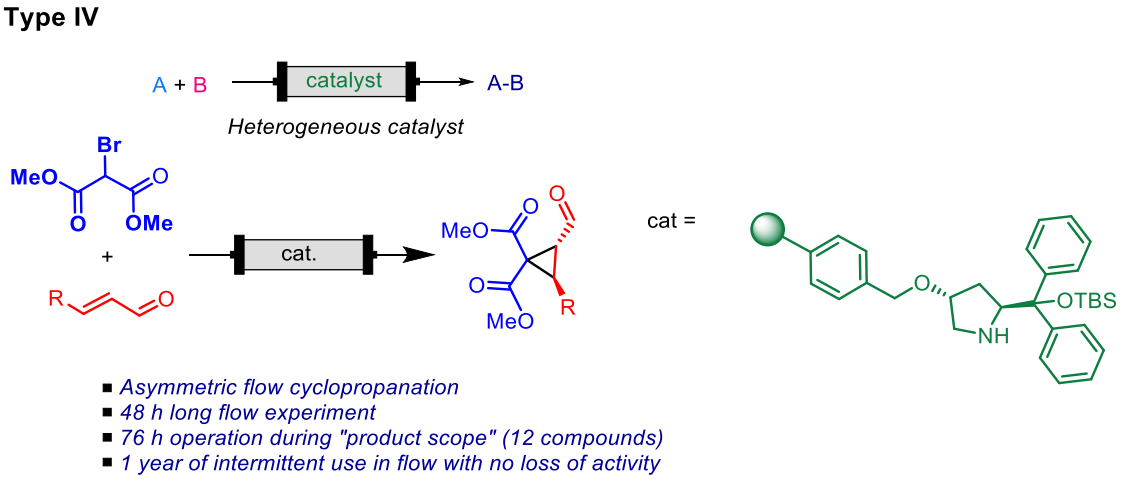

Figure 10. Type IV flow and organocatalytic enantioselective continuous-flow cyclopropanation.[62]

In Figure 10, one example is reported how a solid-supported diarylprolinol organocatalyst could be used for a cyclopropanation reaction. It has to be noted that once the catalyst was charged in the reactor it was not removed and, therefore, it was possible to do not only the optimization of the reaction conditions, a 48-h continuous flow experiment but also the synthesis of a scope of 12 compounds. Furthermore, the catalyst isolated inside the reactor could be used over a period of one year without observable deactivation.
In a perfect **Type IV** system as the above-mentioned example, the eluting stream is not contaminated by the catalyst and the immobilized catalyst retains its activity. This simplifies eventual inline purification steps to remove possible byproducts or reagents used in excess, and creates a perfect approach for a multistep synthesis. In this respect, the synthesis of Rolipram reported by the Kobayashi group shows the effectiveness of this approach.[50]

[60] a) S. Cañellas, P. Alonso and M. A. Pericàs, *Org. Lett.* **2018**, *20*, 4806–4810; b) P. Etayo, E. C. Escudero-Adán and M. A. Pericàs, *Catal. Sci. Technol.* **2017**, *7*, 4830-4841; c) P. Etayo, C. Ayats and M. A. Pericàs, *Chem. Commun.* **2016**, *52*, 1997-2010.
[61] a) J. Lai, M. Fianchini and M. A. Pericàs, *ACS Catal.* **2020**, *10*, 14971-14983; b) J. Lai, R. M. Neyyappadath, A. D. Smith and M. A. Pericàs, *Adv. Synth. Catal.* **2020**, *362*, 1370-1377; c) S. Cañellas, C. Ayats, A. H. Henseler and M. A. Pericàs, *ACS Catal.* **2017**, *7*, 1383-1391; d) J. Izquierdo and M. A. Pericàs, *ACS Catal.* **2016**, *6*, 348-356.
[62] P. Llanes, C. Rodríguez-Escrich, S. Sayalero and M. A. Pericàs, *Org. Lett.* **2016**, *18,* 6292–6295.

1.5 Thesis aim and outline

CO_2 has become a relevant and versatile chemical in synthetic organic chemistry replacing conventional carbon feedstock such as (tri)phosgene and related chemicals. Its use in the preparation of heterocyclic structures has matured significantly over the last decade and will undoubtedly continue to inspire the synthetic communities devising new types of reductive and non-reductive transformations. Due to its high kinetic stability, the most successful methodologies take advantage of metal catalysis and high reaction temperatures, while high energy reagents help to overcome the thermodynamic challenge. Organocatalysts represent potential sustainable alternatives to metal catalysts offering cheap, accessible and modular structures.

A merger between organocatalysis and flow chemistry is an appealing approach to increase the sustainability of a chemical process and its scalability, thus making it more attractive for future commercial applications. We noted that at the start of this thesis work that the use of CO_2 as a reagent in combination with a heterogeneous organocatalyst under flow operation was severely underdeveloped. Therefore, the **main objective of this doctoral thesis** was the design and development of heterogeneous organocatalytic processes that can be used to valorize CO_2 under (mild) continuous flow conditions thereby offering also scalability. In particular, we have focused on processes that either can avoid the use of potentially corrosive additives (halides) and offer simple separation between the product(s) and reagents.

In **Chapter 2**, we describe a supported organocatalyst (TBD@PS) that can be used as a single-component system for the activation of CO_2. The synthesis of glycerol carbonate was selected as target, with the supported *N*-heterocyclic base TBD allowing the coupling of glycidol and CO_2 under comparative mild reaction conditions. With this catalyst design, we took advantage over the swelling properties of the low-crosslinked polystyrene resin, and the continuous flow system could be operated under stable conditions for at least 48 h thereby preparing 147 mmol of glycerol carbonate (17.3 g) without any noticeable loss of catalytic performance or leaching.

In **Chapter 3**, we aimed to extent the synthesis of heterocyclic products (i.e., from carbonates to oxazolidinones) with a single-component supported (TBD) organocatalyst. Using a non-swellable catalyst, we targeted the selective synthesis of 2-substituted oxazolidinones from readily accessible epoxy amines and CO_2. The continuous flow system proved to be stable for several weeks during which a small library of 16 oxazolidinone scaffolds could be prepared. Furthermore, a sequential synthesis of 7 distinct oxazolidines were prepared by switching alternately the feed from “substrate” to “solvent” showing the approach to have potential in drug discovery/development programs.

In **Chapter 4**, we describe for the first time the use of a heterogeneous organocatalyst in the selective formylation of various amines providing *N*-formamides. Cheap and accessible trimethoxy silane was used as a reducing agent and the continuous flow process allowed to prepare a series of *N*-formamides in batch mode, which was extended to a longer-run flow synthesis of 450 minutes preparing a selected target compound with a productivity of 2.32 mmol h^{-1}.

Chapter 2: Organocatalytic and Halide-Free Synthesis of Glycerol Carbonate under Continuous Flow

The results described in this chapter have been published in:

N. Zanda, A. Sobolewska, E. Alza, A. W. Kleij and Miquel À. Pericàs *ACS Sustainable Chem. Eng.* **2021**, *9*, 4391−4397.

2.1 Introduction

2.1.1 CO_2 valorization and cycloaddition to epoxides

Contemporary research in carbon dioxide (CO_2) valorization catalysis has offered a plethora of new transformations towards products with value in fine chemical synthesis [1-4] pharmaceutical development [5,6] and polymer science.[7-10] CO_2 is cheap and widely available, though highly stable and thus much less reactive compared to other C_1 sources.

Without a doubt, nonreductive catalytic conversions of CO_2 are among the most widely studied transformations in the area of CO_2 catalysis. In these reactions, the thermodynamic challenge posed by this carbon feedstock is met by using higher-energy reactants such as organometallic reagents (such as organolithiums, Grignards and zincates)[11,2] or strained molecules. In this regard, cyclic ethers (epoxides, oxetanes and aziridines) are the most common reaction partners reported in nonreductive CO_2 catalysis and offer productive routes to heterocyclic[12-14] and polymeric products.[15,16] The chemoselectivity in these processes is often dictated by the nature of the catalyst and a detailed mechanistic understanding[17] of the reaction is vital to optimize the overall performance. Hence, In the last years efforts were made to unravel structure-activity relationships of both metal-based and metal-free catalysts. These data allow to benchmark catalytic performances more accurately.[18]

Thus, considering the well-established nature of the catalytic cycloaddition of CO_2 to epoxides giving cyclic carbonates as products, recent attention has shifted from classical catalyst development to increasing process sustainability.[19]

---

1 J. Artz, T. Müller, K. Thenert, J. Kleinekorte, R. meys, A. Sternberg, A. Bardow and W. Leitner, *Chem. Rev.* **2018**, *118,* 434-504.
2 Q. Liu, L. Wu, R. Jackstell and M. Beller, *Nat. Comm.* **2015**, *6,* 5933-5948.
3 J. Vaitla, Y. Guttormosen, J. K. Mannisto, A. Nova, T. Repo, A. Bayer and K. H. Hopman, *ACS Catal.* **2017**, *7,* 7231-7244.
4 Q.-W Song, Z.-H Zhou and L.-N He, *Green. Chem.* **2017**, *19,* 3707-3728.
5 W. Guo, V. Laserna, J. Rintjema and A. W. Kleij, *Adv. Synth. Catal.* **2016**, *358,* 1602-1607.
6 À. Cristofòl, C. Böhmer and A. W. Kleij, *Chem. – Eur. J.* **2019**, *25,* 15055-15058.
7 M. I. Childers, J. M. Longo, N. J. Van Zee, A. M. LaPointe and G. W. Coates, *Chem. Rev.* **2014**, *114,* 8129-8152.
8 B. Grignard, S. Gennen, C. Jérôme, A. W. Kleij and C. Detrembleur, *Chem. Soc. Rev.* **2019**, *48*, 4466– 4514.
9 A. K. Kamphuis, F. Picchioni and P. P. Pescarmona, *Green Chem.* **2019**, *21*, 406–448.
10. Y. Y. Wang and D. J. Darensbourg, *Coord. Chem. Rev.* **2018**, *372*, 85–100.
11 K. Huang, C.-L. Sun and Z.-J. Shi, *Chem. Soc. Rev.*, **2011**, *40*, 2435-2452.
12 S. Wang and C. Xi, *Chem. Soc. Rev.* **2019**, *48*, 382–404.
13 B. Yu and L.-N He, *ChemSusChem* **2015**, *8*, 52–62.
14 S. Dabral and T Schaub, *Adv. Synth. Catal.* **2019**, *361*, 223– 246.
15 S. Paul, Y. Zhu, C. Romain, R. Brooks, P. K. Saini and C. K. Williams, *Chem. Commun.* **2015**, *51*, 6459–6479.
16 M. Scharfenberg, J. Hilf and H. Frey, *Adv. Funct. Mater.* **2018**, *28*, 1704302.
17 F. Della Monica and A. W. Kleij, *Catal. Sci. Technol.* **2020**, *10*, 3483–3501.
18 a) P. Yingcharoen, C. Kongtes, S. Arayachukiat, K. Suvarnapunya, S. V. C. Vummaleti, S. Wannakao, L. Cavallo, A. Poater and V. D' Elia, *Adv. Synth. Catal.* **2019**, *361*, 366–373; b) C. J. Whiteoak, A. Nova, F. Maseras and A. W. Kleij, *ChemSusChem* **2012**, *5*, 2032– 2038; c) M. Alves, B. Grignard, R. Mereau, C. Jerome, T. Tassaing and C. Detrembleur, *Catal. Sci. Technol.* **2017**, *7*, 2651–2684; d) J. Rintjema and A. W. Kleij, *ChemSusChem* **2017**, *10*, 1274–1282.
19 a) R. R. Shaikh, S. Pornpraprom and V. D'Elia, *ACS Catal.* **2018**, *8*, 419–450; b) J. W. Comerford, I. D. V. Ingram, M. North and X. Wu, *Green Chem.* **2015**, *17*, 1966–1987; c) C. Martín, G. Fiorani, A. W. Kleij, *ACS Catal.* **2015**, *5*, 1353–1370.
20 a) J. A. Castro-Osma, K. J. Lamb and M. North, *ACS Catal.* **2016**, *6*, 5012–5025; b) F. Liu, Y. Gu, P. Zhao, J. Gao and M. Liu, *ACS Sustainable Chem. Eng.* **2019**, *7*, 5940–5945; c) A. Decortes and A. W. Kleij, *ChemCatChem* **2011**, *3*, 831–834.

In these sustainable approaches, parameters like reaction temperature and pressure have played an important role over the years[20] but a more recent development is the use of organocatalysts[18c,21] and halide-free systems[22,23] for the preparation of cyclic carbonates.

2.1.2 CO_2 valorization and cycloaddition to epoxides in continuous flow

Flow chemistry is a recently added, efficient tool to increase the sustainability of a process[24] and notably great progress has been made in recent years in the continuous flow preparation of cyclic carbonates. However, in all these contributions reported in the literature, the catalytic system consisted of a metal- and/or halide-based system.[25]

A recent and important development was reported by Jamison *et al*. They demonstrated the effective use of a combination of simple *N*-bromo-succinimide (NBS) and benzoyl peroxide as a binary homogeneous organocatalyst at elevated temperature (120 ºC).[26] In a separate study, the same authors reported a stoichiometric approach for the two-step transformation of several alkenes into their respective cyclic carbonates.[27]

Of particular relevance is the work reported by Young.[25a] Aluminum(salen) complexes combined with a halogen co-catalyst incorporated into the ligand framework, were supported onto silica and these could efficiently promote the formation of ethylene carbonate. This bifunctional catalyst showed over time some degree of deactivation by leaching of bromide. Even though the catalyst could be reactivated, the leached bromide contaminated the eluting stream containing the product. The same group also demonstrated the possible use of flue gas for the synthesis of cyclic carbonates.[25b]

---

[21] a) Y. Hu, S. Peglow, L. Longwitz, M. Frank, J. D. Epping, V. Brueser and T. Werner, *ChemSusChem* **2020**, *13*, 1825–1833; b) M. Cokoja, M. E. Wilhelm, M. H. Anthofer, W. A. Herrmann and F. E. Kühn, *ChemSusChem* **2015**, *8*, 2436–2454; c) G. Fiorani, W. Guo and A. W. Kleij, *Green Chem.* **2015**, *17*, 1375–1389.

[22] X. Wu, C. Chen, Z. Guo, M. North and A. C. Whitwood, *ACS Catal.* **2019**, *9*, 1895–1906.

[23] S. Sopeña, M. Cozzolino, C. Maquilón, E. C. Escudero-Adán, M. Martínez Belmonte and A. W. Kleij, *Angew. Chem., Int. Ed.* **2018**, *57*, 11203–11207.

[24] M. B. Plutschack, B. Pieber, K. Gilmore and P. H. Seeberger, *Chem. Rev.* **2017**, *117*, 18, 11796–11893.

[25] a) M. North, P. Villuendas and C. Young, *Chem. - Eur. J.* **2009**, *15*, 11454–11457; b) M. North, B. Wang and C. Young, *Energy Environ. Sci.* **2011**, *4*, 4163–4170; c) X. Wu, M. Wang, Y. Xie, C. Chen, K. Li, M. Yuan, X. Zhao and Z. Hou, *Appl. Catal., A* **2016**, *519*, 146–154; d) A. Rehman, A. M. Lopez Fernandez, M. F. M. G. Resul and A. Harvey, *J. CO_2 Util.* **2018**, *24*, 341–349; e) L. Guo, L. Deng, X. Jin, Y. Wang and H. Wang, *RSC Adv.* **2018**, *8*, 26554–26562; f) B. R. James, J. A. Boissonnault, A. G. Wong-Foy, A. J. Matzger and M. S. Sanford, *RSC Adv.* **2018**, *8*, 2132–2137; g) A. A. Sathe, A. M. K. Nambiar, R. M. Rioux, *Catal. Sci. Technol.* **2017**, *7*, 84–89.

[26] J. A. Kozak, J. Wu, X. Su, F. Simeon, T. A. Hatton and T. F. Jamison, *J. Am. Chem. Soc.* **2013**, *135*, 18497–18501.

[27] J. Wu, J. A. Kozak, F. Simeon, T. A. Hatton and T. F. Jamison, *Chem. Sci.* **2014**, *5*, 1227–1231.

2.1.3 Aims and objectives

Our group has become interested in the development of new approaches for CO_2 activation and conversion into heterocyclic products through conceptually distinct substrate-controlled reactivity. In these manifolds, the substrate contains apart from an oxirane unit a second functional group (typically an alcohol or amine group) that activates CO_2 to form a carbonic/carbamic acid hemi-ester intermediate with increased nucleophilicity. This formal proton relay event allows for intramolecular attack on the oxirane providing the heterocyclic target under essentially halide-free conditions (Scheme 1).[23,28]

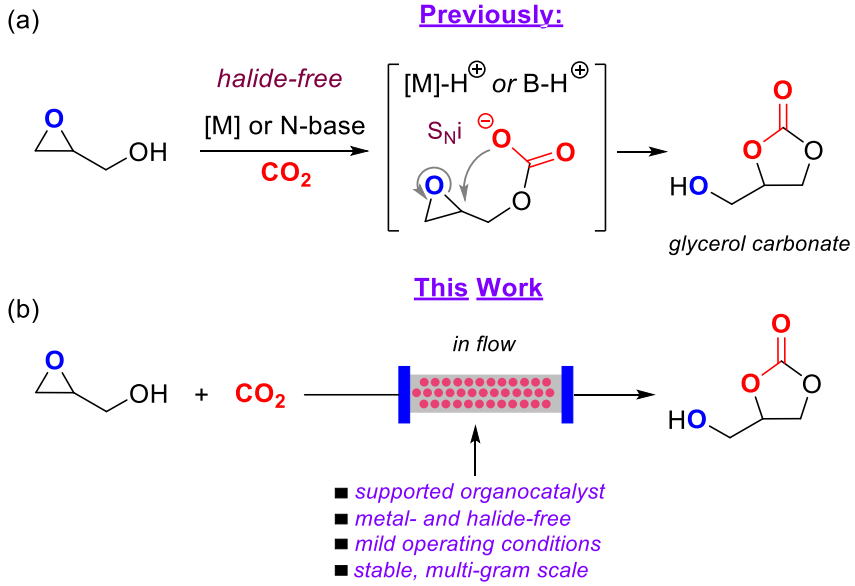

Scheme 1. Overall approach towards the synthesis of glycerol carbonate using an immobilized organocatalyst.

Inspired by the apparent limitation in catalyst development in the context of continuous flow operation, we anticipated that a proper immobilization of an appropriate catalyst with substrate activation potential could offer an appealing strategy to design a continuous flow synthesis of cyclic carbonates under mild metal- and halide-free conditions (Scheme 1b).

Among the known cyclic carbonates, glycerol carbonate (GC) stands out as it represents a valuable and versatile bifunctional building block in polymer and small molecule synthesis, and biomedical applications.[28] Therefore, by merging substrate-assisted CO_2 conversion with organocatalytic flow processes,[29] we envisioned that we could develop a heterogeneous

---

[28] a) W. Natongchai, J. A. Luque-Urrutia, C. Phungpanya, M. Solà, V. D'Elia, A. Poater and H. Zipse, *Org. Chem. Front.* **2021**, *8*, 613–627; b) J. Rintjema, R. Epping, G. Fiorani, E. Martín, E. C. Escudero-Adán and A. W. Kleij, *Angew. Chem. Int. Ed.* **2016**, *55*, 3972–3976; c) R. Huang, J. Rintjema, J. González-Fabra, E. Martín, E. C. Escudero-Adán, C. Bo, A. Urakawa and A. W. Kleij, *Nat. Catal.* **2019**, *2*, 62–70; d) C. Qiao, A. Villar-Yanez, J. Sprachmann, B. Limburg, C. Bo and A. W. Kleij, *Angew. Chem., Int. Ed.* **2020**, *59*, 18446–18451.

[29] a) S. Christy, A. Noschese, M. Lomelí-Rodriguez, N. Greeves and J. A. Lopez-Sanchez, *Curr. Opin. Green Sustain. Chem.* **2018**, *14*, 99–107; b) G. Fiorani, A. Perosa and M. Selva, *Green Chem.* **2018**, *20*, 288–322.

[30] a) S. Cañellas, C. Ayats, A. H. Henseler and M. A. Pericàs, *ACS Catal.* **2017**, *7*, 1383–1391; b) R. M. Neyyappadath, R. Chisholm, M. D. Greenhalgh, C. Rodríguez-Escrich, M. A. Pericàs, G. Hähner and A. D. Smith, *ACS Catal.* **2018**, *8*, 1067–1075; c) N. R. Guha, R. M. Neyyappadath, M. D. Greenhalgh, R. Chisholm, S. M. Smith, M. L. McEvoy, C. M. Young, C. Rodriguez-Escrich, M. A. Pericas, G. Hahner and A. D. Smith, *Green Chem.* **2018**, *20*, 4537–4546; d) S. B. Ötvös, P. Llanes, M. A. Pericàs, and O. C. Kappe, *Org. Lett.* **2020**, *22*, 8122–8126.

catalytic process under attractive and stable flow conditions[30] to prepare GC in relevant quantities and purity.

2.2 Results and discussion

2.2.1 Catalyst design and batch reactions

With these ideas in mind, we have recently developed two types of organocatalysts for the efficient conversion of epoxides and CO_2 into cyclic carbonates. They were based on resorcin[4]arene[31] and pyrogallol[32] and both of them were successfully supported onto polystyrene based beads, easily recyclable and reusable. With these bifunctional catalytic systems, the coupling between various epoxides and CO_2 could be promoted to afford various mono- and disubstituted cyclic organic carbonates.

These bifunctional catalysts, based on a halide nucleophile, provided us a blueprint for the development of a suitable continuous flow catalyst system for the synthesis of GC. Related to our envisioned design, Sartorio and co-workers previously reported that 1,5,7-triazabicyclodec-5-ene (TBD) supported on mesoporous silica (MCM41) provides a bifunctional catalyst with both TBD and silanols as active species for the coupling of various epoxides and CO_2. However, these reactions proceeded only under harsh conditions (140 ºC, 50 bar CO_2) and required long reaction times of up to 70 h. This can be explained by the slow diffusion of the reactants into the mesoporous catalyst structure.[33]

We envisioned that employing a polystyrene (PS) based organocatalyst could avoid these diffusion related limitations and, by using an appropriate anchoring strategy, could offer a cheap and modular system for catalyst optimization.

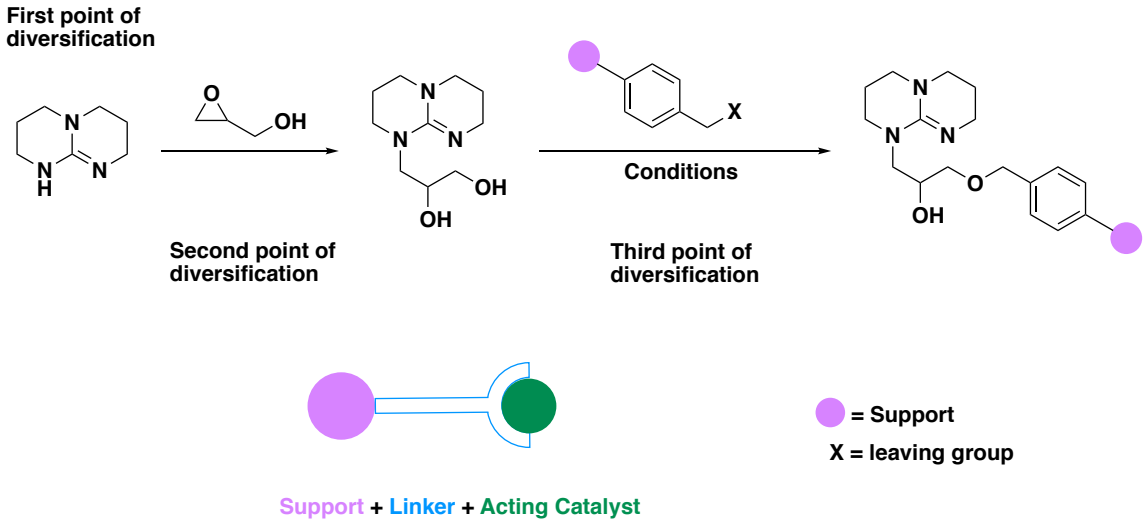

Figure 1. Catalyst design strategy.

The approach towards the catalyst structure was designed to be divergent, giving access to a three-component type catalyst containing an inert support, a linker and the module containing the active site displaying thus a high degree of variability. The first step (Figure 1) was the

[31] T. Jose, S. Cañellas, M. A. Pericàs and A. W. Kleij, *Green Chem.* **2017**, *19*, 5488–5493.
[32] C. J. Whiteoak, A. H. Henseler, C. Ayats, A. W. Kleij and M. A. Pericàs, *Green Chem.* **2014**, *16*, 1552–1559.
[33] A. Barbarini, R. Maggi, A. Mazzacani, G. Mori, G. Sartori and R. Sartorio, *Tetrahedron Lett.* **2003**, *44*, 2931–2934.

aminolysis of glycidol by TBD, and the as-generated monomer can then be anchored onto various polystyrene based supports. Thus, several TBD-supported catalysts became accessible through this preparation (see the Experimental Section and Figure 2), and their activity was tested and compared with other types of heterogeneous organocatalysts.

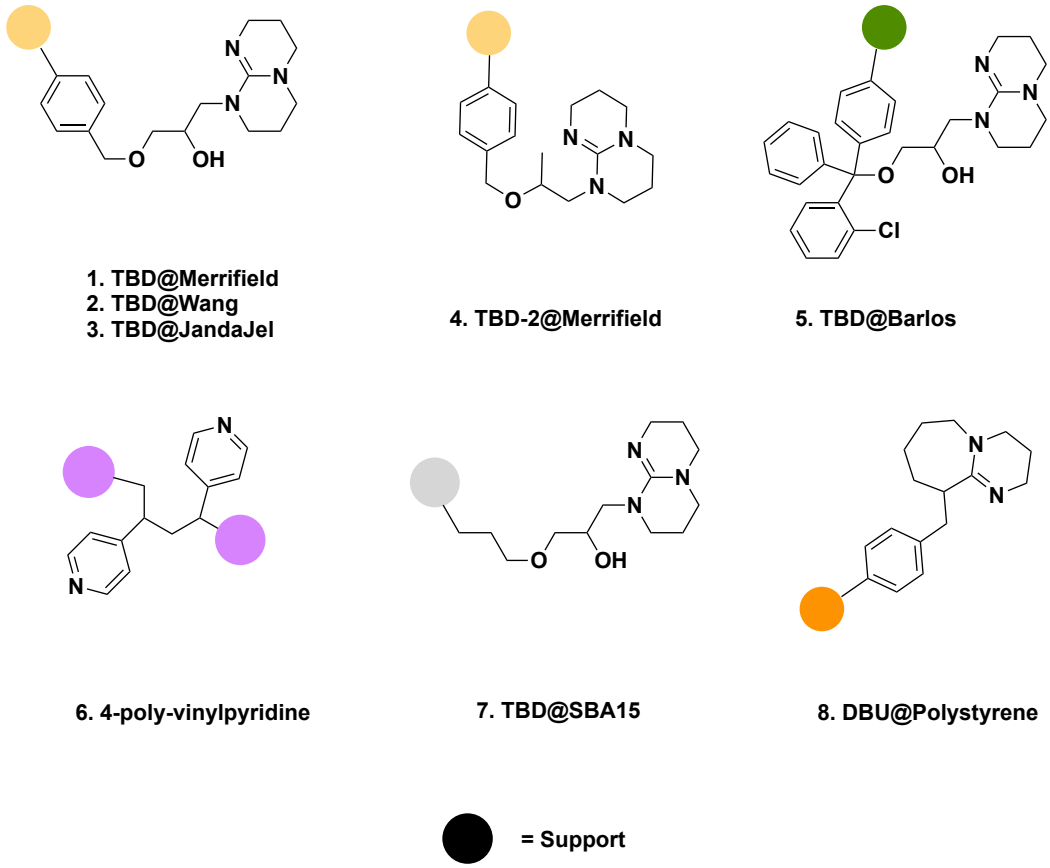

Figure 2. Structures of the heterogeneous catalysts and their corresponding supports used for the catalytic studies.

To gain meaningful and transferable knowledge from batch to continuous flow conditions we chose to run the screening experiments on an AMTECH SPR16 multiphase parallel reactor. An important feature of this system is that it allows to run parallel reactions at a constant pressure (isobaric mode) as would also be desired in a flow reactor set up.

The catalyst screening was carried out using glycidol as substrate. Initially, the carbon dioxide inlet pressure, reaction temperature and substrate concentration were optimized providing a starting point for the comparison between the various supported organocatalysts. The reaction set up performed best under neat conditions and much worse in a solvent (i.e., under diluted conditions, Table 1).

Table 1. Effect of the glycidol concentration in the synthesis of GC.[a]

Entry	Concentration (mol/L)	^{1}H NMR yield (%)	Glycerol (%)
1	neat	95	5
2	3.33	91	–
3	1.67	82	7
4	0.83	66	–

[a] 5 bar CO_2 (isobaric conditions), glycidol in methyl ethyl ketone (MEK), glycidol (1.0 mmol), catalyst **1** (0.30 mmol), 70 ºC, 18 h. Durene was used as an internal NMR standard.

Table 2. Batch screening of the influence of the reaction temperature.[a]

Entry	Temperature (ºC)	^{1}H NMR yield (%)	Glycerol (%)
1	50	28	0
2	60	58	0
3	70	78	7
4	80	76[b]	16

[a] 5 bar CO_2 (isobaric conditions), 1.8 M glycidol in methyl ethyl ketone (MEK), glycidol (1.0 mmol), catalyst **1** (0.30 mmol), 18 h. Durene was used as an internal NMR standard. [b] At higher temperature, hydrolysis of either glycidol or glycerol carbonate becomes an issue giving glycerol as by-product.

The screening of the reaction temperature (Table 2) gave us information about the formation of glycerol, which appears to be the main side reaction. While increasing the temperature was favorable for the formation of GC, at the same time it also increased the amount of glycerol by-product. As a compromise between attractive process kinetics and process selectivity, a temperature of 70 ºC was selected for further studies (see below).

Having assessed the effect of temperature and concentration, we ran a screening of the various heterogeneous catalysts (Figure 2) using a 1.8 M solution of glycidol (1 mmol) in MEK, 70 ºC as operating temperature and a catalyst loading of 0.30 mmol.

Table 3. Batch screening of the influence of the catalyst in the formation of GC.[a]

Entry	Catalyst	^{1}H NMR yield (%)	Glycerol (%)
1	TBD@Merrifield, **1**	82	7
2[b]	TBD@Merrifield, **1**	88	4
3	TBD@Wang, **2**	72	6
4	TBD@JandaJel, **3**	77	6
5	TBD-2@Merrifield, **4**	79	4
6	TBD@Barlos, **5**	73	5
7	4-polyvinylpyridine, **6**	56	22
8	TBD@SBA15, **7**	83	<1
9	DBU@polystyrene, **8**	80	4
10	MTBD	95	3
11	–	0	0

[a] 5 bar CO_2 (isobaric conditions), 1.8 M glycidol in methyl ethyl ketone (MEK), glycidol (1.0 mmol), catalyst 0.30 mmol %, 70ºC ,18 h. Durene was used as internal NMR standard. [b] Using dry MEK.

Based on our previous work using TBD or DBU as a homogeneous catalyst,[23,28c] we selected the supported organocatalysts (**1-8**) shown in Figure 2, derived from these *N*-heterocyclic bases. For comparison purposes the pyridine-supported system (**6**) was also included in the screening. The comparative performances of **1-8** demonstrated that both TBD- and DBU-based catalysts are productive systems with overall high substrate conversion, and high selectivity for GC. Merrifield-supported TBD appeared to be one of the most efficient ones (Table 3, entries 1 and 2) providing up to 88% yield of the carbonate product, whereas the presence of other supported catalyst gave somewhat inferior results (entries 2-9), with the supported pyridine catalyst being markedly less active.

The use of an anhydrous solvent (entry 2 versus entry 1) provided a bit higher chemoselectivity with smaller amounts of glycerol byproduct formed as a result of epoxide hydrolysis under the experimental conditions. Importantly, we also tested MTBD (*N*-methyl-TBD) as a homogeneous reference system, which provided as expected a higher substrate conversion and yield of product. Among the immobilized species, the catalyst system TBD@Merrifield **1** exhibited the best performance, with only marginal decrease in performance with respect to the homogeneous reference (compare entries 2 and 9). Thus, this system was finally selected as the preferred heterogeneous catalysts for developing a continuous flow process.

2.2.2 Continuous flow set-up

We next turned our focus towards the design of an appropriate flow system that could exploit the properties of catalyst **1**. The schematic set-up of the continuous flow system is illustrated in Scheme 2 (for a picture of the setup, see the experimental section).

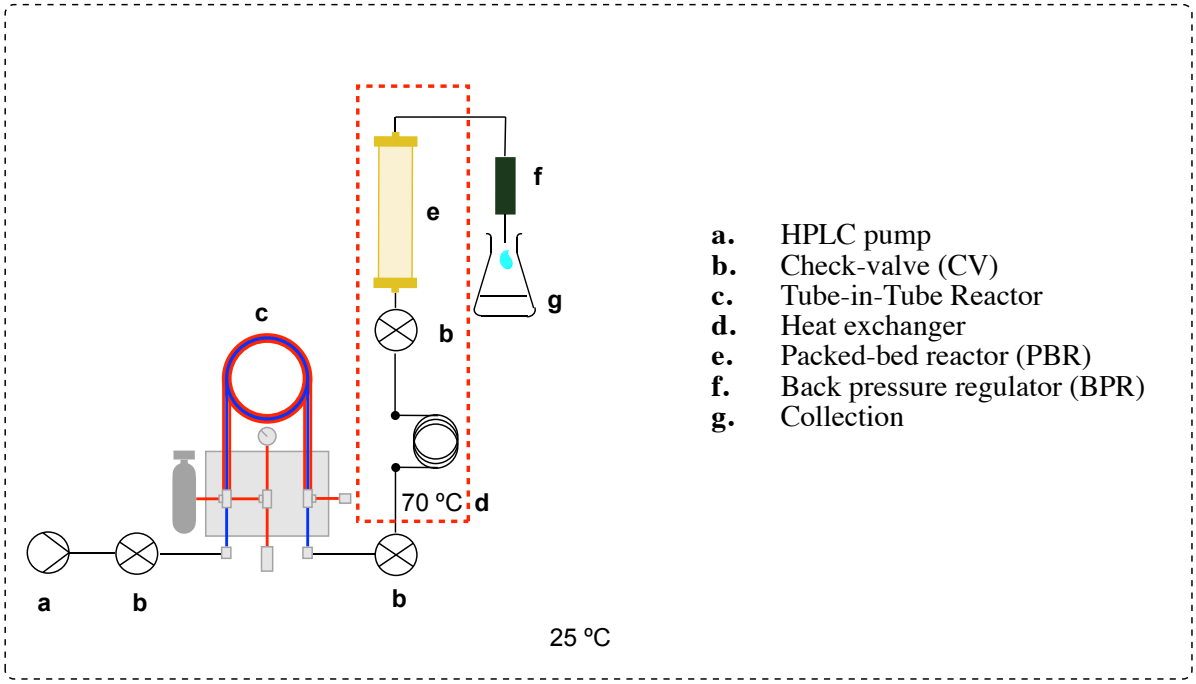

Scheme 2. Schematic diagram of the flow setup

In our design, the feed of starting material (glycidol) dissolved in methyl ethyl ketone (MEK) was provided by a Knauer Azura P4.1 pump with an integrated pressure sensor (a). The feed was flowed through a check-valve (CV, b) into the tube-in-tube reactor (T-i-T, c = 0.6 mL inner tube volume), employed in the traditional configuration, where it was saturated in CO_2 and passed through a second CV into a 1.0 mL pre-heating coil warmed to 70 ºC by an oil bath. The reactant stream was then passed through a third CV into the packed bed reactor (PBR, e), which was used in the up-flow configuration. The PBR was assembled using a Diba Omnifit® SolventPlus™ volum-adjustable column, equipped with Chemraz O-rings resistant to the reaction media. The column was kept at the desired temperature by a hermetically adapted glass external jacket heated by circulation of an oil stream provided by a Julabo oil heater. The jacketed glass reactor and all the tubing subject to heating were additionally insulated by external coating with glass wool, epoxy resin and aluminum tape. Finally, a back-pressure regulator (BPR) from IDEX was used to pressurize the system. The liquid stream was finally collected in an Erlenmeyer from which the samples were taken and analyzed by ^{1}H NMR spectroscopy.

To show the suitability of our setup for the selected catalytic system (TBD@Merrifield **1**), we first carried out a stability test. The purpose of this was to examine in which manner and to what extent the applied pressure would change the nature of the supported, swollen catalyst. The results provided in Table 4 demonstrate that a stable gel structure could be maintained when the pressure inside the tube-in-tube reactor (outer tube region) was in the range of 3-8 bar and at 60-70 ºC while operating the back-pressure regulator at 13.3-17.2 bar.

Table 4. Results of the physical stability test for catalyst **1**.[a]

Entry	T (ºC)	CO_2 in T-i-T (bar)	BPR (bar)	PBR
1	rt	8	8	gel
2	50	8	8	dry
3	60	8	8	dry
4[b]	70	–	8	gel
5	r.t.	8	17.2	gel
6	60	8	17.2	gel
7	70	8	17.3	gel
8[c]	70	3	13.4	gel

[a] The PBR was equipped with 800 mg of catalyst. The system was tested flowing MEK at 0.11 mL/min, τ 30 min, at a constant pressure of CO_2 of 8 bar in the tube-in-tube reactor. The system was operated for 4 h and then visually checked. [b] This experiment, in the absence of CO_2, was performed to exclude that MEK was responsible for drying of the reactor. [c] This experiment was performed as a test for the long-run flow catalysis. Since we decreased the pressure of CO_2 down to 3 bar, it was possible to decrease the overall pressure of the system through a lower BPR, which was followed the general trend of CO_2 solubility in 2-butanone (MEK) reported by Gui.[34]

The potential of swellable catalysts can be fully exploited when they are maximally swollen, exposing the highest possible number of active sites to the reaction media. Our tests confirmed that the pressure approximations from Henry's law could be applied. Under inadequate conditions of pressure and temperature, the catalyst could lose its gel structure (i.e., drying), which may result from a reduction of CO_2 dissolved into the solution phase resulting into a biphasic (gas and liquid) flow. Therefore, we performed these experiments under conditions assuring that catalyst **1** was acting in a gel-phase and that there was no out-gassing of CO_2 while heating.

2.2.3 Continuous flow process optimization

To optimize the performance of the flow system illustrated in Scheme 2, several reactions under continuous flow were conducted primarily focusing on the glycidol conversion and productivity (Table 5). The residence time (τ) had an obvious influence on both parameters with the glycidol conversion increasing from 36 to 76% (entries 1-3), though a longer residence was not necessarily beneficial for the catalyst productivity. To balance both τ and the catalyst productivity, increasing the amount of catalyst **1** in the PBR was probed while varying the flow rate, the volume of the PBR and the substrate feed concentration (entries 4-12). The best glycidol conversion (>99%, entry 10) was attained combining a τ of 45 min with a substrate feed concentration of 0.22 mol/L resulting in a GC throughput of 1.201 mmol/h and a catalyst productivity of 1.52 mmol of GC/mmol of **1**. Further attempts were done to increase this throughput (entries 13-15) showing that by lowering the CO_2 pressure in the outer region of the tube-in-tube reactor, increasing the catalyst amount (1.59 g, 1.48 mmol) and volume of the

[34] X. Gui, Z. Tang and W. Fei, *J. Chem. Eng. Data* **2011**, *56*, 2420-2429.

PBR (4.65 mL), and having a substrate feed concentration of 0.33 mol/L, virtually complete glycidol conversion was achieved with a 30 min residence time. The GC throughput under these latter conditions was also substantially higher (entry 15, 3.04 mmol/h) and the BPR settings could be lowered to 194 psi (= 13.3 bar) while performing the reaction at 70 ºC.

Table 5. Optimization of the continuous flow reaction conditions for the synthesis of glycerol carbonate using (**1**).[a]

Entry	pCO_2 (bar)	BPR (psi)	Cat. **1** (mmol)	Flow rate (mL/min)	PBR (mL)	τ (min)	[Feed][b]	Conv. (%)[b]	GC[c] (mmol)	P[d]
1	8	250	0.17	0.089	2.67	30	0.14	36	0.269	1.58
2	8	250	0.17	0.059	2.67	45	0.14	65	0.322	1.89
3	8	250	0.17	0.045	2.67	60	0.14	76	0.287	1.69
4	8	250	0.17	0.089	2.67	30	0.07	36	0.135	0.79
5	8	250	0.17	0.059	2.67	45	0.07	65	0.161	0.95
6	8	250	0.28	0.059	4.71	45	0.13	59	0.272	0.97
7	8	250	0.28	0.053	4.71	90	0.13	84	0.347	1.24
8	8	250	0.28	0.105	4.71	45	0.22	59	0.810	2.92
9	8	250	0.28	0.053	4.71	90	0.23	78	0.570	2.04
10	8	250	0.79	0.091	4.08	45	0.22	>99	1.201	1.52
11	8	250	0.79	0.204	4.08	20	0.22	89	2.397	3.03
12	8	250	0.79	0.136	4.08	30	0.22	93	1.670	2.11
13	5	250	0.79	0.136	4.08	30	0.22	95	1.705	2.15
14	3	250	0.79	0.136	4.08	30	0.22	90	1.616	2.04
15	**3**	**194**	**1.48**	**0.155**	**4.65**	**30**	**0.33**	**99**	**3.038**	**2.05**
16[e]	8	250	0.28	0.122	5.50	45	0.21	31	0.477	1.70
17[f]	8	250	0.28	0.075	3.77	45	0.24	55	0.594	2.86

[a] Typical conditions unless stated otherwise: pCO_2 (isobaric) in the outer-region of the tube-in-tube reactor, MEK, 70 ºC, **1** as catalyst (entries 1-9, 16 +17: f_{exp} = 0.307 mmol/g; entries 10-14: f_{exp} = 0.740 mmol/g; entry 15: f_{exp} = 0.933 mmol/g), 250 psi = 17.2 bar, BPR = back pressure regulator, PBR = packed back reactor, τ = residence time. [b] The [feed] refers to the concentration of the glycidol feed (mol/L), and the conversion is at steady state conditions. [c] GC produced per hour (mmol/h). [d] P is productivity expressed as mmol of produced GC per mmol of catalysts per hour (mmol/(h·mmol**1**)). [e] Using 2-methyl-THF as solvent. [f] Using ethyl acetate as solvent

We considered that a conversion around 90% at a 0.22 M substrate feed (cf., Table 2: entry 14) would be a good starting point to study the stability of the catalyst under the flow reaction conditions. To achieve this conversion value, we examined the effect of reducing the local pressure of CO_2 in the tube-in-tube reactor (entries 12-15). Reducing this pressure from 8 down to 3 bar did not cause any significant change in substrate conversion suggesting that the CO_2 concentration in the liquid was not a limiting parameter. This was further substantiated by the observation of outgassing beyond the BPR while working at this lower pressure value. Thereto, several flow catalysis cycles were performed, and in each cycle a steady state conversion of glycidol was maintained for 4-6 h, with the NMR yield of GC being quantified by ^{1}H NMR

spectroscopy (Table 6). After each flow cycle, the system was purged with MEK to remove unreacted substrate and product, following re-initiating of the subsequent flow cycle.

Table 6. Flow synthesis of glycerol carbonate and reuse of the catalyst.[a]

Cycle	Conversion[b] (%)	Cycle	Conversion[b] (%)
1	90	5	78
2	88	6	76
3	84	7	65
4	85	8	57

[a] Conditions: 3 bar CO_2 (isobaric conditions), 0.22 M glycidol in methylethyl ketone (MEK), **1** in PBR (0.792 mmol), 70 ºC, 4-6 h at steady state, BPR at 250 psi. [b] Conversion at a steady state determined by ^{1}H NMR using durene as internal standard.

Eight reaction cycles were performed with the same sample of catalyst in the PBR, using a substrate flow (0.22 M solution of glycidol in MEK) of 0.136 mL/min into the tube-in-tube reactor having a local CO_2 pressure of 3 bar. The catalyst roughly retained its activity for 4 cycles, after which a gradual loss of activity was noted with the conversion decreasing from 90 to 57% in the final cycle. This reduction in catalyst performance was mainly attributed to mechanical damage of the support structure at this operative pressure, as it was observed that the catalyst could not re-swell to its original volume inside the PBR when the flow experiment was completed. This was also confirmed by swelling tests performed in batch mode once the catalyst was removed from the flow system.

Based on these observations, some further experiments were planned to design a longer continuous flow conversion of glycidol/CO_2 taking into account the results reported in Tables 5 and 6. In order to produce GC with a continuous high and selective substrate conversion under the optimized reaction conditions (3 bar CO_2 in isobaric mode, 70 ºC), both the catalyst amount (1.59 g, 1.48 mmol) and substrate concentration (0.33 mol/L) were adjusted to provide nearly full conversion. Continuous preparation of GC was achieved under these modified conditions for a total of 48 h at the steady-state. Note that to avoid the mechanical degradation of the catalyst support, the pressure provided by the BPR was reduced from 250 psi (17.2 bar) to 190 psi (13.1 bar). The product was continuously collected in separate fractions and each fraction was analyzed by ^{1}H NMR spectroscopy to determine the substrate conversion and GC selectivity (Figure 3).

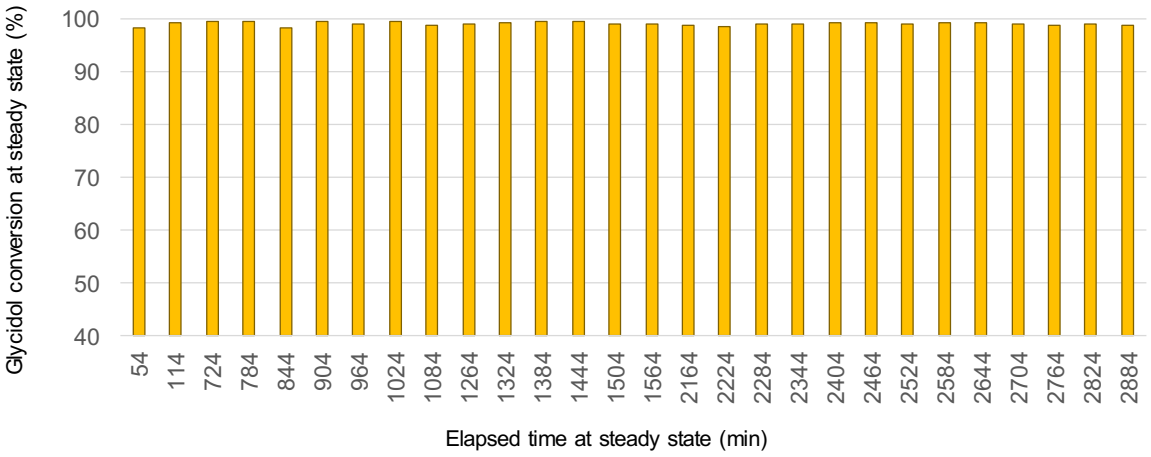

Figure 3. Glycidol conversion (%) with time in a long run (48 h) flow experiment using heterogeneous organocatalyst **1** under the optimized conditions.

To our delight, these spectroscopic analyses related to the fractions collected (cf., Figure 3) unambiguously showed that this flow set-up was highly stable during the entire time frame providing eventually 17.3 g (147 mmol) of cyclic carbonate with an accumulated TON of 99 and a productivity of 2.04 mmol/(h·mmol$_1$) at the steady state. Moreover, there appears to be no difference in spectroscopic purity between the collected and column-purified GC,[35] supporting that high efficiency and selectivity of the heterogeneous organocatalyst **1** in this process operation window.

2.3 Conclusions

In summary, the research described in this Chapter demonstrates the development of a heterogeneous, metal- and halide-free catalyst that can be effectively used for the continuous flow synthesis of one of the commercially most attractive cyclic carbonates reported to date. This new flow process features high stability, excellent substrate conversion and high chemo-selectivity producing multi-gram quantities of carbonate product from readily available glycidol and CO_2. The approach illustrated here creates a new foundation for the sustainable synthesis of similar heterocyclic structures and related polycarbonates, while capitalizing on the use of a cheap, renewable and accessible carbon feedstock. The use of the tube-in-tube reactor, while convenient for small scale preparations, would need further optimization and the developed catalytic flow process requires re-design in order to be useful on a larger scale.

[35] N. Zanda, A. Sobolewska, E. Alza, A. W. Kleij and Miquel À. Pericàs, *ACS Sustainable Chem. Eng.* **2021**, *9*, 4391−4397.

2.4 Experimental section

2.4.1 General information

Unless otherwise noted, all commercial reagents were used as received without further purification or drying, including CO_2 which was purchased from PRAX-38 AIR. Flash chromatography was carried out using 60 mesh silica gel and dry-packed columns. Thin layer chromatography was carried out using Merck TLC silica gel 60 F254 aluminum sheets. Components were visualized by UV light ($\lambda = 254$ nm) and stained with $KMnO_4$. NMR spectra were recorded at 298 K on a Fourier 300 MHz Bruker, a Bruker Avance 400 Ultrashield or a Bruker Avance 500 Ultrashield apparatus. Chemical shifts are reported in ppm relative to the residual solvent peaks in $CDCl_3$ (δ = 7.26 ppm) or DMSO-d_6 (δ = 2.50 ppm). Elemental analyses were performed by MEDAC Ltd, United Kingdom. IR spectra were recorded on a Bruker Tensor 27 FT-IR spectrometer.

2.4.2 Experimental setup

The tube-in-tube (T-i-T) reactor is a membrane reactor with a shell configuration. In the traditional configuration, which we employed, the liquid stream flows inside the inner tube and the gas is located in the outer space between the two tubes. The properties of the Teflon AF-2400 allows to saturate the stream with the desired gas in matter of seconds according to the providers. During all our experiments, the residence time (the time the feed was in contact with the reactor) was always in the order of minutes. The pressure of the CO_2 applied in the inner tube was between 3 and 8 bar, with the total pressure of the system being around 17 bar.

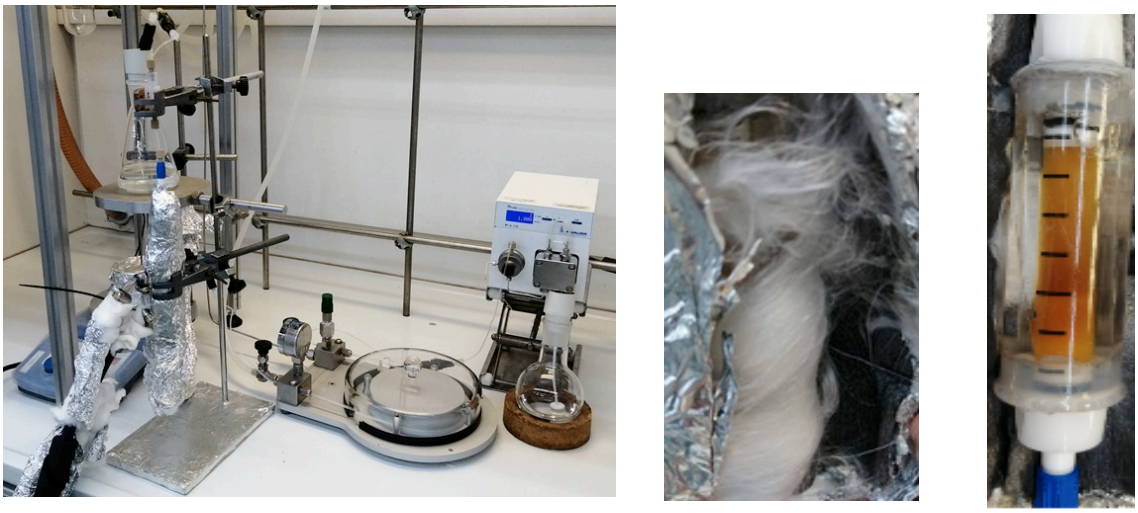

Figure 4. Picture of the set up (left); wrapping of the reactor with glass wool and poly-epoxy resin (center) and catalyst bed inside the column (right).

2.4.3 Experimental flow protocol

- The system is first primed with solvent and the catalyst is swollen
- The solvent is exchanged for the feed solution and flowed through the system
- When the feed arrives and fills the tube-in-tube reactor, the CO_2 manometer is opened at the desired pressure. The tube-in-tube reactor is then primed three times with cycles opening and closing the gas exit. At the end the exit key is closed
- The heat exchanger is then turned on at the desired temperature
- When the feed solution is about to finish, the feed container is rinsed with solvent

- Finally, the system is cleaned with solvent

2.4.4 Swelling test studies on catalyst 1

The swelling test was performed according the procedure reported by North and Routledge.[36] The desired resin (43–89 mg) was transferred to a 2 mL syringe fitted with a polypropylene fritted disc with a void volume of 0.15 mL. Solvent (MEK, 2 mL) was added and the syringe agitated for 1 h at room temperature using orbital shaking/stirring. Excess solvent was removed by compressing the syringe piston before slowly withdrawing the piston and allowing the resin to return to its maximum volume. The volume was recorded and the degree of swelling calculated using the formula:

$$Swelling\ (mL\ g^{-1}) = \frac{measured\ volume - void\ volume}{mass\ of\ resin}$$

Table 7. Comparison of the swelling of fresh catalyst **1** employed in the stability test (ST) and the long-run (LR) flow process. Here the results refer to the "high" and "central" part of the packed-bed reactor.

Catalyst	Weight (mg)	Volume after 1 h (mL)	Volume after 18 h (mL)	Volume after 2 d (mL)	Swelling after 1 h (mL/g)	Swelling after 18 h (mL/g)	Swelling after 2 d (mL/g)
fresh ST	87.9	0.3	0.3	0.4	3.4	3.4	4.55
ST h[a]	83.4	0.15	0.15	0.2	1.8	1.8	2.4
ST c[b]	87.3	0.2	0.2	0.2	2.3	2.3	2.3
fresh LR	84.2	0.4	0.4	0.4	4.8	4.8	4.8
LR h[c]	43.4	0.2	0.15	0.2	4.6	3.5	4.6
LR c[d]	89.0	0.3	0.25	0.4	3.37	2.8	4.5

[a] ST h = catalyst from top portion of PBR. [b] ST c = catalyst from central portion of PBR. [c] LR h = catalyst from top portion of PBR. [d] LR c = catalyst from central portion of PBR

Since the swelling tests after 1 h and 18 h were not conclusive enough, the catalyst was left in contact with the solvent for 48 h (2 days = 2 d), and in this case it was evident that mechanical damage of the catalyst was affecting the swelling. This was even more evident for the catalyst batches used in the stability test (cycles) compared to the long run experiment. These combined swelling tests gave a simple confirmation of what is possible to observe from a visual analysis of the packed bed reactor. After the experiments regarding the stability of the catalyst, the catalyst was not able to fill the original volume it initially occupied, whereas the physical state of the catalyst before and after the long run continuous flow process was the same.

[36] C. Amadi-Kamalu, H. Clarke, M. McRobie, J. Mortimer, M. North, Y. Ran, A. Routledge, D. Sibbald, M. Tickias, K. Tse and H. Willway, *Chemistry Open* **2020**, *9*, 431–441.

2.4.5 FT-IR comparison between fresh and used catalyst

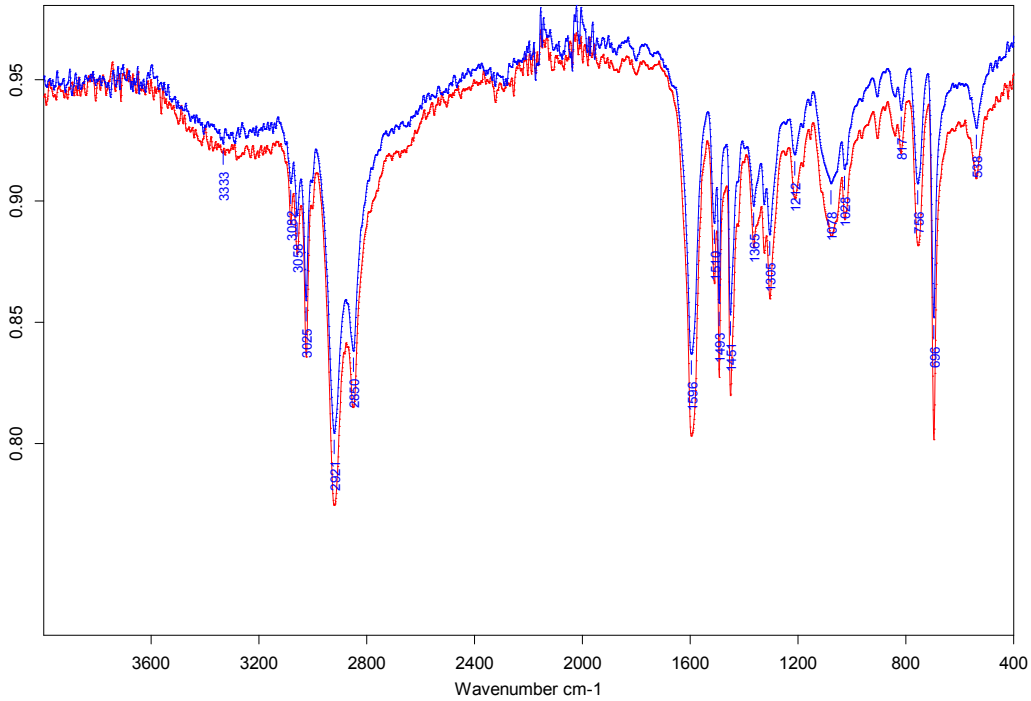

Figure 8. FT-IR spectroscopic analysis of the fresh catalyst (red color) and the used one (blue color).

From the comparison of the IR spectra of the fresh and used catalyst employed in the stability tests in flow (8 cycles in total), there is no evident sign of chemical modification of the structure.

2.4.6 General procedure for the batch experiments

In a typical experiment we weighed the appropriate amount of catalyst and charged the reactor (a 10 mL stainless steel autoclave). The reactor was then sealed and a leak test was performed using CO_2 as gas (15-20 bar). The reactor was pressurized at 2 bars with a constant flow of CO_2 while charging it with a solution of the substrate (glycidol) and closed. Then, the reaction mixture was stirred and the reactor was first heated at the desired temperature after which it brought to the desired isobaric pressure by adding CO_2. After the chosen reaction time, the system was cooled down, the product collected and the reactor washed with EtOAc. The combined organic layers were then filtered and concentrated in vacuo. To an aliquot of the reaction mixture was added DMSO-d_6 and a known amount of an internal standard (durene) following analysis by ^{1}H NMR.

2.4.7 Characterization data for the precursors

Precursor 1:

8-Tetrahydro-2*H*-pyrimido[1,2-a]pyrimidin-1(6*H*)-yl)propane-1,2-diol. Freshly distilled oxiran-2-ylmethanol (2.64 mmol, 1 equiv) was added to a stirred solution of 1,3,4,6,7,8-hexahydro-2*H*-pyrimido[1,2-a] pyrimidine (2.64 mmol, 1 equiv) in toluene (8.8 mL) at 50 ºC. The reaction mixture was stirred at 50 ºC for 24 h and filtered with a PTFE filter (0.45 micron), and the solvent was removed under reduced pressure. Yield: 99%. **^{1}H NMR** ($CDCl_3$, 400 MHz): δ = 1.75 – 1.81 (m, 2H), 1.89 – 1.98 (m, 2H), 3.07 – 3.12 (m, 4H), 3.15 – 3.28 (m, 4H), 3.34 – 3.45 (dd, 2H), 3.48 – 3.49 (d, 1H), 3.67 – 3.72 (m, 1H); **^{13}C-NMR** ($CDCl_3$, 100 MHz): δ = 22.7, 22.8, 42.2, 47.9, 48.2, 48.4, 53.3, 63.7, 71.0, 152.7. **CHNO (%)** analyses found (theoretical): C 55.28 (56.32), H 10.51 (8.98), N 19.94 (19.69), O 14.25 (15.01); **HRMS** (ESI+, MeOH): *m/z* 214.1546 (calc. 214.1550); **FT-IR** (neat, ν in cm^{-1}): 3296, 2847, 1577, 1515, 1035, 1044.

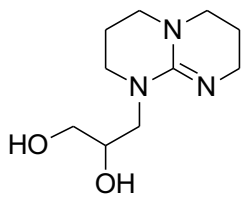

Precursor 2:

1-(3,4,7,8-Tetrahydro-2*H*-pyrimido[1,2-a]pyrimidin-1(6*H*)-yl)propan-2-ol:[37] 2-methyl-oxirane (5.39 mmol, 1.5 equiv) was added to a stirred solution of 1,3,4,6,7,8-hexahydro-2*H*-pyrimido[1,2-a]pyrimidine (3.59 mmol, 1 equiv) in toluene (10 mL). The mixture was stirred at 80 ºC for 16 h. Then the crude was cooled down to r.t., and the solvent was removed under reduced pressure. Yield: 99%. The NMR data of the product were compared against the previously reported data described in the literature. **^{1}H NMR** (toluene-d_8, 400 MHz): δ = 1.18 (d, 3H), 1.46 (m, 4H), 2.50 (m, 1H), 2.58 (m, 1H), 2.64 (m, 2H), 2.69 (m, 1H), 2.82 (m, 1H), 2.97 (dd, 1H),3.22 (m, 2H), 3.51 (dd, 1H,), 4.24 (qdd, 1H): **^{13}C NMR** (toluene-d_8, 101 MHz): δ 154.2, 68.4, 60.8, 48.8, 48.7, 48.5, 43.2, 24.9, 22.4.

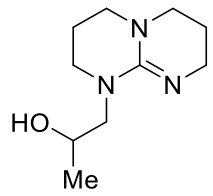

[37] P. Horeglad, A. Litwińska, G. Z. Żukowska, D. Kubicki, G. Szczepaniak, M. Dranka and J. Zachara, *Appl. Organomet. Chem.* **2013**, *27*, 328-336.

2.4.8 Synthesis of the heterogeneous catalysts

General procedure A for supported catalysts: NaH (95%, 3 equiv) was added portion-wise to a stirred solution of 3-(3,4,7,8-tetrahydro-2*H*-pyrimido[1,2-a] pyrimidin-1(6*H*)-yl)propane-1,2-diol (1 equiv) at 0 ºC and under N_2 atmosphere. The suspension was stirred for 15 min and then added through a cannula to a closed flask containing the respective resin support (0.5 equiv) in DMF (20 mL) under N_2. Then, the suspension was shaken for 2 days at r.t. The obtained heterogeneous catalyst was characterized by IR to assess the presence of C=N "stretching" absorptions. Elemental analysis was additionally performed to quantify the amount of precursor (functionalization degree, *f*) onto the support, and finally gel phase ^{13}C NMR analysis was also carried out where possible.

General procedure B for supported catalysts: A solution of 3-(3,4,7,8-tetrahydro-2*H*-pyrimido[1,2-a]pyrimidin-1(6*H*)-yl)propane-1,2-diol (1 equiv) in DCM (10 mL) was added at 0 ºC and under N_2 atmosphere to a shaken suspension of a Barlos resin (0.5 equiv) and triethylamine (TEA, 2 equiv) in DCM. Then the reaction suspension was shaken for 3 days at r.t. The obtained catalyst was characterized by IR to assess the presence of C=N "stretching" absorptions. Elemental analysis was additionally performed to quantify the amount of precursor (functionalization degree, *f*) onto the support, and finally gel phase ^{13}C NMR analysis was also carried out where possible.

Synthesis of Merrifield supported catalyst TBD@Merrifield (1): NaH 95% (3 equiv) was added portion-wise to a stirred solution of 3-(3,4,7,8-tetrahydro-2*H*-pyrimido[1,2-a] pyrimidin-1(6*H*)-yl)propane-1,2-diol (1 equiv) at 0 ºC and under a N_2 atmosphere. The suspension was stirred for 15 min and then added through a cannula to a closed flask containing (chloromethyl)polystyrene (Novabiochem, 1.5 mmol/g, 1% DVB, 100-200 mesh) (0.5 equiv) in DMF (20 mL) under N_2. Then the suspension was shaken for 5 days at r.t. **CHNO** (%) analyses: C 82.98, H 7.78, N 3.92, O 3.02; f_{exp}**:** 0.933 mmol/g (note: entry 15, Table 1); **FT-IR** (neat, ν in cm^{-1}): 3024, 2921, 1596, 1450, 696; **^{13}C NMR** ($CDCl_3$, 126 MHz): δ = 152.09, 70.23, 64.09, 55.71, 48.22, 41.52, 22.92, 22.66.

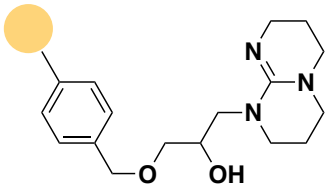

Note that also the catalyst batches with other functionalization degrees (*f*) were prepared similarly, and this refers to Table 1: entries 1-9, 16 + 17: f_{exp} = 0.307 mmol/g, using 0.6 mmol/g, 1% DVB, 100-200 mesh, Merrifield resin, and Table 1: entries 10-14: f_{exp} = 0.740 mmol/g

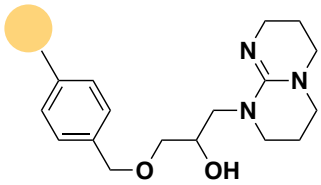

Synthesis of Wang supported catalyst (2): This catalyst was prepared according general procedure A using Wang resin (IRIS biotech, 1.2 mmol/g, 1% DVB, 100-200 mesh). **CHN** (%) analyses: C 80.23, H 7.31, N 2.70; f_{exp}: 0.643 mmol/g; **FT-IR** (neat, ν in cm^{-1}): 3024, 2921, 1599, 1450, 697.

Synthesis of JandaJel supported catalyst (3): This catalyst was prepared according general procedure A from Jandajel (Aldrich, 1 mmol/g resin. 1% cross-linked, 100-200 mesh). **CHN** (%) analyses: C 87.09, H 7.55, N 1.79. f_{exp}: 0.426 mmol/g; **FT-IR** (neat, ν in cm^{-1}): 3025, 2919, 1600, 1451, 696; **^{13}C NMR** ($CDCl_3$, 126 MHz): δ = 145.01, 69.67, 63.64, 55.21, 48.80, 47.85, 43.14, 22.77, 22.49.

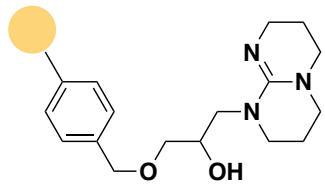

Synthesis of Merrifield supported catalyst TBD-2@Merrifield (1-(3,4,7,8-tetrahydro-2*H*-pyrimido[1,2-a]pyrimidin-1(6*H*)-yl)propan-2-ol supported catalyst) (4): This catalyst was synthesized according general procedure A employing a Merrifield resin (Novabiochem, 0.6 mmol/g 1% DVB, 100-200 mesh). **CHN** (%) analyses: C 89.50, H 7.69, N 1.59; f_{exp}: 0.379 mmol/g; **FT-IR** (neat, ν in cm^{-1}): 3025, 2921, 1600, 1451, 695.

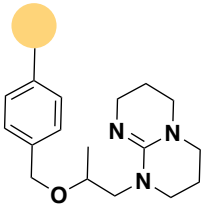

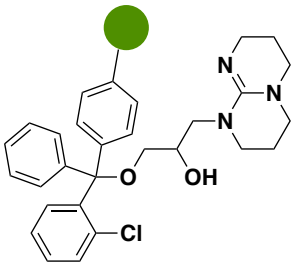

Synthesis of Barlos supported catalyst (5): This catalyst was prepared according general procedure B from Barlos resin (IRIS biotech, 1.6 mmol/g, 1% DVB, 100-200 mesh). **CHN** (%) analyses: C 74.84, H 6.54, N 4.25; f_{exp}: 0.993 mmol/g; **FT-IR** (neat, ν in cm^{-1}): 3314, 3024, 2922, 1594, 1446, 698.

Chapter 3: Continuous organocatalytic flow synthesis of 2-substituted oxazolidinones using carbon dioxide.

The results described in this chapter have been published in:

N. Zanda, L. Zhou, E. Alza, A. W. Kleij and Miquel À. Pericàs, *Green Chem.* **2022**, *24*, DOI: 10.1039/D2GC00503D

3.1 Introduction

3.1.1 Oxazolidinones

Oxazolidinones, also known as cyclic carbamates, are interesting synthetic targets as they represent sub-structures of pharmaceutically relevant and structurally diverse compounds (Figure 1).[1] Well-known strategies reported for their synthesis involve the combination of (tri)phosgene and amino alcohols,[2] the reaction between isocyanate reagents and epoxides[3] and recently disclosed (photo)catalytic and/or transition metal mediated cross-coupling or cyclization protocols.[4] Another and rather attractive approach to their preparation involves the use of carbon dioxide (CO_2) to generate these heterocyclic compounds by combining this C_1 building block with aziridines.[5]

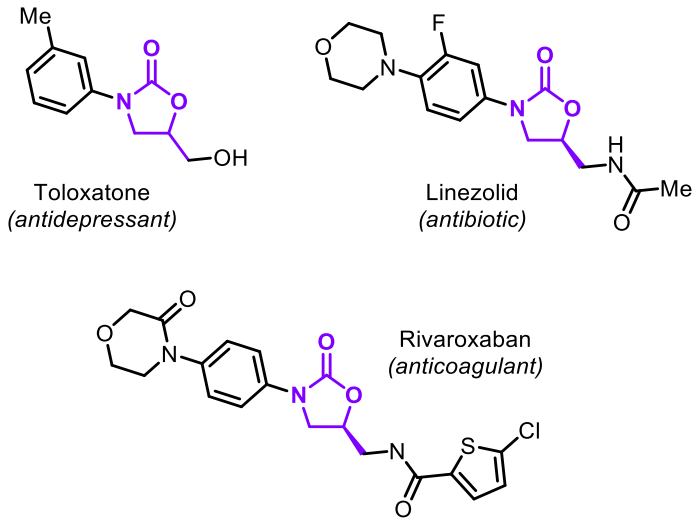

Figure 1. Examples of commercial drugs containing the 2-substituted oxazolidinone moiety.

While the aforementioned methodologies are intrinsically effective towards the creation of structurally diverse oxazolidinones, they either require toxic reagents, (transition) metal catalysts and/or pre-functionalization of the precursors. Approaches that can alleviate these downsides while focusing on potentially more sustainable processes may create new opportunities for oxazolidinone synthons and their derivatives in synthetic and pharmaceutical science. An interesting approach was provided by Kim and co-workers in 2017, taking advantage of a ionic liquid (IL) deposited directly in a microfluidic device. In this manner, 2-

---

1 a) S. Arshadi, A. Banaei, S. Ebrahimiasl, A. Monfared and E. Vessally, *RSC Adv*. **2019**, *9*, 19465-19482; b) M. E. Dyen and D. Swern, *Chem. Rev*. **1967**, *67*, 197–246; c) F. Sun, E. V. Van der Eycken and H. Feng, *Adv. Synth. Catal*. **2021**, *363*, 5168-5195.

2 N. Alouane, A. Boutier, C. Baron, E. Vrancken and P. Mangeney, *Synthesis* **2006**, *5*, 860-864.

3 a) J. A. Castro-Osma, A. Earlam, A. Lara-Sánchez, A. Otero and M. North, *ChemCatChem* **2016**, *8*, 2100-2108; b) Y. Toda, S. Gomyou, S. Tanaka, Y. Komiyama, A. Kikuchi and H. Suga, *Org. Lett*. **2017**, *19*, 5786–5789; c) X. Wu, J. Mason and M. North, *Chem. Eur. J.* **2017**, *23*, 12937-12943; d) Y. Toda, K. Hashimoto, Y. Mori and H. Suga, *J. Org. Chem*. **2020**, *85*, 10980-10987.

4 a) Q. Guo, X. Ren and Z. Lu, *Org. Lett.* **2019**, *21*, 880-884; b) W. Mahy, P. K. Plucinskim and C. G. Frost, *Org. Lett*. **2014**, *16*, 5020-5021; c) S. T. Heller, T. Fu and R. Sarpong, *Org. Lett*. **2012**, *14*, 1970-1973; d) T. Nagai, N. Mimata, Y. Terada, C. Sebe and H. Shigehisa, *Org. Lett*. **2020**, *22*, 5522-5527.

5 a) F. Fontana, C. C. Chen and V. K. Aggarwal, *Org. Lett*. **2011**, *13*, 3454-3457; b) M. Sengoden, M. North and A. C. Whitwood, *ChemSusChem* **2019**, *12*, 3296-3303. c) H. Seo, L. V. Nguyen, T. F. Jamison, *Adv. Synth. Catal.* **2019**, *361*, 247-264.

oxazolidinones and quinazoline-2,4-(1*H*,3*H*)-diones could be prepared by treatment of CO_2 with propargylic amines or 2-aminobenzonitriles, respectively.[6]

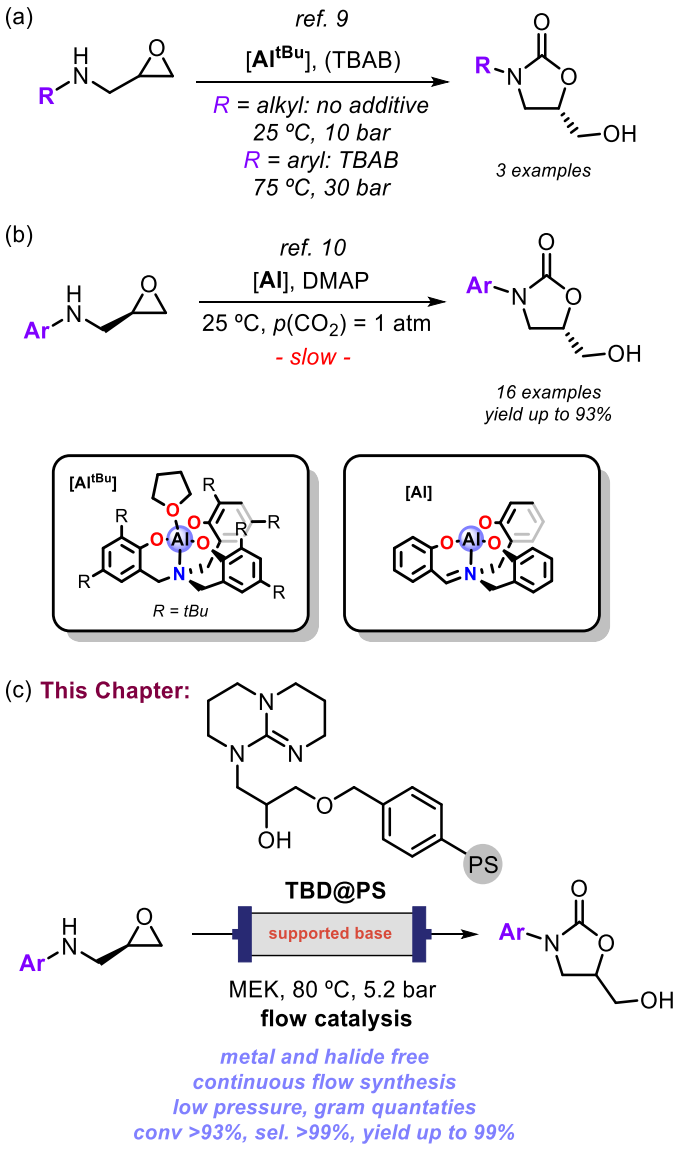

Scheme 1. Previous work under (a) and (b), and current approach towards *N*-aryl oxazolidinones (c) using a heterogenized TBD based organocatalyst.

Another attractive approach is the reaction between epoxy amines and CO_2. Whereas CO_2 represents a cheap and abundant reaction partner for the development of new synthetic methodology,[7] epoxy amines are readily available and prepared in few steps.[8]

---

6 N. K. Vishwakarma, A. K. Singh, Y.-H. Hwang, D.-H. Ko, J.-O. Kim, A. G. Babu and D.-P. Kim, *Nat. Commun*. **2017**, *8*, 14676-14684.

7 a) Q. Liu, L. Wu, R. Jackstell and M. Beller, *Nat Commun*. **2015**, *6*, 5933. b) A. Polyzos, M. O'Brien, T. P. Petersen, I. R. Baxendale and S. V. Ley, *Angew. Chem. Int. Ed*, **2011**, *50*, 1190-1193. c) H. Seo, A. Liu and T. F. Jamison, *J. Am. Chem. Soc,* **2017**, *139*, 13969–13972.

8 Epoxy amines can be easily prepared in high yields from ring-opening of epichlorohydrin by anilines followed by treatment with a base, see: *a*) A. K. Chakraborti, S. Rudrawar and A. Kondaskar, *Eur. J. Org. Chem*. **2004**, *17*,3597-3600; *b*) M. M Islam, P. Bhanja, M. Halder, S. K. Kundu and S. M. Islam, *RSC Adv.* **2016**, *6*, 109315;

Admittedly, organic reactions based on CO_2 as a reagent do not have the potential to remediate the negative effects ascribable to global emissions, but this greenhouse gas offers a green and sustainable alternative to fossil fuel-derived carbon reagents. In 2016, we reported a few examples of the coupling of epoxy amines bearing *N*-alkyl groups and CO_2 providing access to 2-substituted-oxazolidinones in excellent yields and selectivity. Despite the lower reactivity of *N*-aryl based epoxy amines, the drug Toloxatone could be prepared via a similar methodology in 74% yield under binary Al/halide catalysis (Scheme 1a).[9] The chemo-selectivity (81%) in this latter example was not complete, as the formation of small amounts of a cyclic carbonate was also observed.

Later, Kim and co-workers further extended this protocol by using a modified Al-complex and reported the conversion of chiral epoxy amines and CO_2 into enantiopure *N*-aryl oxazolidinones in the presence of DMAP under mild temperature conditions.[10] This latter protocol could be additionally used to complete a formal synthesis of Linezolid (Figure 1), though in general the reactions were slow (likely due to limited CO_2 solubility in the solvent), with typical reaction times being 1-4 days and for most of the scope of products, the reactions were performed at a milligram scale.

3.1.2 Aims and objectives

Having the limitations discussed in Section 2.1.1 in mind, we considered the possibility to translate these batch processes into continuous flow ones to enable larger-scale synthesis. Key aspects in our approach are the optimization of the contact time between reagents (to favor high chemoselectivity), the avoidance of a metal catalyst and halide additives and the promise of a scalable approach for the target compounds. A flow catalysis approach has as additional advantages that it combines improved safety, control and, in some cases, sustainability depending on the type of catalyst and ease of catalyst/product separation[11], making it also very attractive from a practical point of view.

Organocatalytic methodologies remain of high interest in the area of green chemistry, and we have reported both the development of easily prepared heterogenized organocatalysts[12], and the organocatalytic valorization of CO_2 using catalysts of this type.[13] By merging these two strategies, we have been recently able to develop a continuous flow organocatalytic approach for glycidol carbonate. With this approach, we have shown the feasibility of performing coupling reactions of

c) V. T. Kamble and N.S. Joshi, *Green Chem. Lett. Rev*. **2010**, *3*, 275-281; d) J. J. Lim and K. Arrington, *Org. Process Res. Dev*. **2020**, *24*, 1927-1937.

9 J. Rintjema, R. Epping, G. Fiorani, E. Martin, E. C. Escudero-Adan and A. W. Kleij, *Angew. Chem. Int. Ed*. **2016**, *55*, 3972-3976.

10 Y. Lee, J. Choi and H. Kim, *Org. Lett*. **2018**, *20*, 5036-5039.

11 a) B. Gutmann, D. Cantillo and C. O. Kappe, *Angew. Chem. Int. Ed*. **2015**, 54, 6688-6728; b) C. J. Mallia and I. Baxendale, *Org. Process Res. Dev*. **2016**, 20, 327-360; c) M. Brzozowski, M. O'Brien, S. Ley and A. Polyzos, *Acc. Chem. Res*. **2015**, 48, 349-362.

12 For some recent examples, see: a) L. Zhou, S. Perulli, M. M. Mastandrea, P. Llanes, J. Lai and M. A. Pericàs, *Green Chem*. **2021**, 23, 8859-8864; b) J. Lai, M. Fianchini and M. A. Pericàs, *ACS Catal*. **2020**, 10, 14971-14983; c) S. Wang, C. Rodrìguez-Escrich, and M. A. Pericàs, *Angew. Chem. Int. Ed*. **2017**, 56, 15068-15072; d) P. Llanes, S. Sayalero, C. Rodrìguez-Escrich and M. A. Pericàs, *Green Chem*. **2016**, 18, 3507-3512. For a recent review, see: e) C. Rodríguez-Escrich and M. A. Pericàs, *Chem. Rec*. **2019**, 19, 1872-1890.

13 *a*) C. J. Whiteoak, A. H. Henseler, C. Ayats, A. W. Kleij and M. A. Pericàs, *Green Chem*. **2014**, *16*, 1552-1559; *b*) T. Jose, S. Cañellas, M. A. Pericàs and A. W. Kleij, *Green Chem*. **2017**, *19*, 5488-5493; c) S. Sopeña, E. Martín, E. C. Escudero-Adán and A. W. Kleij, *ACS Catal*. **2017**, *7*, 3532-3539.

gaseous CO_2 with epoxides under comparatively mild (3 bar, 70 ºC) reaction conditions[14] as opposed to a recently disclosed pyridine-based homogeneous catalytic approach (10 bar, 60 ºC).[15] Though epoxy amines should have different reactivity than epoxy alcohols,[13] the flexibility offered by packed bed reactors for flow application and the easy optimization of their use should allow to develop a catalytic process with a suitably immobilized organocatalyst that enables the selective and high-yield preparation of *N*-aryl oxazolidinones. Here, we demonstrate that a single-component polystyrene-supported 1,5,7-triazabicyclodec-5-ene (**TBD@PS**, Scheme 1c) is an effective, robust and recyclable catalyst for the sequential and continuous formation of a wide range of *N*-aryl oxazolidinones.

3.2 Results and discussion

3.2.1 Design of the flow setup

By taking advantage of our previously attained knowledge,[13] we designed a flow setup (figure to Table 1) that uses CO_2 as a gaseous stream. To control the volume of gas flowed in the system, we employed a Bronkhorst mass flow controller (MFC). The reaction feed was then provided by a micro HPLC pump (details in the Experimental Section). The two streams met in a static Tee mixer and then were flowed through a packed bed reactor (PBR) held in a vertical position and with a down-flow configuration. This proved to be beneficial for the overall stability of the system. The system was heated by a vent oven at the desired temperature and the pressure was maintained by a back-pressure regulator (BPR). The collection of reaction product was performed by a homemade auto-collector, programmed in Python and controlled by a Raspberry pi 4b (single board computer) used as microcontroller. The use of this computer controlled MFC allowed to quickly assess the stability of the gas flow, a stable gas flow meant that stable reaction conditions could be achieved, and the automatic collector, to determine the steady state by carefully examining the collected fractions of product.

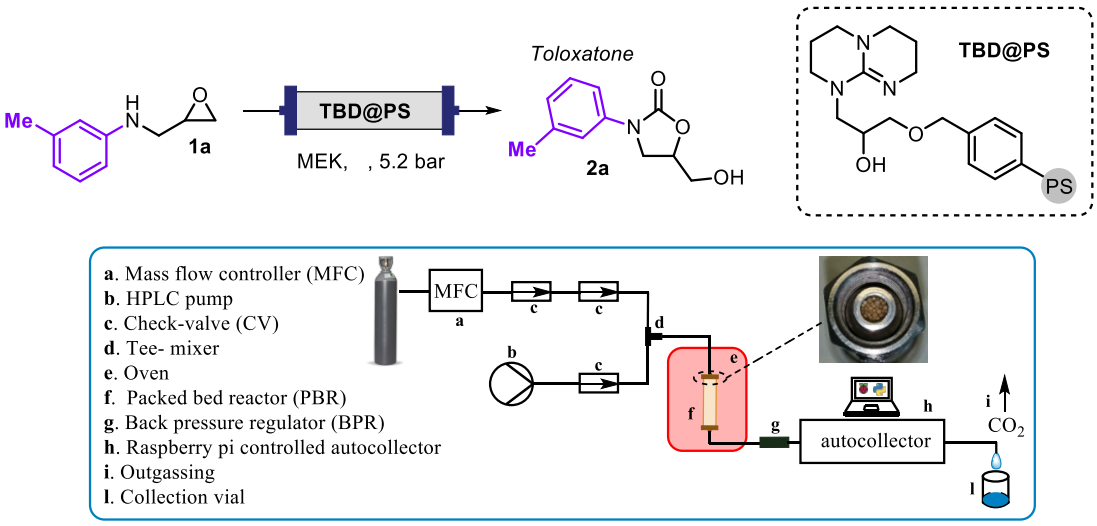

Figure 2. Schematic diagram of the flow setup described in this chapter.

[14] N. Zanda, A. Sobolewska, E. Alza, A. W. Kleij and M. A. Pericàs, *ACS Sustainable Chem. Eng*. **2021**, *9*, 4391–4397.

[15] W. Natongchai, J. A. Luque-Urrutia, C. Phungpanya, M. Solà, V. D'Elia, A. Poater and H. Zipse, *Org. Chem. Front*. **2021**, *8*, 613-627.

To take full advantage of the physical properties of the system, we decided to employ a similar TBD-based organocatalyst as we described before.[22] However, in the present case the TBD moiety was anchored onto a highly cross-linked Merrifield (polystyrene, PS) resin with 5.5 % 1,4-divinylbenzene (DVB). The catalyst will be further denoted as **TBD@PS**. The advantage of the resulting PS-like support is that it does not swell under the operating conditions, favoring stable catalyst operation. Similar kind of supports were previously prepared and used in continuous flow in a liquid-gas-solid system by the Kobayashi group.[16]

3.2.2. Optimization of the reaction conditions

Once the stability of the flow system was established, we explored the chemistry of the targeted transformation. We decided to use epoxy amine **1a** as the benchmark to optimize the catalytic process. The coupling of **1a** with CO_2 produces oxazolidinone **2a**, i.e. the antidepressant Toloxatone, whose formal synthesis from an epoxy amine was first reported by Kleij et al.[9] In the flow catalysis setup (Figure 1, Table 1), optimal results were obtained when a combined flow of 5.1 mL/min was employed (see the Experimental Section for more extensive optimization data). The reaction solvent was chosen according to our previous findings,[13,17]since the favorable solubility of CO_2 in MEK usually results in better reaction rates. DMSO was chosen as co-solvent to avoid the precipitation of the oxazolidinone product inside the reactor (Table 1, entry 2 vs. 1), which was experimentally observed to occur at substrate conversion around 80% and in the absence of this co-solvent. Thus, a small amount (6.5 %, v/v) of DMSO was added to avoid reactor clogging. The use of other polar co-solvents such as DMF, 1,4-dioxane and CH_3CN were also considered but proved to less effective than DMSO (see the Experimental Section).

Better catalytic performance of the **TBD@PS** was generally observed at higher temperature (80 ºC). While the highest conversions (96%) were recorded at lower substrate (**1a**) flow−rates (Table 1, entries 4 and 5), the highest productivities were achieved when more concentrated (0.15-0.2 M) solutions of **1a** were circulated through the PBR at 0.10 mL/min (entries 1 and 6). It is worth noting that conversion of **1a** appeared to be rather insensitive to its concentration, and this tends to indicate that the limiting factor of the process efficiency is the availability of CO_2 at the catalytic sites (cf. entries 1 and 3).

To achieve high chemo-selectivity (>99%) for Toloxatone **2a**, it was needed to carefully dry the epoxy amine **1a** under vacuum to remove traces of water arising from the aqueous work-up in the isolation of this precursor. After having identified the optimal conditions for the synthesis of **2a** (Table 1, entry 5), we tested whether a continuous flow catalysis preparation of Toloxatone could be realized for a longer period of time (26 h, Figure 2) under steady state conditions. Gratifyingly, the flow-catalytic preparation of the *N*-aryl oxazolidinone product was operationally stable, providing a total of 1.56 g of Toloxatone with a 93% yield after isolation by flash column purification. The reaction conditions were specifically chosen such that nearly complete substrate conversion was possible in order to facilitate product isolation without the need for extensive purification. They also allowed to examine possible product precipitation, which may occur especially at high substrate conversion.

[16] T. Yasukawa, R. Masuda and S. Kobayashi, *Nat. Catal*. **2019**, *2*, 1088-1092.
[17] A. Decortes and A. W. Kleij, *ChemCatChem* **2011**, *3*, 831-834.

Table 1. Optimization of reaction conditions using epoxy amine **1a** as substrate to produce oxazolidinone **2a**.

Entry	Feed of **1a** mL/min	T ºC	Conc. mol/L	Conv. %[b]	Yield %[b]	**TBD@PS** mmol	**2a** mmol·h^{-1}	Productivity mmol·h^{-1}·mmol·cat^{-1}
1	0.10	80	0.20	80	79	0.551	0.960	1.742
2[c]	0.10	80	0.20	NA	NA	0.551	NA	NA
3[d]	0.10	80	0.20	52	NA	0.551	0.624	1.132
4	0.05	80	0.20	96	90	0.487	0.622	1.277
5[e]	0.05	80	0.10	96	93	0.487	0.311	0.639
6[f]	0.10	80	0.15	85	84	0.573	0.765	1.335
7	0.10	25	0.15	5	NA	0.551	0.045	0.082
8	0.10	70	0.20	57	50	0.551	0.684	1.241

[a] General reaction conditions: pCO_2 (*inlet pressure*) 10 bar, CO_2 5 mL/min, solvent MEK, 280 mg **TBD@PS** catalyst, f_{exp} = 1.96 mmol/g, BPR at 75 psi (= 5.2 bar). The experiments were carried out for 3 hours at steady state and then the reactor was washed with the reaction solvent. [b]Conversion and isolated yields refers to steady state conditions. [c]Reaction without DMSO as co-solvent, the reactor was blocked. [d] CO_2 feed at 2 mL/min. [e]Measured flow-rate was 0.0557 mL/min, with an estimated 1.04 mmol of CO_2 and 0.00557 mmol of substrate entering the reactor every minute. [f] f_{exp} was 2.04 mmol/g. Abbreviations used: BPR = back pressure regulator, PBR = packed back reactor. NA stands for "not assessed".

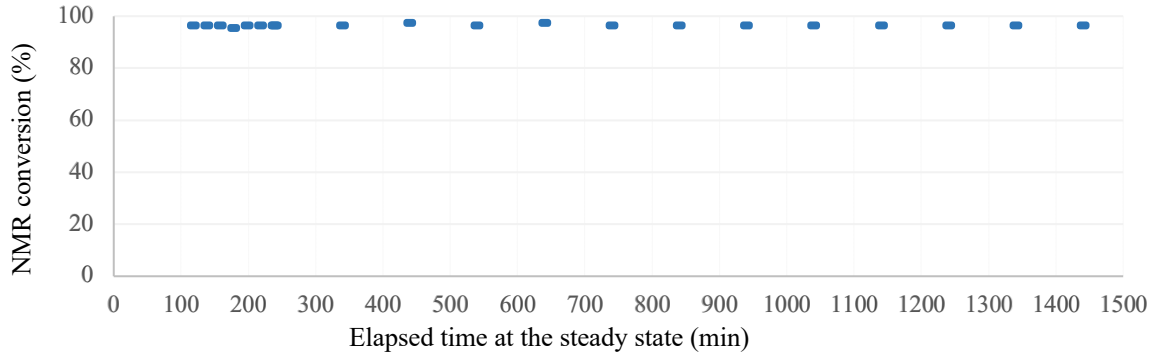

Figure 3. Extended time catalytic flow formation of Toloxatone **2a** mediated by **TBD@PS** under the reaction conditions of ***entry 5*** in Table 1.

3.2.3 Product scope of the reaction

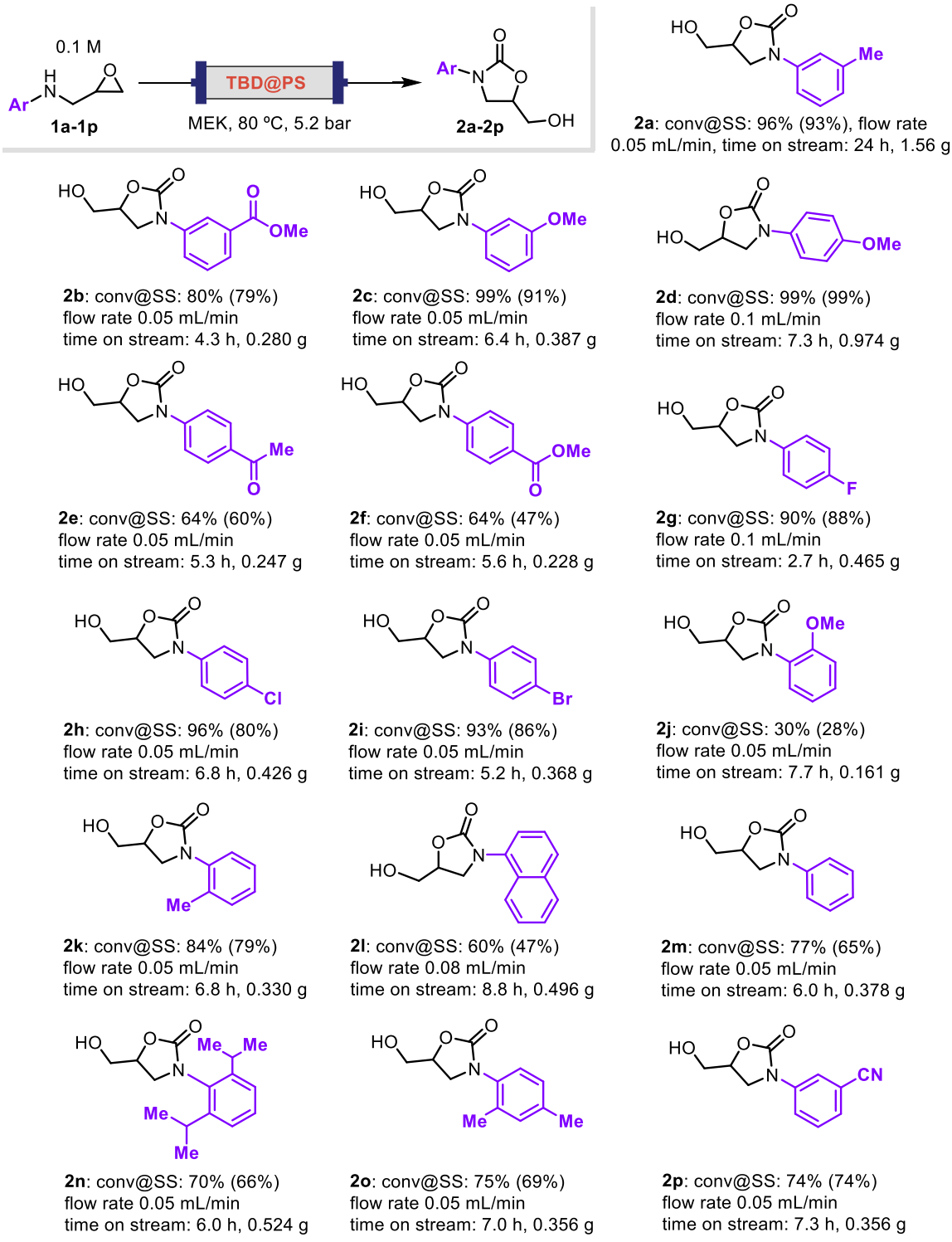

Figure 4. Scope of *N*-aryl oxazolidinone products **2a-2p** using epoxy amine/CO_2 coupling reactions promoted by **TBD@PS**. Typical conditions unless stated otherwise: pCO_2 (inlet pressure) 10 bar, CO_2 5.0 mL/min MFC flowrate, MEK/DMSO (100:6.5 v/v), 0.1 M feed (**note**: for the synthesis of **2g** 0.15 M), PBR containing 270 mg of **TBD@PS** with f_{exp} = 1.77 mmol/g or, for compounds **2d**, **2g**, **2m**, **2l** and **2n**, f_{exp} = 1.96 mmol/g, BPR loaded at 75 psi (= 5.2 bar).

Next, the scope of *N*-aryl oxazolidinone products that can be produced from various epoxy amines and CO_2 was examined using in all cases samples of the same **TBD@PS** batch (see Figure 4, **2a**-**2p**). For some of the epoxy amine substrates, higher reactivity was expected and, in these cases, we decided to use a flow rate of 0.1 mL/min. The experiments were carried out for the desired interval of time and under stable operating conditions, after which the reactor content was washed with the reaction solvent and kept wet before reuse. The conversion at stead state (SS) was determined by ^{1}H NMR. Isolated yields of product are reported in brackets, and the selectivity was >99% (**note**: the selectivity for **2m** was 95% and for **2f** 92 %). The reaction temperature for **2n** was 75 ºC, as the system operation was not stable at 80ºC.

To avoid further optimization of the amount of DMSO, we ran all reactions at 0.1 M (except for **2g**: 0.15 M). Epoxy amines with *para* electron-donating substituents on the *N*-aryl groups (**2a**, **2c** and **2d**) showed higher reactivity (i.e., conversion at steady state) giving excellent yields (≥ 91%) of the oxazolidinones. *Ortho*-substituted *N*-aryl epoxy amines such as **2j**, **2k**, **2n** and **2o** showed lower reactivity, which can be rationalized by a higher degree of steric requirement upon ring-closure during the formation of the oxazolidinone product. Substrates with either ester or acyl groups on the *N*-aryl (**2b**, **2e** and **2f**) showed lower conversion levels at steady state, whereas halide-containing substrates provided smooth access to the heterocyclic products **2g**-**2i** in good yields (80-88%). Sterically more frustrated substrates such as those leading to **2l** and **2n** could still be converted into their respective oxazolidinones with appreciable yields. The synthesis of the cyano-aryl derivative **2p** was also feasible affording the product in a yield of 74%. The successful execution of various oxazolidinone syntheses using the presented flow set up demonstrates that the catalyst systems is versatile and widely applicable.

3.2.4 Sequential experiment

Finally, we wondered whether a continuous and sequential experiment could be designed with a single batch of **TBD@PS** offering thus a way to rapidly produce a small library of oxazolidinones (Table 2). Between each of the reactions, a washing step was applied to avoid cross-impurities in the next product in the sequence. The total duration of this sequential flow experiment was around 64 h (*carried out in a period of two weeks*), during which various oxazolidinones were prepare with nearly the same or similar substrate conversion levels as compared to the separate synthesis of these heterocyclic products. Notably, the chemo-selectivity observed throughout the entire experiment remained very high, and only during the preparation of **2p** (entry 7) a small drop (>99→90%) in selectivity was noted.

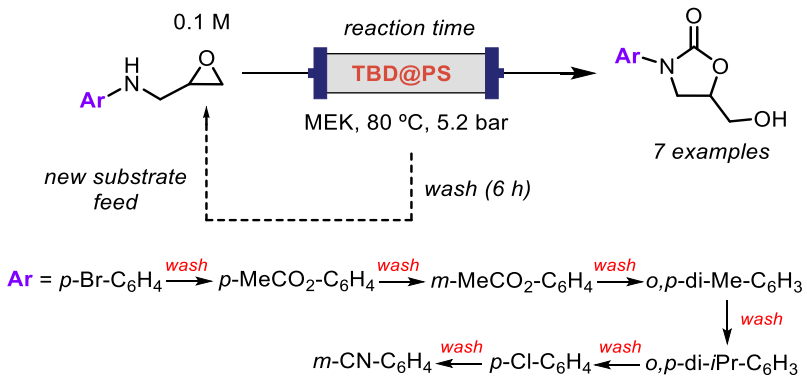

Figure 5. Conceptual design of the sequential experiment.

Table 2. Formation of various oxazolidinone products using a sequential flow catalysis approach using the same **TBD@PS** catalyst.[a]

Entry	Product	T (h)	C_1 (%)	C_2 (%)	Selectivity (%)[b]	Yield (%)[c]
1	**2i**	4.7	93	93	>99 (>99)	86
2	**2f**	5.6	64	65	92 (88)	49
3	**2b**	4.3	81	80	>99 (>99)	79
4	**2o**	6	75	75	>99 (>99)	70
5	**2n**	4	66	70	>99 (>99)	60
6	**2h**	4	78[d]	96	>95 (>99)	NA
7	**2p**	5	70	74	90(>99)	60

[a] **TBD@PS** (270 mg), f_{exp} = 1.77 mmol/g, pCO_2 (inlet pressure) 10 bar, CO_2 5.0 mL/min MFC flowrate, MEK/DMSO (100:6.5 v/v), 0.1 M feed, BPR 75 psi (= 5.2 bar), total reaction time (*T*) indicated after reaching a steady state; reactor washing time in-between the experiments was 6 h. [b] Chemo-selectivity observed for the oxazolidinone product with in brackets the selectivity reported in Figure 2. [c] Isolated yield after flash column purification. [d] Due to clogging of the reactor, the product could not be isolated with a representative yield. Abbreviations used: C_1 = conversion at the steady state achieved with the same catalyst batch in this multi-sequence process, C_2 = conversion at steady state with fresh catalyst as reported in Figure 3. NA means "not assessed".

The byproduct that formed was the corresponding cyclic organic carbonate. The latter was identified by comparison with reported ^{1}H NMR spectra in literature. To note, the peak multiplicity and specific NMR displacement of the carbonate products are characteristic and easily assigned. The observation that the carbonate product arises when the starting material is not dried overnight under vacuum and over time, after re-using, the catalyst suggests that adventitious water may be involved in its formation. The analysis of the catalyst by ESEM (Figure 8, Experimental Section) showed white crystals that likely is NaCl formed during the grafting of the catalyst. A small amount of water could dissolve the salt effectively thereby providing chloride as a potential nucleophile that can ring-open the epoxide ring favoring the formation of the carbonate rather than the carbamate.

Considering the results of the long-run (Figure 3) and catalyst re-use experiments (Figure 5 and Table 2), it seems reasonable to assume that the supported **TBD@PS** organocatalyst has good stability and remains active for prolonged periods of time.

3.3 Conclusion

In summary, the research described in this chapter shows that a supported organocatalyst (**TBD@PS)** is an active and stable catalyst for the application under continuous flow in the preparation of a wide variety of pharmaceutically relevant *N*-aryl oxazolidinones. The process combines a number of attractive features, making it a sustainable alternative for the valorization of CO_2 into added-value organics, turning waste into value added products. First, the catalytic resin can be easily prepared in two steps from cheap, commercially available starting materials. The process can be operated under comparative mild pressure and temperature conditions and

utilizes a simple, metal-free *N*-heterocyclic catalyst and does not require a halide additive. Pure oxazolidinone products can be isolated by quick filtration through a pad of silica. Lastly, the heterogeneous catalyst can be stored to up to a year under air at r.t. without any loss in activity and remains stable under continuous flow operation for at least two weeks. The activity could be further extended by employing distilled solvents and/or flushing the catalytic bed with dry air at high temperatures to remove the water that might accumulate in the reactor.

Compared to batch operations, continuous flow conversion of CO_2 has the advantage of maintaining a constant operating pressure, thus maximizing process kinetics and process efficiency. Similar catalytic flow syntheses that are based on a renewable carbon feedstock hold promise to be implemented in fine-chemical and pharmaceutical development programs and will become even more attractive when the non-utilized (excess) CO_2 could be re-used. It is expected that this type of reaction will find application in future continuous flow multi-step procedures for the synthesis of fine chemicals.

3.4 Experimental section

3.4.1 Experimental flow setup

The feed of starting material, amino epoxide dissolved in a methylethyl ketone (MEK) and dimethyl sulfoxide (DMSO), was provided by a Thales nano micro HPLC pump. The feed was flowed through a Swagelok® check-valve (CV) (1/3 psi) and joined the gas stream in a static Tee-mixer. The gas stream was provided by a Bronkhorst EL-Flow Prestige mass flow controller (MFC) and passed through two Swagelok® CV (1/3 psi) before reaching the Tee. After the mixer the mixed stream entered the Packed Bed Reactor (stainless steel, ϕ 0.46 cm x 5 cm, 0.83 mL). The PBR was located inside of a vent oven heated by an heating plack, the temperature was doublechecked by a digital thermometer. The system was closed by a back-pressure regulator (BPR) from IDEX. Finally, the gas liquid stream was directed into an homemade autocollector (containing Bruphny Micro Servo Motor SG90 9G) and controlled by a Raspberry pi4b programmed in Python3. The collection was performed into glass vials (ϕ 5.0 cm, 10 mL) the outgassing was performed via a cotton thread located at the end of the tubing.

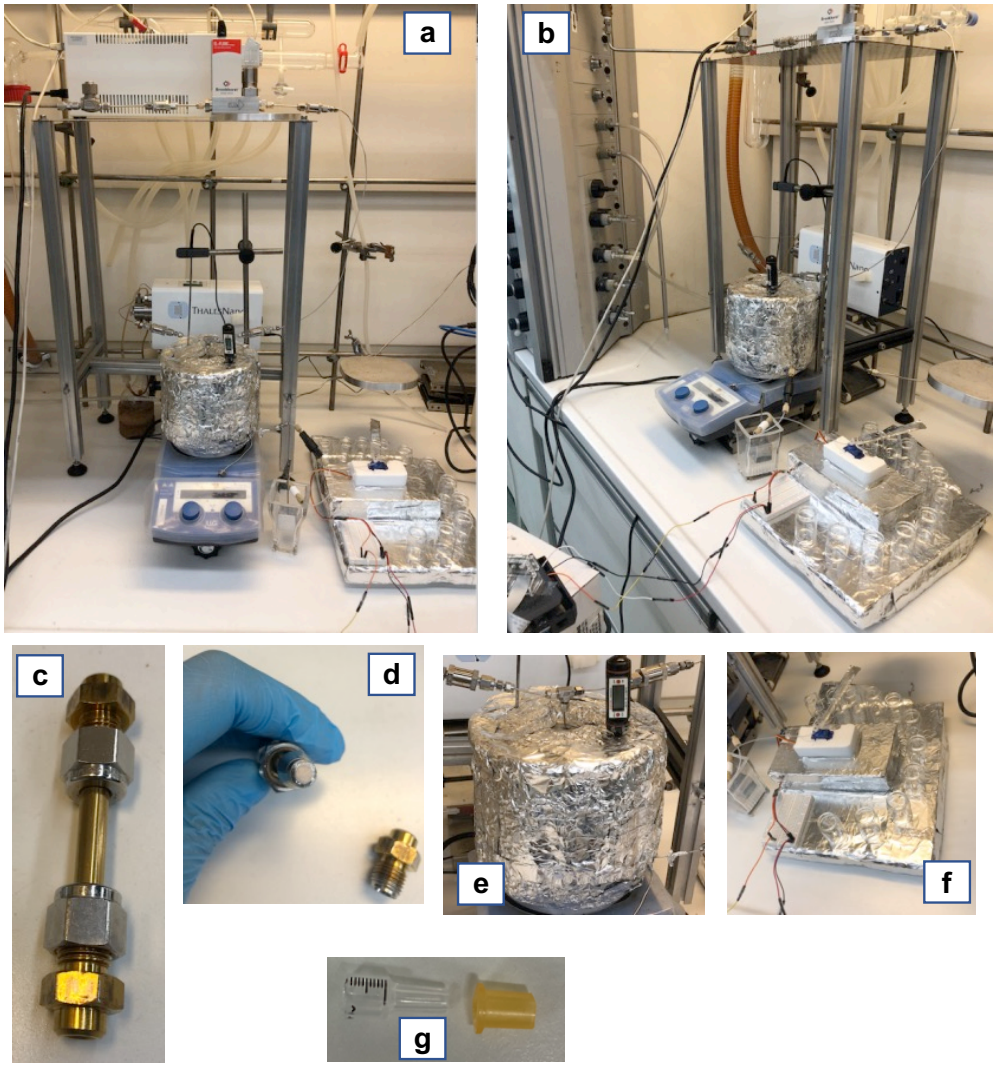

Figure 6. Pictures of the setup (a and b), PBR (c and d), the vented oven (e), auto-collector (f) and the degassing at the outlet of the system (g) in order to avoid to spill the droplets.

3.4.2 Experimental flow protocol

- MFC is turned on and connected to the PC
- Gas manometer is opened at the desired inlet pressure
- Gas flow is started
- Leak test is performed
- Calibration of the auto-collector
- HPLC pump is turned on and set at the desired flow rate (flows only solvent)
- Wait for system stabilization (usually 5-10 minutes)
- Solvent flask is exchanged for reaction feed
- Heating plate is turned on
- Auto-collector is set to collect the desired fraction in the desired timeframe
- When the feed is about to end rinse the flask with reaction solvents
- Finally exchange the flask for a clean one with reaction solvent and wash

3.4.3 System stability test

The flow setup described in Figure 6a-b was equipped with a Knauer Azura P4.1 pump with integrated pressure sensor to determine the necessary pressure to efficiently flow the gas (5 to 24 hours long).

Selected Examples:

Flowing stream: MEK/DMSO 6.5% (0.1 mL/min) + CO_2 (5 mL_n/min)
BPR: 5.17 Bar
Knauer pressure read: 8 bar
Necessary gas inlet pressure to achieve a stable flow: 9 bar

Flowing stream: 0.1 M solution of toloxatone amino epoxide precursor in MEK/DMSO 6.5% (0.1 mL/min) + CO_2 (5 mL_n/min)
BPR: 5.17 Bar
Knauer pressure read: 9 bar
Necessary gas inlet pressure to achieve a stable flow: 10 bar

The designed setup proved to be stable under several flow-rates if the inlet pressure was kept above 9 bar. During the reactions we kept the inlet pressure at 10 bar to maintain a stable system and to avoid the influence of any possible variation of pressure from the line. This was done mainly because the line is shared with all the institute and because the solution of different compounds could have properties that could influence the pressure in the reactor.

With regard to the PBR configuration, when it was used in horizontal position the output of the MFC was not stable, the same applies to the vertical up-flow configuration. The CO_2 flow rate can be changed in a range between 2 mL_n/min and 20 mL_n/min and the stability of the system it is not affected. The system was operated in blank tests in temperatures between 25ºC and 110ºC. More supports were tested for the TBD derivative such as SBA15 and Porous glass beads both with and without filler; the problem of this type of support is that it leads to very high column pressure (>10 bar) under the reaction conditions and therefore the CO_2 could not flow with the inlet pressure provided by our institutional gas line.

3.4.4 First catalytic tests

Table 3. Comparison between glycidol and epoxy amine precursor **2a** to Toloxatone **3a**.[a]

Entry	substrate	mL/min	Conversion at SS
1	Glycidol	0.1	75
2	Glycidol	0.05	100
3	**2a**	0.1	25
4	**2a**	0.05	40

[a] General reaction conditions: the feed, substrate 0.1 M in MEK was flowed at the indicated flow rate and with 20 mL_n/min of CO_2 (10 bar inlet pressure), the PBR was heated at 70ºC, BPR 40 psi, catalyst 270 mg. The crude was collected at intervals of 30 minutes and in the table is reported the conversion at the steady state (SS) and analyzed by ^{1}H- NMR spectroscopy.

These experiments showed a preliminary difference in the reactivity between glycidol and epoxy amine **2a**, and thus the conditions needed to be adjusted to achieve high yields with these substrates.

3.4.5 Tables with additional screening results

Table 4. Further reaction optimization.[a]

Entry	Feed **1a**	CO_2	T	Conc.	Conv.	Yield	**TBD@PS**	**2a**	$\mathbf{P_{2a}}$[b]
	mL/min	mL_n/min	ºC	mol/L	%	%	mmol	mmol·h^{-1}	
1	0.1	5	80	0.2	80	79	0.551	0.960	1.742
2[c]	0.1	5	80	0.2	NA	NA	0.551	NA	NA
3	0.1	2	80	0.2	52	NA	0.551	0.624	1.132
4	0.05	5	80	0.2	96	90	0.487	0.622	1.277
5	0.05	5	80	0.1	96	93	0.487	0.311	0.639
6	0.1	5	80	0.15	85	84	0.573	0.765	1.335
7	0.1	5	25	0.15	5	NA	0.551	0.045	0.082
8[c]	0.1	5	90	0.15	85	73	0.551	0.765	1.388
9	0.1	5	70	0.2	57	50	0.551	0.684	1.241
10	0.1	5	70	0.1	52	NA	0.551	0.312	0.566
11	0.1	20	70	0.1	20	NA	0.434	0.120	0.276
12	0.07	5	80	0.15	88	86	0.551	0.554	1.006
13	0.12	5	90	0.15	79	74	0.551	0.853	1.548
14	0.12	4	90	0.15	77	74	0.551	0.832	1.509
15	0.05	5	80	0.1	0	NA	0	NA	NA
16	0.1	10	70	0.2	48	NA	0.551	0.576	1.045
17[d]	0.1	10	70	0.1	30	NA	0.434	0.180	0.415
18[d]	0.1	10	80	0.1	26	NA	0.551	0.156	0.283
19[d]	0.1	5	70	0.1	27	NA	0.434	0.162	0.373
20[d]	0.1	20	70	0.1	45	NA	0.551	0.270	0.490

[a]Unless stated otherwise pCO_2 (*inlet pressure*) 10 bar, MEK, 270 mg catalyst f_{exp} = 1.96 mmol/g (entry 6: f_{exp} = 2.04 mmol/g; entry 13: f_{exp} = 1.55 mmol/g), BPR 75 psi (= 5.17 bar), experiments were carried out for 3 hours at the steady state (ss) then reactor was washed with the reaction Conv = Conversion at the steady state with fresh catalyst, determined by ^{1}H NMR collecting fractions at the steady state , unless stated otherwise selectivity was > 99% selectivity; BPR = back pressure regulator, PBR = packed back reactor. NA = "not assessed". Yield is calculated according to the fractions collected at the steady state. [b]$\mathbf{P_{2a}}$ = Productivity calculated as such (mmol ·h^{-1}·mmol cat $^{-1}$). [c]Reaction without DMSO as co-solvent, the reactor blocked. [d]BPR was 40 psi (~ 2.76 bar).

The steady state did not depend on the gas flow but only on the feed flow rate and was reached after 50 minutes when 0.1 mL/min were used, and at 100 minutes when 0.05 mL/min were used. In the latter case we determined by volumetric measurements that the real flow rate at which the HLPC pump was working was 0.0557 mL/min and this value was considered in all the calculations. Both increasing the gas flow rate to 10 or 20 mL_n/min or decreasing it to 4 or 2 mL_n/min resulted in a reduced conversion when the amino epoxide precursor of toloxatone was flowed at 0.1 mL/min.

Table 5. Scope and additional experiments with several substrates.[a]

Entry	C	*fr*	Conv. (%)	Y (%)	**TBD@PS** (mmol)	**2a** (mmol·h^{-1})	P	T (h)	$\mathbf{Y_g}$ (g)
1	**2d**	0.1	99	99	0.539	0.594	1.102	7.3	0.974
2	**2g**	0.1	90	88	0.539	0.810	1.500	2.7	0.465
3[b]	**2m**	0.1	42*	NA	0.539	0.252	0.468	–	NA
4[b]	**2m**	0.05	77*	65	0.539	0.386	0.716	6	0.378
5	**2h**	0.05	96	80	0.478	0.288	0.603	7.8	0.426
6	**2j**	0.1	18	NA	0.478	0.108	0.226	–	NA
7	**2j**	0.05	30	28	0.478	0.090	0.188	7.7	0.161
8	**2b**	0.05	80	79	0.478	0.240	0.502	4.3	0.280
9	**2e**	0.05	64	60	0.478	0.192	0.402	5.3	0.247
10	**2k**	0.05	84	79	0.478	0.252	0.527	6.8	0.330
11	**2i**	0.05	93	86	0.478	0.279	0.584	5.2	0.368
12	**2c**	0.1	80	NA	0.539	0.480	0.891	NA	NA
13	**2c**	0.05	99	91	0.478	0.297	0.621	6.4	0.387
14	**2f**	0.05	65	49	0.478	0,195	0.408	5.6	0.228
15	**2n**	0.02	93	NA	0.478	0.112	0.234	–	NA
16	**2n**	0.05	67	60	0.478	0.210	0.439	–	NA
17[c]	**2n**	0.08	70	66	0.539	0.336	0.623	6	0.524
18[c]	**2l**	0.08	60	47	0.539	0.288	0.534	8.8	0.496
19	**2o**	0.05	75	69	0.478	0.225	0.471	7	0.356
20	**2p**	0.05	74	74	0.478	0.222	0.464	7.3	0.356

[a] Unless stated otherwise: pCO$_2$ (*inlet pressure*) 10 bar, CO$_2$ mL$_n$/min (= 5.1 – HPLC flowrate), solvent MEK/DMSO 6.5% 0.1 M (entry 2 0.15M), PBR 270 mg catalyst f_{exp} = 1.77 mmol/g (entry 1-4, 17-18: f_{exp} = 1.96 mmol/g), BPR 75 psi (= 5.17 bar) C = compound; *fr* = Flow rate (mL/min); Conversion at the steady state (ss) with fresh catalyst, it was determined by ^{1}H NMR collecting fractions at the SS, unless stated otherwise the selectivity was >99%; for entry 3: 88%, entry 4: 95% entry 14: 92%; **Y** = yield; $\mathbf{Y^g}$ = overall yield of the whole process (in g); P = productivity defined as mmol·h^{-1}·mmol(cat)$^{-1}$; T = total reaction time; BPR = back pressure regulator, PBR = packed back reactor. [b] Solvent was MEK. [c] Reaction was carried out at 75 ºC.

3.4.6 Sequential experiments

In a typical experiment, the feed of the desired epoxy amine (0.1 M) dissolved in MEK (containing 6.5 v/v % DMSO) was flowed at 0.05 mL/min and the CO_2 (10 bar inlet pressure) was flowed at 5 mL_n/min inside the PBR containing 270 mg of catalyst, which was heated at 80 ºC. The system was pressurized at 5 bar and fractions were collected every 20 minutes. Experiments were carried out for the desired interval of time and under stable conditions after which the reactor was washed with the reaction solvent. The fractions were analyzed by ^1H NMR to determine the conversion, and the final combined crude was also examined. After the desired volume was flowed inside the system the flask containing the feed was rinsed with the solvent mixture and finally exchanged for the solvent mixture in order to fully wash the system.

Note: the reactor was extensively washed for 6 h, with a 2 h purge being generally being sufficient to remove any eventual trace of previous compounds passing through the reactor. The eluting phase was checked by TLC to ensure that no compound stayed behind in the reactor thus avoiding any possible cross contamination. An additional confirmation of this is the FT-IR comparison of the fresh catalyst with the used one (see Figure 7, section 2.4.7).

3.4.7 Catalyst synthesis

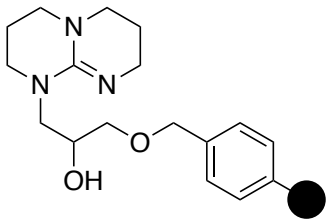

Synthesis of porous polystyrene supported catalyst: NaH 95% (3 equiv) was added portion-wise to a stirred solution of 3-(3,4,7,8-tetrahydro-2H-pyrimido[1,2-a] pyrimidin-1(6H)-yl)propane-1,2-diol[14] (1 equiv) at 0ºC and under a N_2 atmosphere. The suspension was stirred for 15 minand then added through a cannula to a sealed flask containing (chloromethyl)polystyrene (porous polystyrene 5.5% DVB, Aldrich, 16-50 Mesh, 5.5 mmol/g, 0.5 equiv) in DMF (200 mL) under N_2. The suspension was shaken for 5 days at r.t. CHNO (%) analyses: C 69.62, H 7.43, N 7.47, O 3.02; f_{exp}: 1.77 mmol/g; FT-IR (neat, ν in cm^{-1}): 3350, 2922, 1597, 1510, 1321, 1085, 813;

FT-IR examination of the catalyst:

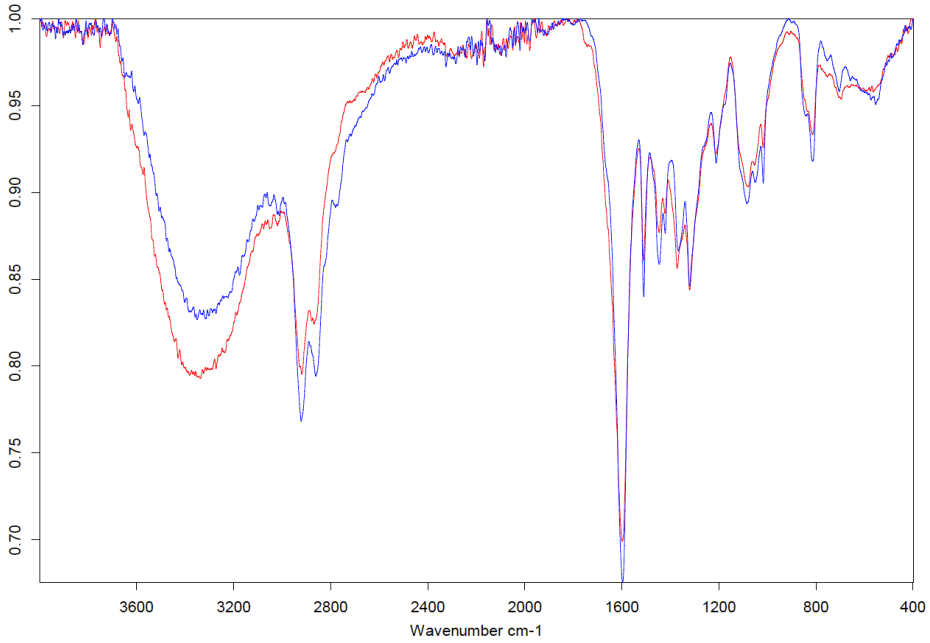

Figure 7. FTIR spectroscopic analysis of the fresh catalyst (blue color) and the used one (red color). No significative difference was detected by comparison of the fresh catalyst and the catalyst used in the reaction; notably, the product did not contaminate the catalyst.

Table 6. Elemental analysis comparison between the fresh and used catalyst.

ELEMENT →	C	H	N	Cl	N/C ratio
Fresh catalyst	69.62	7.43	7.47	2.19	0.107
Used catalyst	67.21	7.56	7.08	2.04	0.105

The N/C ratio does not show any significant difference. The same holds for the Cl/C ratio.

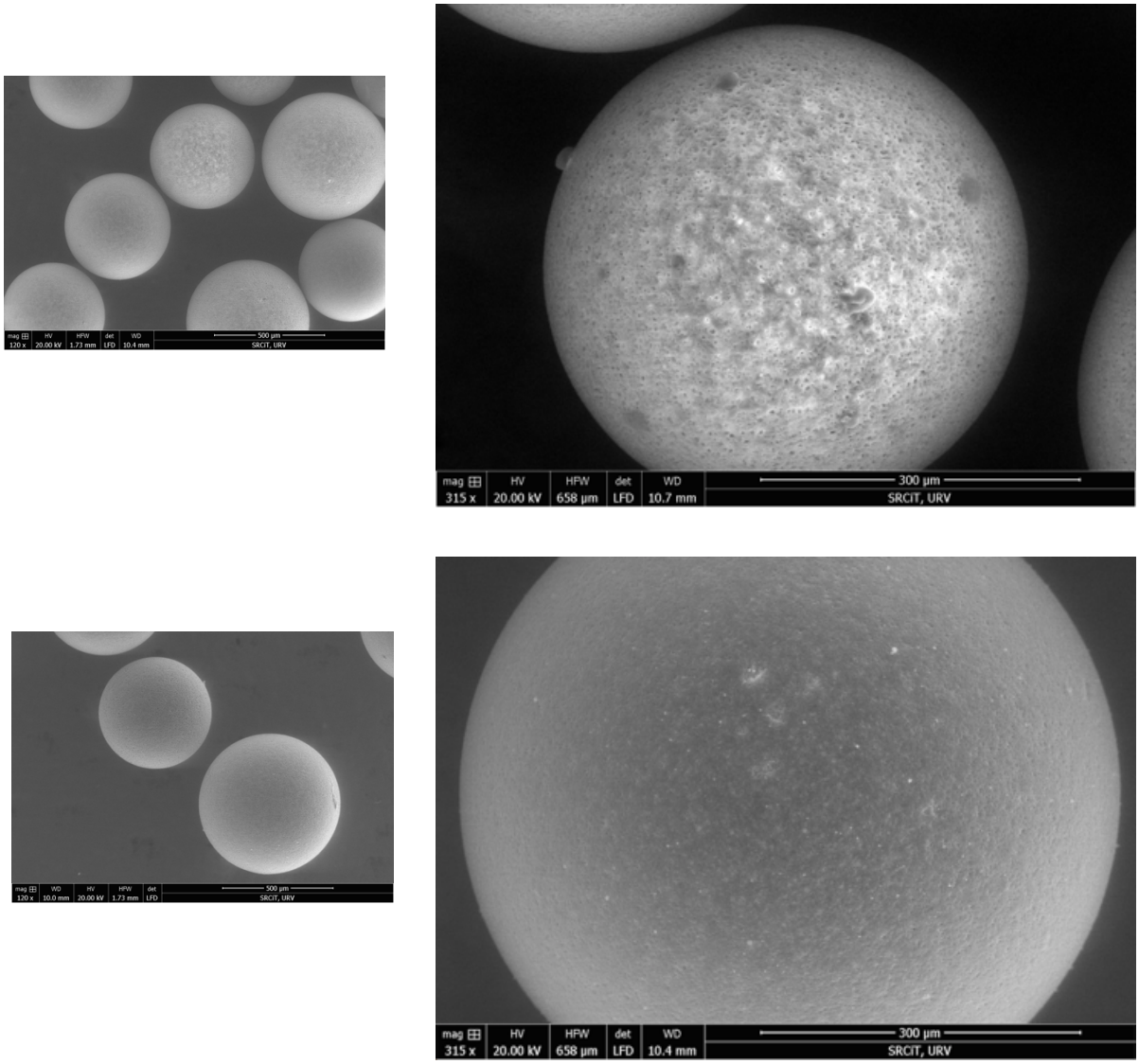

Figure 8. SEM pictures of the polystyrene bead morphology in Merrifield resin (5.5% DVB) with a mass of 120.315 au.

Notes: The presence of NaCl crystals could justify the decreased selectivity towards the oxazolidinone when the substrate is not well dried, and over time due to increasing water accumulation in the reactor. Traces of water can dissolve NaCl thus releasing a halogen nucleophile that can ring-open the epoxide and mediate the formation of the cyclic organic carbonate. In general, the presence of water favors the formation of the carbonate (4% identified in the non-dried toloxatone precursor. This was determined by comparing known ^{1}H-NMR spectra with the experimentally obtained one in our work.

The NaCl crystals originated during the grafting of the monomer, and it was not possible to remove the salt by washing with water or water/organic solvent mixtures (i.e., water/dioxane and water/THF). The intrinsic properties of the polymer made the removal of the salt difficult. However, this did not affect the selectivity when the amino epoxide was well-dried. Curiously, the solvents employed were not dried and probably did not contain enough water to dissolve a meaningful amount of the salt.

3.4.8 Synthesis of oxazolidinones products

General procedure: In a typical experiment, the feed of the desired amino-epoxide dissolved in MEK/DMSO (DMSO at 6.5 v/v %) was flowed at 0.05 mL/min and the CO_2 (10 bar inlet pressure) was flowed at 5 mL_n/min inside the PBR (containing 270 mg of catalyst) heated at 80ºC. The system was pressurized at 75 psi. After the desired volume was flowed inside the system, the flask containing the feed was rinsed with the solvent mixture and finally the feed was exchanged for the solvent mixture in order to fully wash the system. Then all the fractions were joined and the solvents removed. DMSO was then removed first by washing with water (three times) and brine (one time). The organic fractions were combined and the solvent removed under reduced pressure. Minor traces of DMSO were removed under vacuum and the crude product was then purified by flash chromatography to obtain the desired oxazolidinone.

5-(hydroxymethyl)-3-(*m*-tolyl)oxazolidin-2-one (2a) (Toloxatone).[18] Synthesized according the general procedure (0.05 mL/min, 0.1 M, 5 mL_n/min CO_2) 1.560 g, white solid, 93% yield. **^{1}H NMR** (400 MHz, $CDCl_3$) δ 7.38 (s, 1H), 7.34 – 7.28 (m, 1H), 7.28 – 7.21 (m, 1H), 6.98 – 6.92 (m, 1H), 4.76 – 4.67 (m, 1H), 4.05 – 3.90 (m, 3H), 3.79 – 3.69 (m, 1H), 2.79 – 2.70 (m, 1H), 2.36 (s, 3H), 1.77 (bs, 1H). **^{13}C NMR** (126 MHz, $CDCl_3$) δ154.9, 139.0, 138.0, 128.9, 125.1, 119.1, 115.5, 72.9, 62.8, 46.5, 21.6. **FT-IR** (neat, *v* in cm^{-1}): 1724 (C=O).

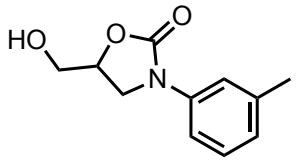

Methyl 3-(5-(hydroxymethyl)-2-oxooxazolidin-3yl)benzoate (2b).[19] Synthesized according the general procedure (0.05 mL/min, 0.1 M, 5 mL_n/min CO_2) 0.280 g, white solid, 79% yield. **^{1}H NMR** (400 MHz, DMSO-d_6) δ 7.29 (t, *J* = 8.2 Hz, 1H), 7.23 (t, *J* = 2.3 Hz, 1H), 7.10 (dd, *J* = 8.2, 0.9 Hz, 1H), 6.70 (ddd, *J* = 8.3, 2.5, 0.8 Hz, 1H), 5.21 (t, *J* = 5.6 Hz, 1H), 4.73 – 4.63 (m, 1H), 4.11 – 4.03 (m, 1H), 3.82 (dd, *J* = 8.9, 6.3 Hz, 1H), 3.75 (s, 3H), 3.71 – 3.63 (m, 1H), 3.61 – 3.50 (m, 1H). **^{13}C NMR** (101 MHz, DMSO-d_6) δ 166.0, 154.5, 139.0, 130.3, 129.4, 123.8, 122.1, 118.0, 73.4, 61.7, 52.3, 46.0. **FT-IR** (neat, *v* in cm^{-1}): 1711 (C=O) **ESI-MS** $[C_{12}H_{13}NNaO_5]^+$: calcd, 274.0686; found, 274.0686.

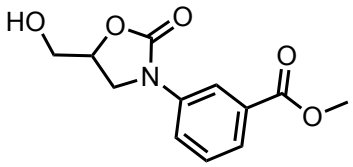

5-(hydroxymethyl)-3-(3-methoxyphenyl)oxazolidin-2-one (2c).[20] Synthetized according the general procedure (0.05 mL/min, 0.1 M, 5 mL_n/min CO_2) 0.387 g, white solid, 91% yield. **^{1}H NMR** (400 MHz, DMSO-d_6): δ 7.29 (t, *J* = 8.2 Hz, 1H), 7.23 (t, *J* = 2.3 Hz, 1H), 7.10 (dd, *J* = 8.2, 0.9 Hz, 1H), 6.70 (ddd, *J* = 8.3, 2.5, 0.8 Hz, 1H), 5.21 (t, *J* = 5.6 Hz, 1H), 4.73 – 4.63 (m, 1H), 4.11 – 4.03 (m, 1H), 3.82 (dd, *J* = 8.9, 6.3 Hz, 1H), 3.75 (s, 3H), 3.71 – 3.63 (m, 1H), 3.61 – 3.50 (m, 1H). **^{13}C NMR** (101 MHz, DMSO-d_6) δ 159.7, 154.4, 139.8, 129.7, 110.0, 108.7, 103.9, 73.1, 61.7, 55.1, 46.1, 40.2, 39.9, 39.7, 39.5, 39.3, 39.1, 38.9. **FT-IR** (neat, *v* in cm^{-1}): 1713 (C=O).

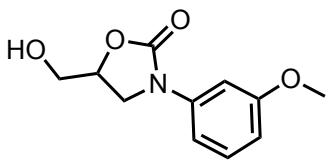

[18] J. Rintjema, R. Epping, G. Fiorani, E. Martin, E. C. Escudero-Adan and A. W. Kleij, *Angew. Chem. Int. Ed.* **2016**, *55*, 3972-3976.
[19] WO2018212534 A1, **2018**-11-22.
[20] A. Ali, K. K. Reddy, H. Cao, S. G. Anjum, M. N. L. Nalam, C. A. Schiffer, T. M. Rana, *J. Med. Chem.* **2006**, *49*, 7342-7356.

5-(hydroxymethyl)-3-(4-methoxyphenyl)oxazolidin-2-one (2d).[21] Synthesized according the general procedure (0.1 mL/min, 0.1 M, 5 mL_n/min CO_2) 0.974 g, white solid, 99% yield. **^{1}H NMR** (400 MHz, DMSO-*d*$_6$) ^{1}H NMR (400 MHz, DMSO-*d*$_6$) δ 7.51 – 7.42 (m, 2H), 7.00 – 6.89 (m, 2H), 5.22 – 5.14 (m, 1H), 4.72 – 4.59 (m, 1H), 4.04 (t, *J* = 3.3 Hz, 1H), 3.79 (t, *J* = 3.3 Hz, 1H), 3.74 (s, 3H), 3.70 – 3.49 (m, 2H). **^{13}C NMR** (101 MHz, DMSO-*d6*) δ 155.4, 154.6, 131.8, 119.7, 114.1, 73.0, 61.7, 55.2, 46.4, 39.5. **FT-IR** (neat, *v* in cm^{-1}): 1714 (C=O).

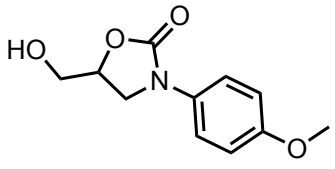

3-(4-Acetylphenyl)-5-(hydroxymethyl)oxazolidin-2-one (2e).[22] Synthesized according the general procedure (0.05 mL/min, 0.1 M, 5 mL_n/min CO_2) 0.247g, white solid, 60% yield. **^{1}H NMR** (400 MHz, DMSO-*d6*) δ 8.10 – 7.94 (m, 2H), 7.76 – 7.63 (m, 2H), 5.23 (t, *J* = 5.5 Hz, 1H), 4.81 – 4.72 (m, 1H), 4.20 – 4.10 (m, 1H), 3.92 – 3.85 (m, 1H), 3.75 – 3.66 (m, 1H), 3.65 – 3.51 (m, 1H), 2.55 (s, 3H). **^{13}C NMR** (101 MHz, DMSO-*d6*) δ 196.6, 154.3, 142.6, 131.3, 129.4, 116.9, 73.4, 61.6, 45.9, 26.5. **FT-IR** (neat, *v* in cm^{-1}): 1738 (C=O), 1662.

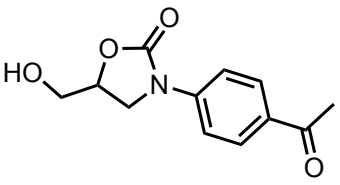

Methyl-4-(5-(hydroxymethyl)-2-oxooxazolidin-3yl)benzoate (2f). Synthesized according the general procedure (0.05 mL/min, 0.1 M, 5 mL_n/min CO_2) 0.228 g, white solid, 47% yield. **^{1}H NMR** (400 MHz, DMSO-*d*$_6$): δ 7.97 (d, *J* = 8.8 Hz, 2H), 7.72 (d, *J* = 8.9 Hz, 2H), 5.30 – 5.19 (m, 1H), 4.79 – 4.66 (m, 1H), 4.20 – 4.06 (m, 1H), 3.88 (dd, *J* = 9.1, 6.2 Hz, 1H), 3.83 (s, 3H), 3.75 – 3.50 (m, 2H). **^{13}C NMR** (101 MHz, DMSO-*d*$_6$) δ 166.2, 154., 143.2, 130.7, 124.3, 117.5, 73.9, 62.1, 52.4, 46.4, 40.0. **FT-IR** (neat, *v* in cm^{-1}): 1739 (C=O), 1701 **ESI-MS** $[C_{12}H_{13}NNaO_5+H]^+$: calcd, 274.0686; found, 274.0695.

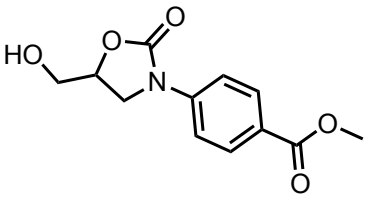

3-(4-Fluorophenyl)-5-(hydroxymethyl)oxazolidin-2-one (2g).[23] Synthesized according the general procedure (0.1 mL/min, 0.15 M, 5 mL_n/min CO_2) 0.465 g, white solid, 88% yield. **^{1}H NMR** (400 MHz, DMSO-*d*$_6$) δ 7.64 – 7.54 (m, 2H), 7.28 – 7.18 (m, 2H), 5.20 (t, *J* = 5.6 Hz, 1H), 4.74 – 4.64 (m, 1H), 4.12 – 4.03 (m, 1H), 3.82 (dd, *J* = 8.7, 6.2 Hz, 1H), 3.72 – 3.61 (m, 1H), 3.61 – 3.51 (m, 1H). **^{13}C NMR** (101 MHz, DMSO-*d*$_6$) δ 157.0, 154.6, 135.0, 119.8, 119.7, 115.6, 115.4, 73.1, 61.6, 46.2. **FT-IR** (neat, *v* in cm^{-1}): 1724 (C=O).

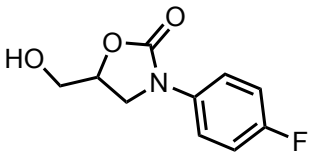

3-(4-chlorophenyl)-5-(hydroxymethyl)oxazolidin-2-one (2h).[7] Synthesized according the general procedure (0.05 mL/min, 0.1 M, 5 mL_n/min CO_2) 0.426 g, white solid, 80% yield. **^{1}H NMR** (400 MHz, DMSO-*d*$_6$) δ 7.64 – 7.54 (m, 2H), 7.48 – 7.38 (m, 2H), 5.27 – 5.16 (m, 1H), 4.76 – 4.64 (m, 1H), 4.07 (s, 1H), 3.82 (dd, *J* = 8.8, 6.2 Hz, 1H), 3.74 – 3.63 (m,

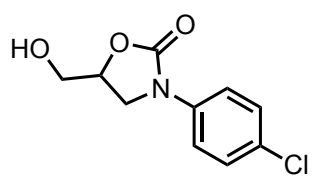

[21] R. Ilg, C. Burschka, D. Schepmann, B. Wünsch and R. Tacke, *Organometallics* **2006**, *25*, 5396-5408.
[22] C. L. J. Wang, W. A. Gregory and M. A. Wuonola, *Tetrahedron* **1989**, *45*, 1323-1326.
[23] Y. Lee, J. Choi and H. Kim, *Org. Lett*. **2018**, *20*, 5036-5039.

1H), 3.63 – 3.50 (m, 2H). **^{13}C NMR** (101 MHz, DMSO-d_6) δ 154.4, 137.5, 128.7, 127.1, 119.3, 73.2, 61.6, 45.9. **FT-IR** (neat, v in cm^{-1}): 1724 (C=O).

3-(4-bromophenyl)-5-(hydroxymethyl)oxazolidin-2-one (2i).[24] Synthesized according the general procedure (0.05 mL/min, 0.1 M, 5 mL$_n$/min CO_2) 0.368 g, light yellow solid, 86% yield. **^{1}H NMR** (400 MHz, DMSO-d_6) δ 7.65 – 7.50 (m, 4H), 5.27 – 5.13 (m, 1H), 4.77 – 4.63 (m, 1H), 4.07 (t, J = 9.0 Hz, 1H), 3.87 – 3.78 (m, 1H), 3.74 – 3.49 (m, 2H). **^{13}C NMR** (101 MHz, DMSO-d_6) δ 154.4, 138.0, 131.6, 119.7, 115.1, 73.2, 61.6, 45.9 **FT-IR** (neat, v in cm^{-1}): 1709 (C=O).

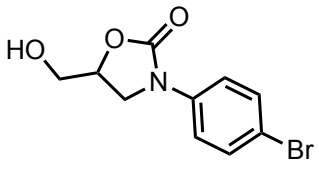

5-(hydroxymethyl)-3-(2-methoxyphenyl)oxazolidin-2-one (2j). Synthesized according the general procedure (0.05 mL/min, 0.1 M, 5 mL$_n$/min CO_2) 0.161 g, white solid, 28% yield. **^{1}H NMR** (400 MHz, DMSO-d_6) δ 7.34 – 7.24 (m, 2H), 7.15 – 7.06 (m, 1H), 7.01 – 6.91 (m, 1H), 5.19 (t, J = 5.7 Hz, 1H), 4.65 (m, 1H), 3.94 - 3.90 (m, 1H), 3.81 (s, 3H), 3.68 – 3.51 (m, 3H). **^{13}C NMR** (101 MHz, DMSO-d_6) δ 156.1, 154.7, 128.6, 128.2, 126.2, 120.5, 112.5, 74.0, 61.9, 55.7, 48.0. **FT-IR** (neat, v in cm^{-1}): 1709 (C=O).

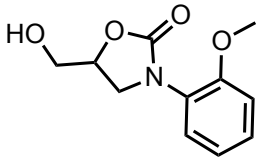

5-(hydroxymethyl)-3-(*o*-tolyl)oxazolidin-2-one (2k).[7] Synthesized according the general procedure (0.05 mL$_n$/min, 0.1 M, 5 mL$_n$/min CO_2) 0.330 g, white solid, 79% yield. **^{1}H NMR** (400 MHz, DMSO-d_6) δ 7.35 – 7.18 (m, 4H), 5.24 (t, J = 5.7 Hz, 1H), 4.75 – 4.65 (m, 1H), 4.01 – 3.91 (m, 1H), 3.74 – 3.64 (m, 2H), 3.61 – 3.52 (m, 1H), 2.22 (s, 3H). **^{13}C NMR** (101 MHz, DMSO-d_6) δ 155.6, 136.6, 135.7, 130.9, 127.6, 126.7, 126.7, 73.9, 61.8, 48.5, 17.4. **FT-IR** (neat, v in cm^{-1}): 1736 (C=O).

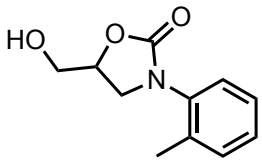

5-(hydroxymethyl)-3-(naphthalen-1-yl)oxazolidin-2-one (2l).[7] Synthesized according the general procedure (0.08 mL/min, 0.1 M, 5 mL$_n$/min CO_2) 75 ºC, 0.496 g, pink solid, 47% yield. **^{1}H NMR** (500 MHz, DMSO-d_6) δ 8.03 – 7.98 (m, 2H), 7.98 – 7.93 (m, 1H), 7.62 – 7.53 (m, 4H), 5.39 (t, J = 5.6 Hz, 1H), 4.88 – 4.81 (m, 1H), 4.15 – 4.07 (m, 1H), 3.88 (dd, J = 8.4, 5.8 Hz, 1H), 3.83 – 3.76 (m, 1H), 3.70 – 3.61 (m, 1H). **^{13}C NMR** (101 MHz, DMSO-d_6) δ 156.5, 134.5, 134.0, 129.8, 128.3, 128.1, 126.7, 126.5, 125.8, 124.9, 123.0, 74.2, 61.9, 49.6. **FT-IR** (neat, v in cm^{-1}): 1711 (C=O).

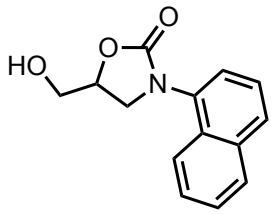

[24] S. M. Kelly, C. Han, L. Tung and F. Gosselin, *Org. Lett.* **2017**, *19*, 3021-3024.

5-(hydroxymethyl)-3-phenyloxazolidin-2-one (2m).[25] Synthesized according the general procedure (0.05 mL/min, 0.1 M, 5 mL_n/min CO_2) 0.378 g, white solid, 65% yield. **^{1}H NMR** (400 MHz, DMSO-d_6) δ 7.58 (m, 2H), 7.44 – 7.33 (m, 2H), 7.11 (m, 1H), 5.21 (t, J = 5.7, 1H), 4.70 (m, 1H), 4.08 (t, J = 9.0 Hz, 1H)), 3.84 (t, J = 9.0 Hz, 1H), 3.72 – 3.63 (m, 1H), 3.72 – 3.51 (m, 1H). **^{13}C NMR** (101 MHz, DMSO-d_6) δ 154.9, 138.6, 128.9, 123.2, 117.7, 73.1, 61.6, 46.0. FT-IR (neat, v in cm^{-1}): 1709 (C=O).

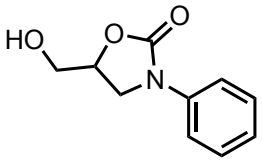

3-(2,6-di-isopropylphenyl)-5-(hydroxymethyl)oxazolidin-2-one (2n). Synthesized according the general procedure (0.08 mL/min, 0.1 M, 5 mL_n/min CO_2) 75ºC, 0.524 g, white solid, 66% yield. **^{1}H NMR** (400 MHz, $CDCl_3$) δ 7.35 (t, J = 7.7 Hz, 1H), 7.23 – 7.18 (m, 2H), 4.86 – 4.76 (m, 1H), 4.06 – 3.96 (m, 1H), 3.85 – 3.66 (m, 3H), 3.13 – 2.93 (m, 2H), 2.65 – 2.55 (m, 1H), 1.35 – 1.15 (m, 12H). **^{13}C NMR** (101 MHz, DMSO-d_6) δ 156.6, 147.4, 147.2, 131.9, 129.0, 124.0, 123.9, 73.8, 61.5, 49.2, 30.7, 28.0, 27.6, 24.3, 24.2, 23.9, 23.7. **FT-IR** (neat, v in cm^{-1}): 1720 (C=O) **ESI-MS** $[C_{16}H_{24}NO_3+H]^+$: calcd, 278.1757; found, 278.1751.

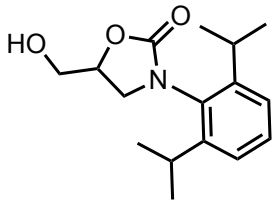

3-(2,4-dimethylphenyl)-5-(hydroxymethyl)oxazolidin-2-one (2o). Synthesized according the general procedure (0.05 mL/min, 0.1 M, 5 mL_n/min CO_2) 0.356 g, white solid, 69% yield. **^{1}H NMR** (400 MHz, DMSO-d_6) δ 7.17 (d, J = 8.0 Hz, 1H), 7.10 (s, 1H), 7.04 (d, J = 2.1 Hz, 1H), 5.28 – 5.17 (m, 1H), 4.74 – 4.60 (m, 1H), 3.93 (s, 1H), 3.72 – 3.62 (m, 2H), 3.61 – 3.51 (m, 1H), 2.27 (s, 3H), 2.17 (s, 3H). **^{13}C NMR** (101 MHz, DMSO-d_6) δ 155.6, 137.0, 135.3, 134.0, 131.3, 127.2, 126.6, 73.8, 61.8, 48.6, 20.5, 17.3. **FT-IR** (neat, v in cm^{-1}): 1723 (C=O) **ESI-MS** $[C_{12}H_{15}NNaO_3+H]^+$: calcd, 244.0944; found, 244.0956

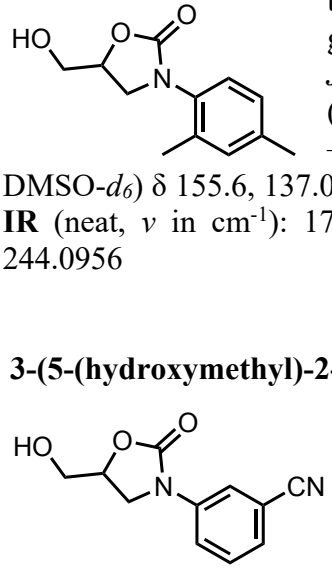

3-(5-(hydroxymethyl)-2-oxooxazolidin-3-yl)benzonitrile (2p). Synthesized according the general procedure (0.05 mL/min, 0.1 M, 5 mL_n/min CO_2), 0.356 g, white solid, 74% yield. **^{1}H NMR** (400 MHz, DMSO-d_6) δ 8.00 (s, 1H), 7.95 – 7.88 (m, 1H), 7.64 – 7.51 (m, 2H), 5.29 – 5.17 (m, 1H), 4.81 – 4.67 (m, 1H), 4.18 – 4.07 (m, 1H), 3.87 (dd, J = 6.1, 1.1 Hz, 1H), 3.77 – 3.64 (m, 1H), 3.64 – 3.53 (m, 1H). **^{13}C NMR** (101 MHz, DMSO-d_6) δ 154.4, 139.4, 130.3, 126.6, 122.1, 120.5, 118.6, 111.8, 73.5, 61.6, 45.8. **FT-IR** (neat, v in cm^{-1}): 1708 (C=O). **ESI-MS** $[C_{11}H_{10}N_2NaO_3]^+$: calcd, 241.0584; found, 241.0584.

[25] E. J. Brnardic, M. E. Fraley, R. M. Garbaccio, M. E. Layton, J. M. Sanders, C. Culberson, M. A. Jacobson, B. C. Magliaro, P. H. Hutson, J. A. O'Brien, S. L. Huszar, J. M. Uslaner, K. L. Fillgrove, C. Tang; Y. Kuo, S. M. Sur and G. D. Hartman, *Bioorg. Med. Chem. Lett.* **2010**, *20*, 3129-3133.

3.4.9. Synthesis and characterization of intermediate epoxy amines

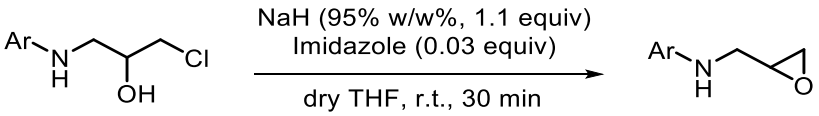

General Procedure:[26] NaH (95%, 1.1 equiv) was added at 0 ºC to a stirred solution of the desired starting material (1 equiv, 0.5 M) and imidazole (0.03 equiv) in dry THF. Then the suspension was warmed up to r.t. and stirred at the same temperature for 30 min. EtOAc was added to this mixture, after which it was washed with water (3 times). The organic fractions were joined and dried over Na_2SO_4, then filtered and the solvents removed under vacuum. The sample was further dried overnight under vacuum to get the epoxy amine target.

3-methyl-*N*-(oxiran-2-ylmethyl)aniline (1a).[2] Yellow oil, 1.320 g, 89% yield. **^{1}H NMR** (400 MHz, $CDCl_3$) δ 7.08 (t, *J* = 1.2 Hz, 1H), 6.56 (d, *J* = 0.9 Hz, 1H), 6.49 – 6.42 (m, 2H), 3.80 (bs, 1H), 3.56 – 3.46 (m, 1H), 3.29 – 3.14 (m, 2H), 2.85 – 2.76 (m, 1H), 2.73 – 2.65 (m, 1H), 2.28 (s, 3H). **^{13}C NMR** (101 MHz, $CDCl_3$) δ 148.0, 139.1, 129.3, 118.9, 113.9, 110.2, 51.1, 45.4, 45.1, 21.7.

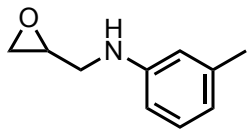

Methyl 3-((oxiran-2-ylmethyl)amino)benzoate (1b). Yellow oil, 0.273 g, 91% yield. **^{1}H NMR** (400 MHz, $CDCl_3$) δ 7.39 (dt, *J* = 7.7, 0.7 Hz, 1H), 7.31 – 7.28 (m, 1H), 7.23 (t, *J* = 7.9 Hz, 1H), 6.81 (ddd, *J* = 8.1, 2.6, 1.0 Hz, 1H), 4.06 – 3.99 (m, 1H), 3.89 (s, 3H), 3.63 – 3.55 (m, 1H), 3.29 – 3.18 (m, 2H), 2.84 – 2.80 (m, 1H), 2.70 – 2.66 (m, 1H). **^{13}C NMR** (101 MHz, $CDCl_3$) δ 167.5, 148.0, 131.3, 129.4, 119.2, 117.8, 113.4, 52.2, 50.9, 45.4, 45.0. **FT-IR** (neat, *v* in cm^{-1}): 3390, 2951, 1712, 1605, 1234, 751 **ESI-MS** $[C_{11}H_{13}NNaO_3]^+$: calcd, 230.0788; found, 230.0782.

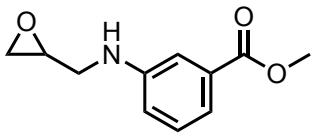

3-Methoxy-*N*-(oxiran-2-ylmethyl)aniline (1c).[27] Brown oil, 0.820 g, 99% yield. **^{1}H NMR** (400 MHz, $CDCl_3$) δ 7.09 (t, *J* = 8.1 Hz, 1H), 6.30 (ddd, *J* = 8.2, 2.4, 0.9 Hz, 1H), 6.26 (ddd, *J* = 8.0, 2.2, 0.8 Hz, 1H), 6.20 (t, *J* = 2.3 Hz, 1H), 3.89 (bs, 1H), 3.77 (s, 3H), 3.58 – 3.49 (m, 1H), 3.29 – 3.17 (m, 2H), 2.84 – 2.78 (m, 1H), 2.73 – 2.65 (m, 1H). **^{13}C NMR** (101 MHz, $CDCl_3$) δ 160.9, 149.3, 130.1, 106.1, 103.0, 99.1, 55.1, 51.0, 45.4, 45.0.

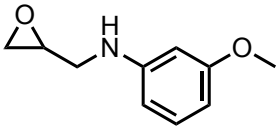

4-Methoxy-*N*-(oxiran-2-ylmethyl)aniline (1d).[28] Brown oil, 0.794 g, 95% yield. **^{1}H NMR** (400 MHz, $CDCl_3$) δ 6.85 – 6.70 (m, 2H), 6.64 – 6.55 (m, 1H), 3.74 (s, 3H), 3.66 – 3.55 (bs, 1H), 3.54 – 3.45 (m, 1H), 3.23 – 3.10 (m, 2H), 2.83 – 2.77 (m, 1H), 2.72 – 2.66 (m, 1H). **^{13}C NMR** (126 MHz, $CDCl_3$) δ 154.0, 140.2, 115.6, 113.8, 54.8, 51.9, 47.6, 45.6.

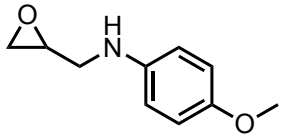

[26] N. Tsiakopoulos, C. Damianakos, G. Karigiannis, D. Vahliotis, D. Papaioannou and G. Sindona, *Arkivoc* **2002**, *13*, 79-104.

[27] K. S. MacMillan, J. Naidoo, J. Liang, L. Melito, N. S. Williams, L. Morlock, P. J. Huntington, S. J. Estill, J. Longgood, G. L. Becker, S. L. McKnight, A. A. Pieper, J. K. Brabander and J. M. Ready, *J. Am. Chem. Soc.* **2011**, *133*, 1428-1437.

[28] D. Bradley and G. Williams, *J. Org. Chem.* **2009**, *24*, 9509–9512.

1-(4-((Oxiran-2-ylmethyl)amino)phenyl)ethan-1-one (1e).[7] White solid, 0.401 g 93% yield.

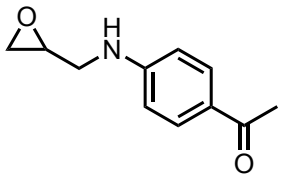

^{1}H NMR (300 MHz, $CDCl_3$) δ 7.95 – 7.79 (m, 2H), 6.73 – 6.57 (m, 2H), 4.41 (bs, 1H), 3.72 – 3.60 (m, 1H), 3.38 – 3.18 (m, 2H), 2.92 – 2.81 (m, 1H), 2.75 – 2.67 (m, 1H), 5.54 (s, 3H). **^{13}C NMR** (101 MHz, $CDCl_3$) δ 196.5, 151.9, 130.9, 127.4, 111.8, 50.7, 45.3, 44.3, 26.2.

Methyl-4-((oxiran-2-ylmethyl)amino)benzoate (1f). White solid, 0.837 g, 98% yield. **^{1}H NMR** (400 MHz, DMSO-d_6) δ 7.73 – 7.61 (m, 2H), 6.75 – 6.70 (m, 1H), 6.69 – 6.63 (m, 2H), 3.74 (d, J = 1.1 Hz, 3H), 3.49 – 3.40 (m, 1H), 3.18 – 3.06 (m, 2H), 2.78 – 2.70 (m, 1H), 2.60 – 2.54 (m, 1H). **^{13}C NMR** (101 MHz, DMSO-d_6) δ 204.0, 190.5, 168.6, 153.8, 148.8, 88.9, 88.2, 82.3, 81.8, 77.8, 77.6, 77.4, 77.2, 77.0, 76.7, 76.5. **FT-IR** (neat, ν in cm^{-1}): 3362, 2946, 1679, 1600, 1278 **ESI-MS** $[C_{11}H_{13}NNaO_3]^+$: calcd, 230.0788; found, 230.0784.

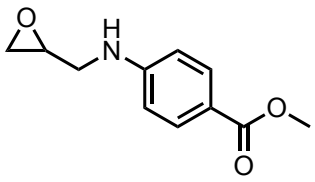

4-Fluoro-*N*-(oxiran-2-ylmethyl)aniline (1g).[7] Violet oil, 0.824 g, 99% yield. **^{1}H NMR** (400 MHz, $CDCl_3$) δ 6.93 – 6.84 (m, 2H), 6.62 – 6.54 (m, 2H), 3.75 (bs, 1H), 3.56 – 3.45 (m, 1H), 3.23 – 3.12 (m, 2H), 2.85 – 2.79 (m, 1H), 2.73 – 2.66 (m, 1H). **^{13}C NMR** (101 MHz, $CDCl_3$) δ 116.0, 115.8, 114.1, 114.0, 77.5, 77.2, 76.8, 51.1, 45.9, 45.5.

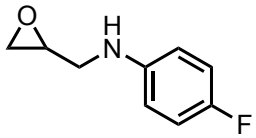

4-chloro-*N*-(oxiran-2-ylmethyl)aniline (1h).[12] Yellow oil, 0.257 g 68% yield. **^{1}H NMR** (400 MHz, $CDCl_3$) δ 7.15 – 7.09 (m, 2H), 6.59 – 6.52 (m, 2H), 3.88 (bs, 1H), 3.58 – 3.47 (m, 1H), 3.23 – 3.14 (m, 2H), 2.84 – 2.79 (m, 1H), 2.70 – 2.65 (m, 1H). **^{13}C NMR** (101 MHz, $CDCl_3$) δ 146.6, 129.3, 122.6, 114.2, 51.0, 45.0, 45.2.

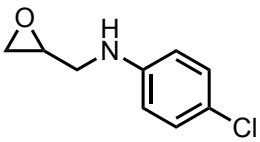

4-Bromo-*N*-(oxiran-2-ylmethyl)aniline (1i).[7] Yellow oil, 0.416 g, 90% yield. **^{1}H NMR** (400 MHz, $CDCl_3$) δ 7.35 – 7.18 (m, 2H), 6.59 – 6.45 (m, 2H), 3.90 (bs, 1H), 3.58 – 3.46 (m, 1H), 3.23 – 3.11 (m, 2H), 2.83 – 2.78 (m, 1H), 2.71 – 2.63 (m, 1H). **^{13}C NMR** (101 MHz, $CDCl_3$) δ 147.0, 132.1, 114.7, 109.6, 50.9, 45.4, 45.1.

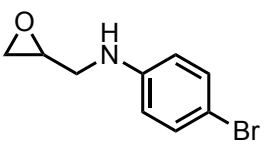

2-Methoxy-*N*-(oxiran-2-ylmethyl)aniline (1j).[29] Dark oil, 99% 0.850 g, 98% yield. **^{1}H NMR** (400 MHz, $CDCl_3$) δ 6.88 (td, J = 7.6, 1.5 Hz, 1H), 6.78 (dd, J = 7.9, 1.5 Hz, 1H), 6.73 – 6.63 (m, 2H), 4.46 (bs, 1H), 3.85 (s, 3H), 3.57 – 3.48 (m, 1H), 3.31 – 3.19 (m, 2H), 2.84 – 2.80 (m, 1H), 2.72 – 2.66 (m, 1H). **^{13}C NMR** (101 MHz, $CDCl_3$) δ 147.0, 137.8, 121.2, 117.1, 110.0, 109.6, 55.4, 51.1, 45.5, 45.1. **FT-IR** (neat, ν in cm^{-1}): 3413, 2936, 1061, 1511, 1220. **ESI-MS** $[C_{10}H_{14}NO_2]^+$: calcd, 180.1019; found, 180.1019

[29] Patent, CN2021-10747869, CN113461629 A 2021-07-01, Preparation of the compound 5-hydroxymethyl-oxazolidin-2-one.

2-Methyl-*N*-(oxiran-2-ylmethyl)aniline (1k).[7] Violet oil, 0.494 g, 82% yield. **^{1}H NMR** (400 MHz, $CDCl_3$) δ 7.16 – 7.10 (m, 1H), 7.07 (d, *J* = 0.9 Hz, 1H), 6.72 – 6.67 (m, 1H), 6.67 – 6.62 (m, 1H), 3.73 (bs, 1H), 3.63 – 3.55 (m, 1H), 3.33 – 3.22 (m, 2H), 2.87 – 2.82 (m, 1H), 2.74 – 2.69 (m, 1H), 2.16 (s, 3H). **^{13}C NMR (101 MHz, $CDCl_3$)** δ 145.9, 130.1, 127.3, 122.50, 117.7, 110.0, 77.5 77.2, 76.8, 51.1, 45.6, 45.1, 17.6.

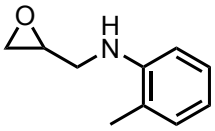

***N*-(oxiran-2-ylmethyl)naphthalen-1-amine (1l).**[7] Brownish solid, 1.01 g, 94% yield. **^{1}H NMR** (300 MHz, $CDCl_3$) δ 7.85 – 7.73 (m, 2H), 7.50 – 7.39 (m, 2H), 7.38 – 7.21 (m, 2H), 6.64 (d, *J* = 1.2 Hz, 1H), 4.56 (bs, 1H), 3.77 – 3.64 (m, 1H), 3.45 – 3.30 (m, 2H), 2.87 (dd, *J* = 3.9, 0.9 Hz, 1H), 2.79 – 2.74 (m, 1H). **^{13}C NMR** (101 MHz, $CDCl_3$) δ 143.2, 134.5, 128.8, 126.6, 126.0, 125.0, 123.7, 120.1, 118.2, 104.8, 51.0, 45.7, 45.2.

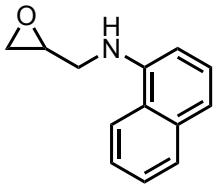

***N*-(oxiran-2-ylmethyl)aniline (1m).**[7,12] Transparent oil, 0.777 g, 97% yield. **^{1}H NMR** (400 MHz, $CDCl_3$) δ 7.22 – 7.14 (m, 2H), 6.74 (tt, *J* = 7.4, 1.1 Hz, 1H), 6.68 – 6.62 (m, 2H), 3.87 (bs, 1H), 3.58 – 3.50 (m, 1H), 3.28 – 3.24 (m, 1H), 3.24 – 3.18 (m, 1H), 2.85 – 2.79 (m, 1H), 2.73 – 2.67 (m, 1H). **^{13}C NMR** (101 MHz, $CDCl_3$) δ 148.0, 129.5, 118.1, 113.1, 77.5, 77.2, 76.8, 51.1, 45.5, 45.1.

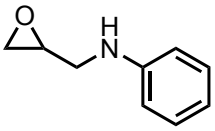

2,6-Di-*iso*-propyl-*N*-(oxiran-2-ylmethyl)aniline (1n). Orange oil, 0.373 g, 99% yield. **^{1}H NMR** (400 MHz, $CDCl_3$) δ 7.14 – 7.04 (m, 3H), 3.37 – 3.17 (m, 4H), 2.91 (dd, *J* = 12.8, 5.6 Hz, 1H), 2.85 (dd, *J* = 5.0, 3.9 Hz, 1H), 2.80 – 2.76 (m, 1H), 1.29 – 1.22 (m, 12H). **^{13}C NMR** (101 MHz, $CDCl_3$) δ 142.9, 142.4, 124.2, 123.8, 53.2, 51.7, 45.6, 27.7, 24.4, 24.4. **FT-IR** (neat, *v* in cm^{-1}): 2960, 1447, 1255, 752 **ESI-MS** $[C_{15}H_{24}NO+H]^+$: calcd, 234.1863; found, 234.1852.

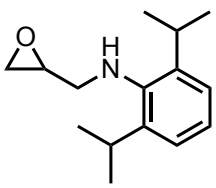

2,4-Dimethyl-*N*-(oxiran-2-ylmethyl)aniline (1o). Dark oil, 0.382 g, 90% yield. **^{1}H NMR** (400 MHz, $CDCl_3$) δ 6.98 – 6.88 (m, 2H), 6.57 (d, *J* = 8.1 Hz, 1H), 3.61 – 3.52 (m, 1H), 3.30 – 3.20 (m, 2H), 2.86 – 2.82 (m, 1H), 2.73 – 2.69 (m, 1H), 2.25 (s, 3H), 2.15 (s, 3H). **^{13}C NMR** (101 MHz, $CDCl_3$) δ 143.6, 131.3, 127.5, 126.8, 122.7, 110.3, 51.2, 45.6, 45.4, 20.4, 17.5. **FT-IR** (neat, *v* in cm^{-1}): 3409, 2917, 1618, 1513 **ESI-MS** $[C_{11}H_{16}NO]^+$: calcd,178.1226; found, 178.1218.

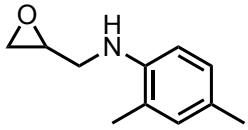

3-((Oxiran-2-ylmethyl)amino)benzonitrile (1p). Yellow oil, 0.310 g, 75% yield. **^{1}H NMR** (400 MHz, $CDCl_3$) δ 7.25 – 7.19 (m, 1H), 7.00 – 6.95 (m, 1H), 6.86 – 6.80 (m, 2H), 4.15 (bs, 1H), 3.63 – 3.52 (m, 1H), 3.24 – 3.15 (m, 2H), 2.84 (dd, *J* = 4.8, 3.8 Hz, 1H), 2.70 – 2.64 (m, 1H). **^{13}C NMR** (101 MHz, $CDCl_3$) δ 148.2, 130.1, 121.5, 119.5, 117.6, 115.2, 50.7, 45.3, 44.7. **FT-IR** (neat, *v* in cm^{-1}): 3380, 2919, 2226, 1601, 1491, 780 **ESI-MS** $[C_{10}H_{11}N_2O+H]^+$: calcd, 175.0866; found, 175.0874.

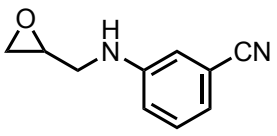

3.4.10. Synthesis and characterization of intermediate halohydrins

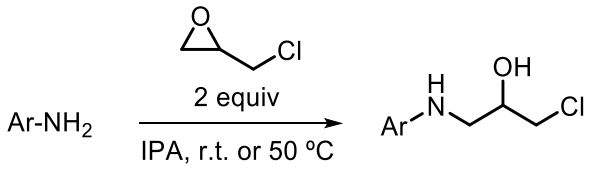

General procedure:[2] To a stirred solution of the respective aniline (25.0 mmol) in *iso*-propanol (6.4 mL, 2 M) at 0 ºC was slowly added epichlorohydrin (50.0 mmol) and then the reaction mixture was further stirred at r.t. for 16 h. The solvent was evaporated and the mixture was purified by column chromatography over silica to obtain the halohydrin product.

3-Methyl-*N*-(oxiran-2-ylmethyl)aniline (1'a).[2] Orange oil, 5.77 g , 57% yield. **^{1}H NMR** (500 MHz, $CDCl_3$) δ 7.16 (m, 1H), 6.64 (m, 1H), 6.54 (m, 2H), 3.89 (bs, 1H), 3.61 –3.52 (m, 1H), 3.28 (m, 2H), 2.87 (m, 1H), 2.75 (m, 1H), 2.40 –2.33 (m, 3H). **^{13}C NMR** (101 MHz, $CDCl_3$) δ 148.0, 139.1, 129.3, 118.9, 113.9, 110.2, 51.1, 45.4, 45.1, 21.7.

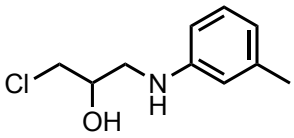

Methyl 3-((3-chloro-2-hydroxypropyl)amino)benzoate (1'b). Yellowish oil, 2.05 g, 51% yield. **^{1}H NMR** (400 MHz, $CDCl_3$) δ 7.43 (ddd, *J* = 7.6, 1.6, 1.0 Hz, 1H), 7.34 – 7.32 (m, 1H), 7.31 – 7.22 (m, 1H), 6.87 (ddd, *J* = 8.1, 2.6, 1.0 Hz, 1H), 4.10 (m, 1H), 3.91 (s, 3H), 3.75 – 3.62 (m, 2H), 3.44 (dd, *J* = 13.2, 4.3 Hz, 1H), 3.29 (dd, *J* = 13.2, 7.3 Hz, 1H). **^{13}C NMR** (101 MHz, $CDCl_3$) δ 167.6, 147.90, 131.3, 129.5, 119.5, 118.1, 113.9, 77.5, 77.2, 76.8, 69.9, 52.3, 47.8, 47.2. **FT-IR** (neat, *v* in cm^{-1}): 3393, 1702, 1604, 1437, 1282. **ESI-MS** $[C_{15}H_{24}NO+H]^+$: calcd, 244.0735; found, 244.0731.

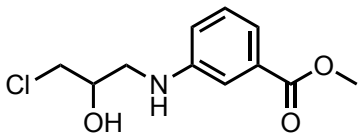

1-Chloro-3-((3-methoxyphenyl)amino)propan-2-ol (1'c).[30] Dark oil, 0.996 g, 26% yield. **^{1}H NMR** (400 MHz, $CDCl_3$) δ 7.10 (t, *J* = 8.1 Hz, 1H), 6.30 (dddd, *J* = 16.8, 8.0, 2.3, 0.9 Hz, 2H), 6.22 (t, *J* = 2.3 Hz, 1H), 4.15 – 4.03 (m, 1H), 3.73 – 3.61 (m, 2H), 3.38 (dd, *J* = 13.3, 4.5 Hz, 1H), 3.24 (dd, *J* = 13.4, 7.1 Hz, 1H), 2.44 (bs, 1H). **^{13}C NMR** (101 MHz, $CDCl_3$) δ 130.1, 106.1, 103.2, 99.2, 69.6, 54.7, 47.6, 46.9.

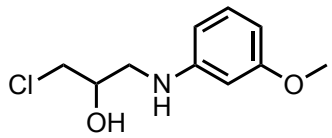

1-Chloro-3-((4-methoxyphenyl)amino)propan-2-ol (1'd).[12] Dark oil, 2.63 g 50% yield. **^{1}H NMR** (400 MHz, $CDCl_3$) δ 6.82 – 6.77 (m, 2H), 6.67 – 6.61 (m, 2H), 4.11 – 4.01 (m, 1H), 3.75 (s, 3H), 3.71 – 3.61 (m, 2H), 3.34 (dd, *J* = 13.1, 4.3 Hz, 1H), 3.19 (dd, *J* = 13.1, 7.2 Hz, 1H), 3.07 – 2.33 (bs, 1H). **^{13}C NMR** (101 MHz, $CDCl_3$) δ 152.9, 142.0, 115.1, 115.0, 70.00 55.9, 48.4, 47.8.

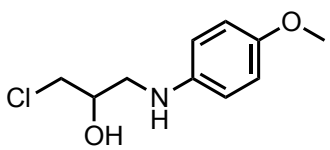

[30] E. Raflee, S. Tangestaninejad, M. H. Habibi and V. Mirkhani, *Synth. Commun.* **2004**, 3673-3681.

1-(4-((3-Chloro-2-hydroxypropyl)amino)phenyl)ethan-1-one (1'e). Transparent oil, 2.05 g, purity 99%, 41% yield (50 ºC, 48 h) **^{1}H NMR** (400 MHz, $CDCl_3$) δ 7.86 – 7.79 (m, 2H), 6.67 – 6.57 (m, 2H), 4.60 (s, 1H), 4.16 – 4.06 (m, 1H), 3.74 – 3.59 (m, 2H), 3.52 – 3.42 (m, 1H), 3.35 – 3.26 (m, 1H), 2.68 (d, *J* = 5.2 Hz, 1H), 2.50 (s, 3H). **^{13}C NMR** (101 MHz, $CDCl_3$) δ 152.0, 131.0, 127.5, 112.0, 69.9, 47.6, 46.3, 26.2. **FT-IR** (neat, *v* in cm^{-1}): 3300, 1644, 1587, 1279, 1174. **ESI-MS** $[C_{11}H_{15}ClNO_2]^+$: calcd, 228.0786; found, 228.0790.

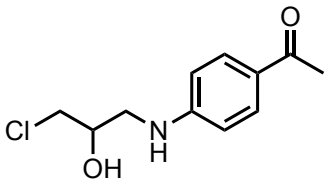

Methyl 4-((3-chloro-2-hydroxypropyl)amino)benzoate (1'f). White solid, 2.05 g, 45% yield **^{1}H NMR** (400 MHz, $CDCl_3$) δ 7.99 – 7.78 (m, 2H), 6.70 – 6.55 (m, 2H), 4.56 – 4.48 (bs, 1H), 4.16 – 4.07 (m, 1H), 3.87 (s, 3H), 3.74 – 3.61 (m, 2H), 3.46 (ddd, *J* = 13.4, 6.7, 4.4 Hz, 1H), 3.31 (ddd, *J* = 13.4, 7.2, 5.4 Hz, 1H), 2.64 (d, *J* = 5.2 Hz, 1H). **^{13}C NMR** (101 MHz, $CDCl_3$) δ 167.4, 151.8, 131.8, 119.2, 112., 69.9, 51.8, 47.6, 46.4. **FT-IR** (neat, *v* in cm^{-1}): 3354, 2947, 1678, 1607, 1280, 1107. **ESI-MS** $[C_{11}H_{14}ClNNaO_3]^+$: calcd, 266.0554; found, 266.0551.

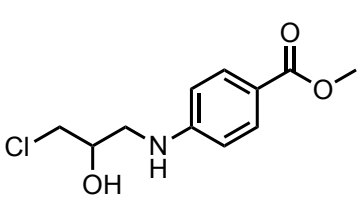

1-Chloro-3-((4-fluorophenyl)amino)propan-2-ol (1'g).[31] Violet oil, 2.62 g, 51% yield. **^{1}H NMR** (400 MHz, $CDCl_3$) δ 6.95 – 6.87 (m, 2H), 6.70 – 6.64 (m, 2H), 4.13 – 4.07 (m, 1H), 3.88 – 3.70 (bs, 1H), 3.70 – 3.59 (m, 2H), 3.34 (dd, *J* = 13.0, 4.2 Hz, 1H), 3.20 (dd, *J* = 13.0, 7.4 Hz, 1H). **^{13}C NMR** (101 MHz, $CDCl_3$) δ 155.8, 144.2, 116.2, 115.9, 115.2, 115.2, 69.7, 48.61, 47.7, 31.0.

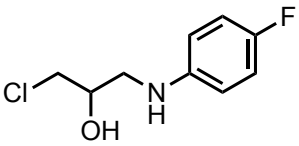

1-Chloro-3-((4-chlorophenyl)amino)propan-2-ol (1'h).[12] Yellow oil, 3.90 g, 45% yield. **^{1}H NMR** (400 MHz, $CDCl_3$) δ 7.19 – 7.09 (m, 2H), 6.62 – 6.54 (m, 2H), 4.11 – 4.03 (m, 1H), 3.72 – 3.58 (m, 2H), 3.35 (dd, *J* = 13.2, 4.3 Hz, 1H), 3.20 (dd, *J* = 13.2, 7.2 Hz, 1H), 2.46 (s, 1H). **^{13}C NMR** (101 MHz, $CDCl_3$) δ 146.4, 129.3, 123.1, 114.6, 69.9, 47.8, 47.4.

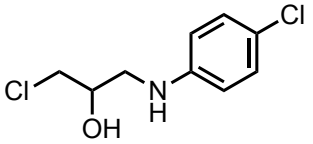

1-chloro-3-((4-bromophenyl)amino)propan-2-ol (1'i).[32] Yellow oil, 2.10 g, 54% yield. **^{1}H NMR** (400 MHz, $CDCl_3$) δ 7.31 – 7.21 (m, 2H), 6.56 – 6.48 (m, 2H), 4.09 – 4.00 (m, 1H), 3.71 – 3.57 (m, 2H), 3.33 (dd, *J* = 13.2, 4.3 Hz, 1H), 3.19 (dd, *J* = 13.2, 7.2 Hz, 1H), 3.06 – 2.21 (m, 1H). **^{13}C NMR** (101 MHz, $CDCl_3$) δ 146.9, 132.2, 115.0, 110.0, 69.9, 47.8, 47.2.

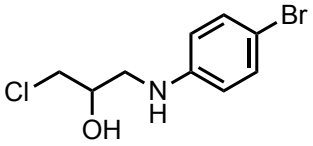

[31] A. Kamal, B. R. Prasad, A. M. Reddy and M. N. A. Khan, *Catal. Commun.* **2007**, *8*, 1876–1880.
[32] V. Mirkhani, S.Tangestaninejad, B. Yadollahi and L. Alipanah, *Catal. Lett.* **2005**, *101*, 93-97.

1-Chloro-3-((2-methoxyphenyl)amino)propan-2-ol (1'j).[33] Dark oil, 2.62 g, 49% yield. **^{1}H NMR** ^{1}H NMR (400 MHz, $CDCl_3$) δ 6.88 (td, *J* = 7.6, 1.5 Hz, 1H), 6.79 (dd, *J* = 8.0, 1.5 Hz, 1H), 6.75 – 6.69 (m, 1H), 6.67 (dd, *J* = 7.8, 1.5 Hz, 1H), 4.53 (bs, 1H), 4.15 – 4.05 (m, 1H), 3.86 (s, 3H), 3.75 – 3.61 (m, 2H), 3.45 – 3.34 (m, 1H), 3.33 – 3.24 (m, 1H), 2.48 (bs, 1H). **^{13}C NMR** (101 MHz, $CDCl_3$) δ 121.4, 117.5, 110.4, 109.8, 70.1, 55.6, 47.9, 47.1.

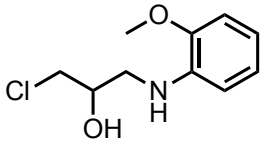

1-Chloro-3-(*o*-tolyl-amino)propan-2-ol (1'k).[34] Dark oil, 1.79 g, 19% yield. **^{1}H NMR** (400 MHz, $CDCl_3$) δ 7.16 – 7.10 (m, 1H), 7.10 – 7.06 (m, 1H), 6.74 – 6.68 (m, 1H), 6.68 – 6.63 (m, 1H), 4.18 – 4.10 (m, 1H), 3.87 (bs, 1H), 3.76 – 3.64 (m, 2H), 3.48 – 3.39 (m, 1H), 3.33 – 3.24 (m, 1H), 2.17 (s, 3H). **^{13}C NMR** (101 MHz, $CDCl_3$) δ 130.5, 127.3, 118.0, 109.8, 67.8, 48.0, 47.2, 17.6.

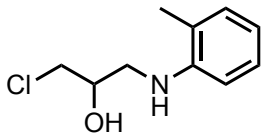

1-Chloro-3-(naphthalen-1-ylamino)propan-2-ol (1'l).[35] Violet oil, 1.26 g, 26% yield. **^{1}H NMR** (400 MHz, $CDCl_3$) δ 7.90 – 7.76 (m, 2H), 7.50 – 7.42 (m, 2H), 7.39 – 7.28 (m, 2H), 6.69 (d, *J* = 1.3 Hz, 1H), 4.32 – 4.20 (m, 1H), 3.82 – 3.67 (m, 2H), 3.64 – 3.53 (m, 1H), 3.48 – 3.37 (m, 1H), 2.61 (bs, 1H). **^{13}C NMR** (101 MHz, $CDCl_3$) δ 129.2, 126.9, 126.4, 125.6, 120.4, 119.1, 105.8, 77.8, 77.5, 77.2, 70.2, 48.4, 47.9.

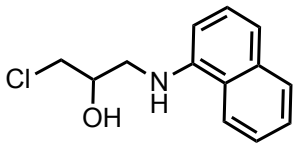

1-Chloro-3-(phenylamino)propan-2-ol (1'm).[36] Yellow oil, 2.36 g, 51% yield. **^{1}H NMR** (400 MHz, $CDCl_3$) δ 7.23 – 7.16 (m, 2H), 6.80 – 6.74 (m, 1H), 6.72 – 6.66 (m, 2H), 4.13 – 4.05 (m, 1H), 3.71 – 3.59 (m, 2H), 3.55 – 3.33 (m, 2H), 3.24 (dd, *J* = 13.3, 7.2 Hz, 1H). **^{13}C NMR** (101 MHz, $CDCl_3$) δ 147.5, 129.6, 118.8, 113.8, 77.5, 77.2, 76.8, 69.9, 47.8, 47.6, 31.1.

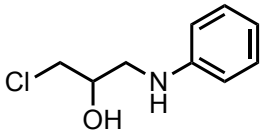

1-Chloro-3-((2,6-di-*iso*-propylphenyl)amino)propan-2-ol (1'n).[37] Reddish solid, 2.94 g, 44% yield. **^{1}H NMR** (500 MHz, $CDCl_3$) δ 7.15 – 7.03 (m, 3H), 4.10 – 4.03 (m, 1H), 3.75 – 3.65 (m, 2H), 3.38 – 3.22 (m, 2H), 3.11 – 3.03 (m, 1H), 3.03 – 2.95 (m, 1H), 2.82 (bs, 1H), 1.25 (d, *J* = 6.9 Hz, 12H). **^{13}C NMR** (101 MHz, $CDCl_3$) δ 143.0, 142.2, 124., 123.81, 70.9, 54.4, 47.9, 27.7, 24.4.

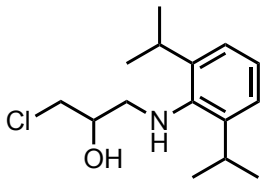

[33] A.V. Nakhate, A.M. Doke and G. D. Yadav, *Ind. Engin. Chem. Res.* **2016**, *41*, 10829-10838.
[34] L. Saikia, J.K. Satyarthi, D. Srinivas and K. Ratnasamy, *J. Catal.* **2007**, *252*, 148-160.
[35] S. Bansal, Y. Kumar, P. Pippal, D. K. Das, P. Pramanik and P. P. Singh, ***New J. Chem.*** **2017**, ***41***, 2668-2671.
[36] A. K. Chakraborti. S. Rudrawar and A. Kondaskar, *Eur. J. Org. Chem*. **2004**, 3597-3600.
[37] Y. L. N. Murthy, B. S. Diwakar, B. Govindh, R. Venu and K. Nagalakshmi, *Chem. Sci. Trans.* **2013**, *3*, 805-812.

1-Chloro-3-((2,4-dimethylphenyl)amino)propan-2-ol (1'o).[38] Dark oil, 2.54 g, 37 % yield.

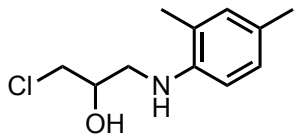

^{1}H NMR (400 MHz, $CDCl_3$) δ 6.95 (d, *J* = 2.1 Hz, 1H), 6.92 (s, 1H), 6.59 (d, *J* = 8.0 Hz, 1H), 4.17 – 4.09 (m, 1H), 3.74 – 3.62 (m, 2H), 3.44 – 3.37 (m, 1H), 3.16 – 2.50 (bs, 1H), 2.24 (s, 3H), 2.16 (s, 3H). **^{13}C NMR** (101 MHz, $CDCl_3$) δ 143.3, 131.4, 127.6, 123.2, 110.9, 69.9, 48.0, 47.7, 20.5, 17.6.

3-((3-Chloro-2-hydroxypropyl)amino)benzonitrile (1'p). Yellow oil, 3.20 g, 36% yield.

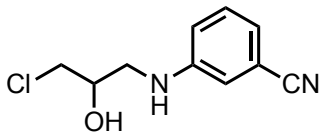

^{1}H NMR (400 MHz, $CDCl_3$) δ 7.29 – 7.19 (m, 1H), 6.99 (dt, *J* = 7.6, 1.2 Hz, 1H), 6.88 – 6.80 (m, 2H), 4.30 (bs, 1H), 4.15 – 4.03 (m, 1H), 3.74 – 3.60 (m, 2H), 3.44 – 3.32 (m, 1H), 3.28 – 3.17 (m, 1H), 2.57 (d, *J* = 5.1 Hz, 1H). **^{13}C NMR** (101 MHz, $CDCl_3$) δ 148.3, 130.1, 121.4, 119.5, 117.8, 115.4, 112.9, 69.8, 47.4, 46.6. **FT-IR** (neat, *v* in cm^{-1}): 3387, 2228, 1724, 1601, 1268. **ESI-MS** $[C_{10}H_{11}ClN_2NaO]^+$: calcd, 233.0452; found, 233.0443.

[38] Z. Du, W. Zhang, Y. Zhang and Z. Wei, *J. Chem. Res.* **2011**, *12*, 726-728.

3.4.11. Schematic illustration of the vent oven

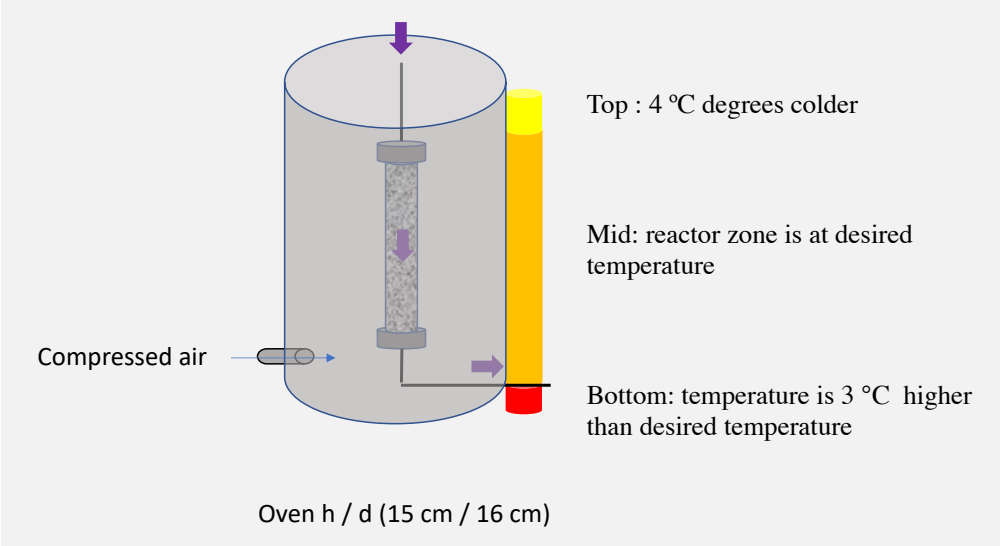

Figure 9. The figure shows the schematic set up of the ventilating oven. A digital thermometer was used to measure the temperature at different heights (*h*) in order to decide where to position the reactor. The oven was heated by an IKA heating plate, the oven was located on the top of the plate and the IKA sensor placed close to the reactor and inserted from a hole in the oven roof. To ensure a "homogeneous" temperature, compressed air was flowed from a channel located at the lower part of the oven and kept at a low flow during the experiments. *d* = diameter.

3.4.12. Auto-collector programming

A raspberry pi 4b was used as microcontroller, it was connected to a the Microservo SG90 (average price ~3€ at Amazon). The Servo was located in a polystyrene platform covered with Aluminum tape to protect it from any possible solvent leakage. The servo was controlled by a code written in Python using Mu a simple python editor. The code was modified from the one that can be found at the following link:
https://www.explainingcomputers.com/pi_servos_video.html

Python3 code for homemade auto-collector

```
# Import libraries
import RPi.GPIO as GPIO
import time

# Set GPIO numbering mode
GPIO.setmode(GPIO.BOARD)
#  f number of fractions to be collected
f = int(input('how many fractions (values between 1 and 10)?'))
#  col number of seconds in which the collector stays still until next impulse
col = int(input('how many seconds do you want to collect?'))
# first fraction
f0 = int(input('how long do you want to collect f0 ?'))

#  Set pin 15 as an output, and set servo1 as pin 11 as PWM
GPIO.setup(15, GPIO.OUT)
# Note 15 is pin, 50 = 50Hz pulse
servo1 = GPIO.PWM(15, 50)

#  start PWM running, but with value of 0 (pulse off)
servo1.start(0)
f_str = str(f)
print('collecting ' + f_str + ' fractions')
col_str = str(col)
print(col_str + ' seconds collecting in every vial')
f0_str = str(f0)
print(f0_str + ' seconds collected in vial 0 ')
time.sleep(f0)

#  Let's move the servo!
print('starting collection')

# Define variable duty
duty = 2

# Loop for duty values from 2 to 12 (0 to 180 degrees)
while duty <= 12:
    servo1.ChangeDutyCycle(duty)
    time.sleep(0.3)
    servo1.ChangeDutyCycle(0)
```

```
        time.sleep(col)
        duty = duty + (10/f)

    # Wait a couple of seconds
    time.sleep(0.3)

    # Turn back to 90 degrees
    print('Turning back to initial position')
    servo1.ChangeDutyCycle(2)
    time.sleep(0.5)
    servo1.ChangeDutyCycle(0)
    time.sleep(1.5)

    #  turn back to 0 degrees
    print('Turning back to 0 degrees')
    servo1.ChangeDutyCycle(2)
    time.sleep(0.5)
    servo1.ChangeDutyCycle(0)

    #  Clean things up at the end
    servo1.stop()
    GPIO.cleanup()
    print('Going back to position 0')
```

Chapter 4: Organocatalytic N-Formylation of Amines by CO_2 under Continuous Flow

4.1 Introduction

4.1.1 N-formylation of amines

Carbon dioxide (CO_2) is one of the most important industrial pollutants but also represents one of the cheapest and most abundant C_1 carbon synthons.[1] It is far less toxic than alternative carbon reagents such as phosgene and its derivatives. Thus, replacing the latter by CO_2 in transformations creates more benign alternative routes within the area of organic synthesis.[2] Among other uses, CO_2 can be reduced to produce compounds such as formic acid, methanol and methane, which are regarded as energy vectors. Alternatively, it can be 'trapped' by organic molecules creating more complex structures.[3] In most of the reported cases that are based on CO_2 conversions, a co-reagent is utilized that typically is a C- or N-centered nucleophile.

Within this realm, the formation of a C–N bond through *N*-formylation reaction is highly interesting because it creates versatile intermediates that can be used in cyclization reactions and as precursors for isocyanates or enaminones, whereas the formyl group also has potential as a protecting group.[4] Considering this, there has been significant interest in the development of suitable methodologies to prepare *N*-formamides.[5] Most of the formyl group donors used in these reactions are derivatives of carbon dioxide (*i.e.*, by in situ reduction of CO_2) using various reducing agents. While the most economical and sustainable reductant would be H_2, its use usually requires high temperature, high pressure and the presence of a (precious) metal-based catalyst. Moreover, in some of these cases the addition of a base additive is also required.[6] Other more easily activated hydride sources are boranes, but these reagents may be sensitive to moisture and air, this behavior limiting practical operations. Another alternative is represented by silanes, and this latter class of compounds combines high stability and modularity, which allows to develop practical reductive approaches and fine-tuning of the reactivity of the Si-H bond.[7]

Several classes of catalysts have been used in the *N*-formylation of amines such as ionic liquids,[8] inorganic salts ($CsCO_3$, K_2CO_3),[9] transition metal complexes,[6,10] and

---

1 a) G. Yuan, C. Qi, W. Wu, H. Jiang, *Curr. Opin. Green Sustain. Chem.* **2017**, *3*, 22-27; b) A. Otto, T. Grube, S. Schiebahn and D. Stolten, *Energy Environ. Sci.,* **2015***, 8,* 3283-3297; c) C. Das Neves Gomes, O. Jacquet, C. Villiers, P. Thuery, M. Ephritikhine and T. Cantat, *Angew. Chem. Int. Ed.* **2012**, *51*, 187-190.

2 a) H. Seo, L.V. Nguyen, T.F. Jamison, *Adv. Synth. Catal.* **2019**, *361*, 247-264; b) Y. Li, X. Cui, K. Dong, K. Junge and M. Beller, *ACS Catal.* **2017**, *7*, 1077–1086; c) Q.-W Song, Z.-H Zhou and L.-N He, *Green Chem.* **2017**, *19*, 3707-3728.

3 Q. Liu, L. Wu, R. Jackstell and M. Beller, *Nat Commun.* **2015**, *6*, 5933.

4 a) Z. Ma, Y. Huang, K. Wan, F. Zhu, C. Sheng, S. Chen, D. Liu and G. Dong, *Bioorg. Med. Chem. Lett.* **2021***, 40*, 127954-127962; b) W. Cao, S. Li, M. Xu, H. Li, X. Xu, Y. Lan and S. Ji, *Angew. Chem. Int. Ed.* **2020**, *59*, 21425-21430; c) T. Miura, Y. Funakoshi, T. Tanaka and M. Murakami, *Org. Lett.* **2014**, *16*, 10, 2760–2763; d) J. O. Rathi and G. S. Shankarling, *Chem. Select* **2020**, *5*, 6861–689; e) S. R. Wilson and M. F. Price, *Synth. Commun*. **1982**, 657-663.

5 For a review, see: M. Nasrollahzedeh, N. Motahharifar, M. Sajjadi, A. M. Aghbolagh, M. Shokouhimehr and R. S. Varma, *Green Chem*. **2019**, *21*, 5144-5167.

6 J. Chen, M. McGraw, E. Y.-X. Chen, *ChemSusChem* **2019**, *12*, 4543-4569.

7 a) Z. Li, Z. Yu, X. Luo, C. Li, H. Wu, W. Zhao, H. Li and S. Yang, *RSC Adv*. **2020**, *10*, 33972-34005; b) Q. Shen, X. Chen, Y. Tan, J. Chen, L. Chen and S. Tan, *ACS Appl. Mater. Interfaces*, **2019**, *11*, 38838-38848.

8 a) T. Murata, M. Hiyoshi, M. Ratanasak, J. Hasegawa and T. Ema, *Chem. Commun*. **2020**, *56*, 5783-5786; b) M. Hulla, F. D. Bobbink, S. Das and P. J. Dyson, *ChemCatChem* **2016**, *8*, 3338-3342; c) X. F. Liu, X. Y. Li, C. Qiao, H. C. Fu and L. N. He, *Angew. Chem. Int. Ed.* **2017**, *56*, 7425-7429.

9 a) K. Motokura, M. Naijo, S. Yamaguchi, A. Miyaji and T. Baba, *Chem. Lett.* **2015**, *44*, 1217-1219; b) C. Fang, C. Lu, M. Liu, Y. Zhu, Y. Fu and B.-L. Lin, *ACS Catal.* **2016**, *6*, 7876-7881; c) D. Nale and B. Bhanage, *Synlett*. **2016**, 1413-1417.

10 Y. Zhang, T. Zhang and S. Das, *Green Chem.* **2020**, *22*, 1800-1820.

organocatalysts.[11] Within this latter family of catalytic systems, NHCs (homogeneous and heterogeneous *N*-heterocyclic carbenes)[12] and organic superbases[13] have clearly dominated the field as preferred and highly efficient modulators. We have recently become interested in the use of *N*-heterocyclic structures such as TBD and DBU as efficient and readily available organocatalysts in the area of CO_2 valorization catalysis.[14] Furthermore, we recently reported that such organic superbases can be easily supported onto different supports providing heterogeneous catalysts with potential for continuous flow synthesis of CO_2-based heterocycles such as glycerol carbonate[15] and related oxazolidinones.[16]

4.1.2 Aims and objectives

Based on these precedents, we envisioned that a combination of a heterogeneous organic superbase with an appropriate silane reducing agent could represent an enabling methodology towards the development of the *N*-formylation of amines under continuous flow operation. A successful flow process offers a potential fast entry into a wider platform of *N*-formamide structures and, importantly, could reduce the reaction time and increase productivity which have been limiting in most of the previous approaches.[7a]

---

[11] H. Lv, Q. Xing, C. Yue, Z. Lei and F. Li, *Chem. Commun.* **2016**, *52*, 6545-6548.

[12] a) F. D. Bobbink, S. Das and P. Dyson, *Nat. Protoc.* **2017***, 12*, 417-428. b) P. K. Hota, S. C. Sau and S. K. Mandal, *ACS Catal.* **2018**, *8*, 11999–12003; c) O. Jacquet, C. Das Neves Gomes, M. Ephritikhine and T. Cantat, *J. Am. Chem. Soc.* **2012**, *134*, 2934-2937; d) H. Lv , W. Wang and F. Li, *Chem. Eur. J.* **2018**, *24* , 16588-16594; e) S. N. Riduan, J. Y. Ying and Y. Zhang, *J. Catal.* **2016**, *343*, 46-51.

[13] a) C. Das Neves Gomes, O. Jacquet, C. Villiers, P. Thuery, M. Ephritikhine and T. Cantat, *Angew. Chem. Int. Ed.* **2012**, *51*, 187-190; b) G. Li, J. Chen, D.-Y. Zhu, Y. Chen and J.-B. Xia, *Adv. Synth. Catal.* **2018**, *360*, 2364-2369; c) R. Nicholls, S. Kaufhold and B. N. Nguyen, *Catal. Sci. Technol.* **2014**, *4*, 3458-3462; d) R. L. Nicholls, J. A. McManus, C. M. Rayner, J. A. Morales-Serna, A. J. P. White and B. N. Nguyen, *ACS Catal.* **2018**, *8*, 3678-3687.

[14] a) G. Fiorani, W. Guo, A. W. Kleij, *Green Chem.* **2015**, *17*, 1375–1389; b) S. Sopeña, M. Cozzolino, C. Maquilón, E. Escudero-Adán, M. Martínez Belmonte, A. W. Kleij, *Angew. Chem. Int. Ed.* **2018**, *57*, 11203–11207; c) W. Guo, J. González-Fabra, N. A. G. Bandeira, C. Bo and A. W. Kleij, *Angew. Chem. Int. Ed.* **2015**, *54*, 11686-11690.

[15] N. Zanda, A. Sobolewska, E. Alza, A. W. Kleij and M. A. Pericàs, *ACS Sustainable Chem. Eng.* **2021**, *9*, 12, 4391–4397.

[16] See Chapter 3 of this thesis.

4.2 Results and discussion

4.2.1 Optimization studies in batch mode

First, we decided to screen common silanes for the reductive functionalization of CO_2 in the presence of *N*-methyl aniline (Table 1). Considering that the reaction will likely not strongly depend on the concentration of carbon dioxide in solution, we ran initial experiments in a reactor under 1 atm of CO_2 pressure (balloon) sealed by a septum. Mixing of the reactants was done by magnetic stirring at 150 rpm to avoid mechanical damage to the heterogeneous catalyst structure (*i.e.*, DBU@PS, Table 1 and Scheme 1, **C1**).

Table 1. Screening of silane reagents in the conversion of *N*-methyl aniline **1a** giving products **2a** and **2a´**.[a]

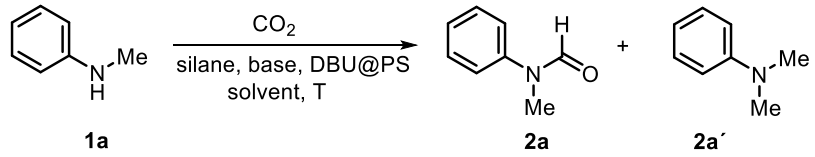

1a **2a** **2a´**

Entry	[SiH] [b]	Conversion (%)	**2a** (%)	**2a´** (%)
1[c]	PHMS	< 45	44	< 1
2	PHMS	0	0	0
3	TMDS	0	0	0
4	Et_3SiH	0	0	0
5	Ph_3SiH	0	0	0
6	$(Me_3Si)_3SiH$	0	0	0
7	$Ph(CH_3)_2SiH$	0	0	0
8	$PhSiH_3$	86	66	20
9	EtO_3SiH	< 98	97	< 1
10	MeO_3SiH	>99	>99	< 1
11[d]	Cl_3SiH	0	0	0

[a] Conditions: 1 atm CO_2 (CO_2 balloon), 0.1 mmol *N*-methyl aniline **1a**, 0.125 mL of dry ACN, 50 ºC, 18 h; DBU@PS **C1** as catalyst (10 mol%). Conversion was determined by ^1H NMR ($CDCl_3$) by relative area integration. [b] Using 6 equiv of silane reagent. [c] Catalyst was DBU as a homogeneous system. [d] Reaction was performed at r.t. since, the b.p. of Cl_3SiH is 32 ºC. TMDS = tetramethyldisilane, ACN = acetonitrile.

PHMS (polymethylhydrosiloxane) was recently reported to be active as reductant when used in combination with DBU for the formylation of *N*-methyl aniline.[17] When we applied our setup to the previously reported reaction conditions (50 ºC, 6 equiv PHMS, 18 h) we achieved

[17] G. Li, J. Chen, D. Zhu, Y. Chen and J. Xia, *Adv. Synth. Catal.* **2018**, *360*, 2364–2369.

comparable results (entry 1). However, when this polysiloxane derivative (with a molecular weight between 1700 and 3200 g/mol) was used in combination with a supported DBU catalyst (DBU@PS, entry 2), no conversion was observed probably due to the lack of efficient contact between both polymeric components. Thus, we then focused further on silane reagents with a lower molecular weight that would remain in solution during the reaction.

Various mono/disilanes failed to deliver the desired product **2a** (entries 3-7), while phenyl silane showed high reactivity but lacked selectivity affording 66% of **2a** but also 20% of over-reduced *N*,*N*-dimethyl aniline **2a´** (entry 8). Fortunately, triethoxysilane and trimethoxysilane proved to be highly reactive (entries 9 and 10) providing **2a** with high selectivity. The use of trichlorosilane was not productive, which we ascribe to the low boiling point of the reagent (31.8 ºC, 1 atm) precluding higher reaction temperature.

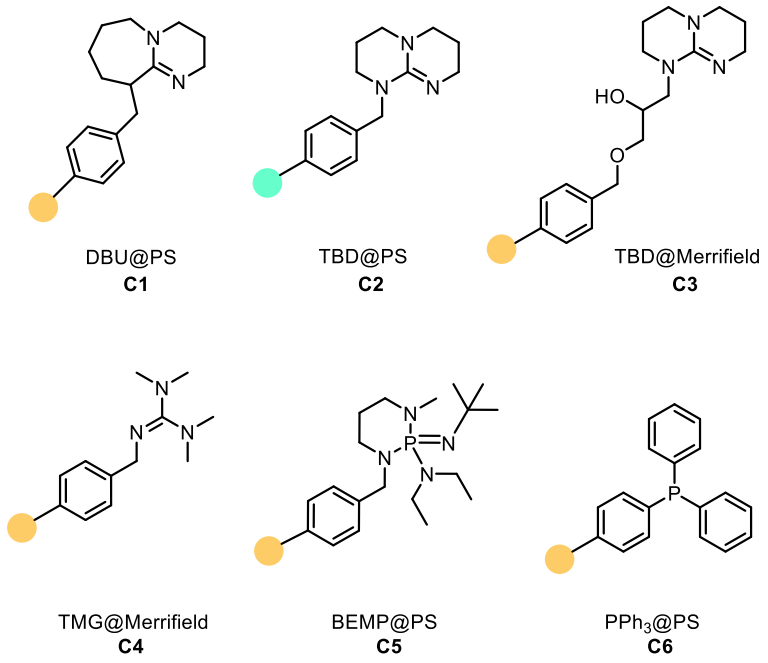

Scheme 1. Catalyst structures **C1**-**C6** used in this chapter.

With the productive siloxanes Me_3OSiH and Et_3OSiH identified, we then screened other potential catalysts (Scheme 1, **C1**-**C6**). We chose catalysts that have either the ability to stabilize a zwitterionic adduct between CO_2 and the amine or directly activate the CO_2 molecule.[18] The supported catalysts TBD@PS, PPh_3@PS, DBU@PS and BEMP@PS were purchased from Sigma Aldrich, whereas TBD@Merrifield[16] and TMG@Merrifield[19] were prepared according to the previously reported procedures.

Catalysts **C1**, **C3**, **C4** and **C5** showed good activity and selectivity for **2a** in the presence of MeO_3SiH (entries 1, 3, 4 and 5 in Table 2), whereas **C2** (entry 2) and **C6** (entry 6) showed poor performance under the reaction conditions applied, and in the absence of catalyst (entry 7) very low conversion of **1a** and yield of **2a** was noted. The result for **C6** was anticipated, but the

[18] For some systems with this potential, see: a) L. F. B. Wilm, T. Eder, C. Mück-Lichtenfeld, P. Mehlmann, M. Wünsche, F. Buß and F. Dielmann, *Green Chem*. **2019**, *21*, 640-648; b) C. Villiers, J.-P. Dognon, R. Pollet, P. Thuéry and M. Ephritikhine, *Angew. Chem. Int. Ed.* **2010**, *49*, 3465–3468.

[19] Z. Wang, R. Gérardy, G. Gauron, C. Damblon and J-C. M. Monbaliu, *React. Chem. Eng.* **2019**, *4*, 17-26.

observed low activity of **C2** seems to suggest that for good activity a delicate balance of *N*-heterocyclic basicity and the presence of additional H-bond donors in the catalyst structure is required. The catalysts **C3** and **C4** appeared to be the most active ones since they could also activate triethoxysilane towards virtually complete substrate conversion at 30 ºC (entries 8-12, with entry 13 as reference). However, further use of catalyst **C4** was discarded because it appeared to suffer some decomposition during operation resulting in leaching of TMG into the eluting stream when used under continuous flow, as we were able to detect free TMG by HPLC analysis of the eluting stream.

Table 2. Screening of catalysts **C1-C6** in the benchmark conversion reported in Table 1.[a]

Entry	catalyst	[SiH] [b]	Conv.[c] (%)	**2a** (%)	**2a´** (%)
1	**C1**	MeO_3SiH	>99	>99	<1
2	**C2**	MeO_3SiH	2	2	0
3	**C3**	MeO_3SiH	>99	>99	< 1
4	**C4**	MeO_3SiH	>99	99	< 1
5	**C5**	MeO_3SiH	>99	>99	<1
6	**C6**	MeO_3SiH	<10	<9	< 1
7	none	MeO_3SiH	6	6	0
8	**C1**	EtO_3SiH	0	0	0
9	**C2**	EtO_3SiH	0	0	0
10	**C3**	EtO_3SiH	< 98	97	< 1
11	**C4**	EtO_3SiH	>99	>99	< 1
12	**C6**	EtO_3SiH	0	0	0
13	none	EtO_3SiH	0	0	0
14	**C2**	TMDS	0	0	0
15	**C3**	TMDS	< 1	< 1	0
16	**C4**	TMDS	0	0	0
17	**C6**	TMDS	0	0	0
18	none	TMDS	0	0	0

[a] Conditions: 1 atm CO_2 (CO_2 balloon), 0.1 mmol *N*-methyl aniline **1a**, 0.125 mL of dry ACN, 30 ºC, 18 h; in each case, 10 mol% of catalyst was used. [b] 5 equiv of siloxane used. [c] Conversion was determined by ^1H NMR ($CDCl_3$).

Table 3. Optimization of the equivalents of the reducing agent MeO_3SiH in the preparation of target **2a**.[a]

Entry	[SiH] (equiv)	Conversion (%)	**2a** (%)	**2a´** (%)
1	5	>99	>99	<1
2	3	<99	98	<1
3	2	<75	74	<1
4	1	<42	41	<1
5	0	0	0	0
6[b]	3	0	0	0

[a] Conditions: 1 atm CO_2 (CO_2 balloon), 0.1 mmol *N*-methyl aniline **1a**, trimethoxysilane (amount indicated), 0.125 mL of dry ACN, 30 ºC, 18 h. Conversion was determined by ^1H NMR ($CDCl_3$). [b] No CO_2 was present.

For the sake of catalyst simplicity, price and availability, we chose to continue our studies with **C1** as catalyst combined with MeO_3SiH as reducing agent. The active site (DBU) in this catalyst is connected to the support via a stable C–C bond, which should enable long-term stability and application. We decided to screen the number of equivalents of the siloxane necessary for the reaction to achieve high conversion after 18 h with the idea of using the outcome in these batch-operated experiments for designing an effective flow process (see below). The use of 3 equiv of siloxane was enough to achieve 99% conversion of the starting material **1a**, as shown by a comparison of the different trials carried out with DBU@PS **C1** as catalyst (Table 3).

4.2.2 *N*-Formamide product scope

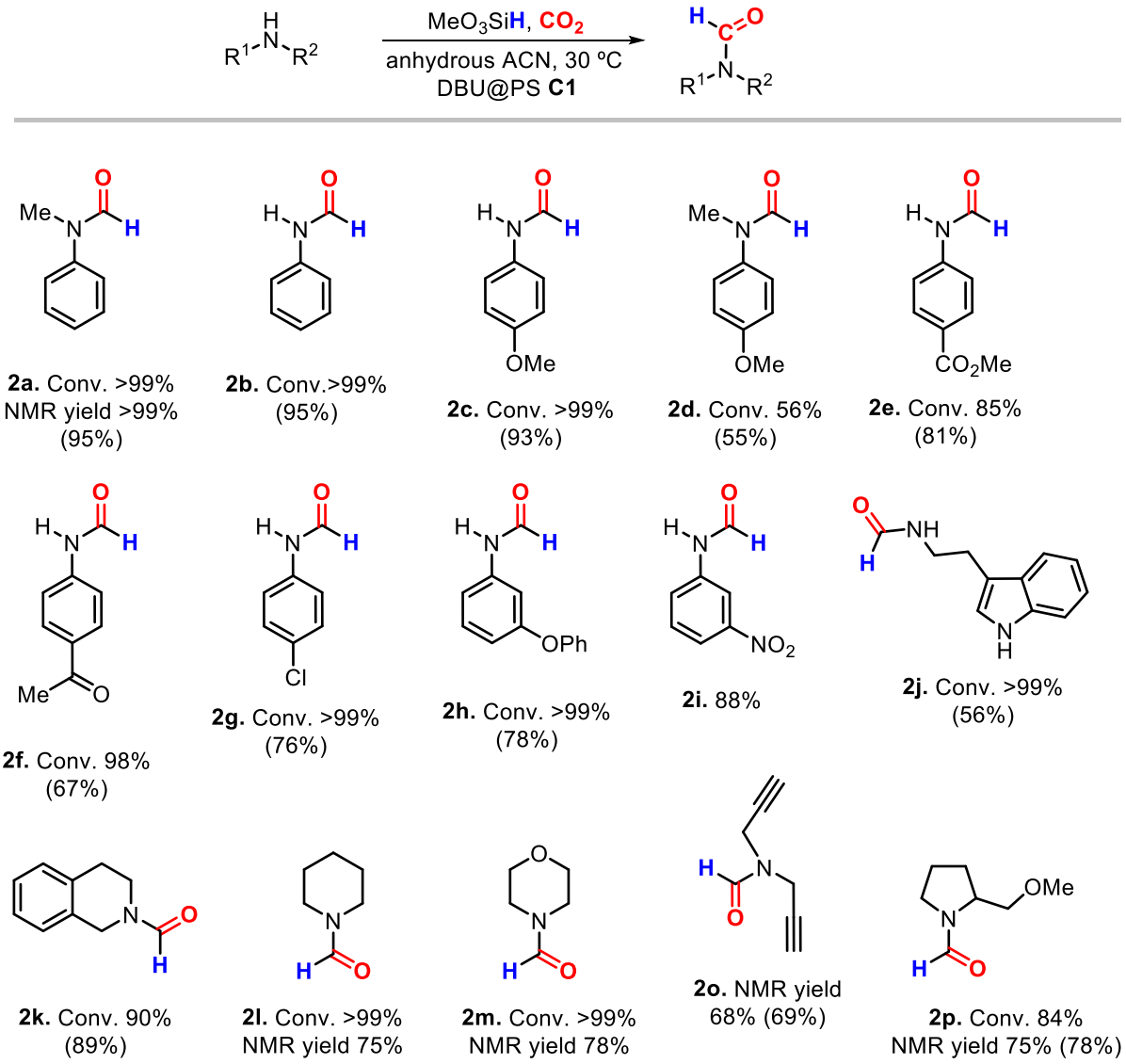

Figure 1. Scope of *N*-formylated products (**2a-2p**) using various amines and promoted by catalyst **C1**. Reaction conditions: CO_2 (balloon), 0.3 mmol **1a-1p**, 3 equiv of Me_3OSiH, 0.45 mL of dry ACN, 18 h, 30 ºC, 150 rpm. Note that for the synthesis of **2a**, **2f**, **2h** and **2i** 5 equiv of siloxane were used, and for **2c**, **2g**, **2k** and **2j** 4 equiv.

However, when we screened other amines to expand the scope of *N*-formylated compounds (Figure 1, synthesis of **2b-2p**; note the higher scale), we noticed that in certain cases a larger excess of the siloxane was required. In the case of the preparation of **2a**, **2c**, **2f-h** and **2i-k**, 4-5 equiv of siloxane were used. In general, different types of (functional) amines can be easily converted by this methodology with different degrees of conversion and product formation depending on the nucleophilic character of the *N*-centers. In all the studied cases, the selectivity for the *N*-formyl compound was >99% as only the desired formamide compounds were detectable. Notably, these transformations are rather practical as no special equipment is required and ambient pressure and low temperature (30 ºC) are sufficient (in most cases) to achieve good to excellent yield of the *N*-formamide.

4.2.3 Continuous flow process optimization

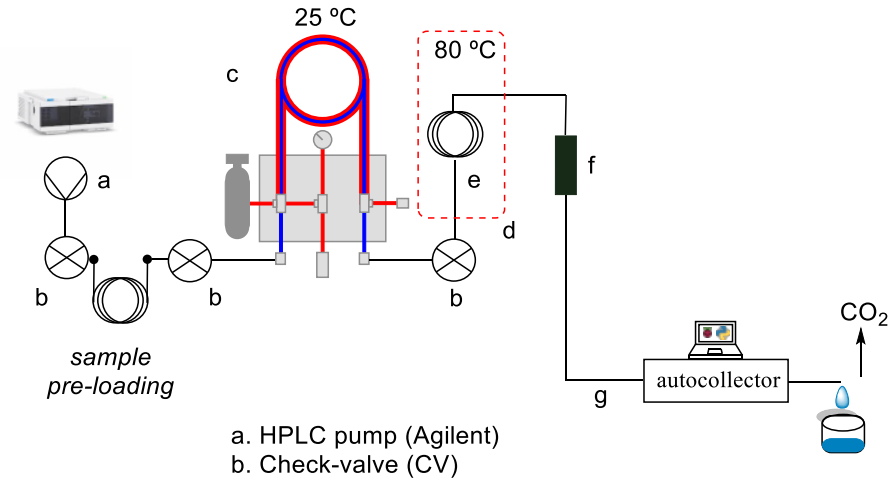

Scheme 2. Schematic diagram of the applied flow setup in the synthesis of *N*-formamide **2a** from *N*-methyl aniline **1a** using DBU@PS **C1**.

We next turned our attention to the design of a flow setup (Scheme 2 and Table 4) that could achieve the synthesis of *N*-formamide **2a** in a continuous way. An HPLC pump provides both the solvent and substrate feed (charged in a loop) into the reactor system. The stream was then passed through a tube-in-tube (T-i-T) reactor operated at 25 ºC and in this traditional configuration charged with CO_2. Subsequently, the CO_2-saturated stream was passed through a coil (¼ inch PTFE tubing containing 6.76 total mmol **C1** loosely packed) heated at the desired temperature (80 ºC). This part of the system was closed by three BPRs (operated at 75 psi, 75 psi and 40 psi, respectively), and the product was then automatically collected.

Table 4. Optimization of the continuous flow conditions.[a]

Entry	Q (mL/min)	τ (min)	T (ºC)	Conversion/ (sel. **2a**) (%)[b]	Productivity in **2a**[c]
1	0.357	30	60	8 (>99)	0.38
2	0.179	60	60	82 (>99)	1.94
3	0.537	20	85	90 (97)	6.17
4	0.357	30	85	96 (96)	4.33
5	0.179	60	80	>99 (98)	2.32
6[d]	0.179	60	80	>99 (98)	2.32

[a] Conditions: 6.76 mmol **C1**, 0.22 M of **1a** in dry ACN, tube-in-tube pressure (at 1 bar), MeO_3SiH (3 equiv), BPR (75 psi/75 psi/40 psi). [b] Selectivity refers to the *N*-formyl-*N*-methyl aniline product **2a**. [c] Productivity of the catalyst system expressed in mmol·h^{-1} of product **2a**. [d] Total reaction time was 480 min. Note that Q stands for the flow (substrate) feed, where τ is the applied residence time.

The stability of the catalyst system was first examined as previously reported.[15] We then tested whether we could perform the reaction at 60 ºC with residence times (τ) inferior to 60 min (Table 4, entry 1). When the flow rate (Q) was decreased to 0.179 mL/min (entry 2), we could achieve 82% conversion of **1a** at the steady state. To increase the rate of this transformation, we then increased the temperature of the reaction mixture to 85 ºC (Scheme 2, zone *e*; entry 3) and this gave 96% conversion of **1a** with 96% selectivity for *N*-formamide **2a**. Finally we found that by performing the reaction at 80 ºC, 1 bar pressure in the T-i-T reactor and with a 60 min residence time optimized results towards the formation of **2a** could be realized. Under these conditions, reproducible full substrate conversion and virtual full selectivity for **2a** is noted (entries 5 and 6).

Lastly, we designed a longer-run experiment (entry 6, 300 min at the steady state) to show that the catalyst was stable enough to be used to produce gram quantities of *N*-formamide **2a** (productivity 2.32 mmol·h^{-1}, 11.6 mmol, 1.57 g). The heterogeneous organocatalyst was exposed to the reagents for a total time of 480 min excluding the washing phase. During this prolonged run, the pressure measured by the HPLC pump varied from 27 bar initially (when the PBR was filled only by the solvent) to 33 bar during the steady state (with the PBR filled by the feed solution). The catalyst did not show any sign of deactivation during this extended run. To gather more evidence for its apparent stability, we removed the catalyst from the PBR and washed it with MeOH and DCM. After carefully drying under vacuum, we performed a batch reaction under the reaction conditions reported in entry 2 of Table 3. The catalyst showed still high activity with the conversion of **1a** >99%.

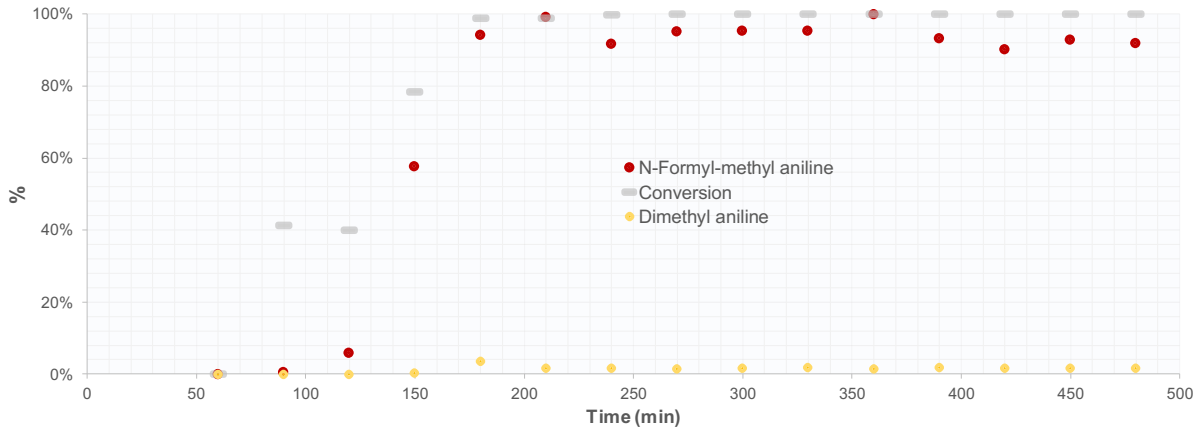

Figure 2. Longer-run continuous flow synthesis of *N*-formamide **2a** monitoring simultaneously the substrate (**1a**) conversion and the formation of by-product **2a´**.

4.3 Conclusion

In this chapter, we have successfully demonstrated the reductive batch formylation of amines by CO_2 using a simple though very effective heterogeneous organocatalyst (DBU@PS, **C1**). Trimethoxysilane, a cheap and commercially available silane was used in combination with **C1** to achieve both high substrate conversion and product yield in the *N*-formylation of a variety of primary and secondary amines Furthermore, we successfully used this heterogeneous organocatalyst for the continuous flow preparation of of *N*-formyl-*N*-methylaniline **2a** with full substrate conversion and excellent selectivity for the target N-arylformamide, and good productivity. Prospectively, this flow approach could be useful for the development of sequential synthesis of a wider variety of *N*-substituted formamide building blocks with a single catalyst batch, thereby expanding the synthetic opportunities for these compounds in multi-step organic transformations.

4.4 Experimental section

4.4.1 Experimental flow protocol

- The catalyst is charged in the tube and connected to the system
- The system is primed with dry solvent and the catalyst is swollen
- The auto-collector is calibrated
- Feed is charged in the loop through a syringe (by hand)
- The flow from the HPLC pump is turned on
- When the feed arrives to the Tube-in-Tube reactor (T-i-T) the CO_2 manometer is opened at the desired pressure. The T-i-T is then primed three times with cycles of opening and closing the gas exit. At the end the exit key is closed
- The heat exchanger is then turned on at the desired temperature
- Changing of the vials of the auto-collector is carried when needed

Note: For additional details about the flow setup please check chapters 2 for an overall view and chapter 3 for the auto-collector.

4.4.2 Reaction optimization under flow using an Omnifit column as PBR

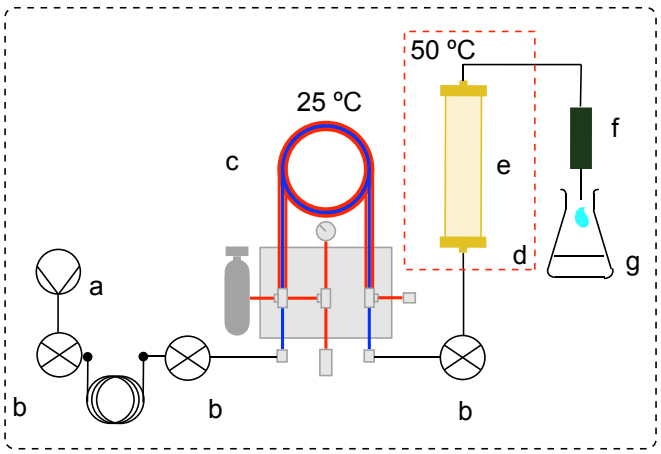

a. HPLC pump
b. Check-valve (CV)
c. Tube-in-Tube Reactor
d. Heat exchanger
e. Packed-bed reactor (PBR)
f. Back pressure regulator (BPR)
g. Collection

Scheme 3: Setup used in the first experiments with an Omnifit column.

In our design, the feed of starting materials *N*-methyl aniline and trimethoxysilane dissolved in acetonitrile (ACN) was first charged into a preloading loop and pushed into the system by an Agilent HPLC pump with integrated pressure sensor controlled by a computer. (**a**) The feed was flowed through a check-valve (CV, **b**) into the tube-in-tube reactor (**c**, T-i-T, 0.6 mL inner tube volume), employed in the traditional configuration. There it was saturated with CO_2 and passed through a second CV directly into the packed bed reactor (PBR, **e**), which was used in the up-flow configuration and heated by a heat exchanger (**d**). The PBR was assembled using a Diba Omnifit® SolventPlus™ volume-adjustable column, equipped with Chemraz O-rings resistant to the reaction media. The column was kept at the desired temperature by a hermetically adapted glass external jacket heated by circulation of an oil stream provided by a Julabo oil heater. The jacketed glass reactor and all the tubing subject to heating were additionally insulated by external coating with glass wool, epoxy resin and aluminum tape. Finally, two back-pressure regulator (BPR, **f**) from IDEX were used to pressurize the system.

The liquid stream was finally collected (**g**) in an Erlenmeyer, from which the samples were taken and analyzed by ^{1}H NMR spectroscopy in $CDCl_3$.

4.4.2.1 Continuous flow process optimization

Table 5. Optimization of the reaction conditions under continuous flow.[a]

Entry	pCO_2 (bar)	BPR (psi)	Flow rate (mL/min)	PBR (mL)	τ (min)	[Feed][b]	[SiH][c]	T (ºC)	Conv. (%)[d]
1	1	150	0.069	4.14	60	0.20	3	70	91
2	1	150	0.139	4.14	30	0.20	3	70	90
3	1	150	0.139	4.14	30	0.20	3	70	90
4	1	150	0.208	4.14	20	0.20	3	70	75
5	1	150	0.208	4.14	20	0.20	3	80	>99
6	1	150	0.208	4.14	20	0.20	3	80	>99[e]
7	2	150	0.277	4.14	15	0.20	2	80	51
8	1	150	0.277	4.14	15	0.20	2	90	66
9	1	150	0.208	4.14	20	0.20	2	90	91[e]

[a] Typical conditions unless stated otherwise: pCO_2 (isobaric) in the outer-region of the tube-in-tube reactor, acetonitrile, DBU@polystyrene (**C1**, 2g, 2.37 mmol), 75 psi = 5.17 bar, BPR = back pressure regulator, PBR = packed back reactor, τ = residence time. [b] The [feed] refers to the concentration of *N*-methyl aniline (in mol/L). [c] [SiH] = MeO_3SiH. [d] The conversion is at steady state conditions, and it was calculated by ^{1}H NMR using relative integration of signals belonging to starting material and the products of the reaction. [e] Selectivity towards the formation of desired product versus *N*,*N*-di-methylaniline for entry 6 is 97%, and for entry 9 it is 74%.

The pressure read on the pump was 33 bar, thus, considering the maximum pressure of 41 bar of an Omnifit column, we decided to use a PFA tubing as a Packed Bed Reactor (PBR).

4.4.3 Synthesis of the heterogeneous catalysts

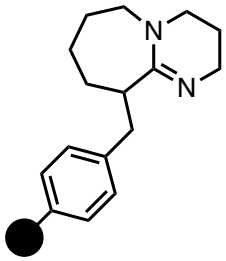

Polystyrene-supported DBU (DBU@polystyrene) C1: was purchased from Sigma Aldrich, CAS: 595128-5g, 1,8-diazabicyclo[5.4.0]undec-7-ene, polymer-bound (1%DVB, 100-200 Mesh). Note that the loading may vary between 1.5-2.5 mmol/g. The catalyst was analyzed by elemental analysis prior to its use in the catalytic studies.

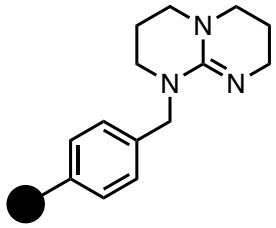

Polystyrene supported TBD (TBD@PS) C2: was purchased from Sigma Aldrich. CAS: 01961-5G-F, 1,5,7-triazabicyclo[4.4.0]dec-5-ene bound, (2% DVB, 100-200 Mesh) loading: 2.4 mmol/g.

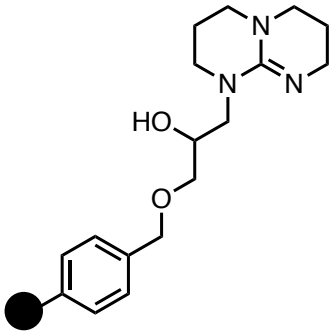

Merrifield supported catalyst TBD@Merrifield C3: Prepared according the reported procedure in chapter 2, f_{exp} = 0.740 mmol/g.

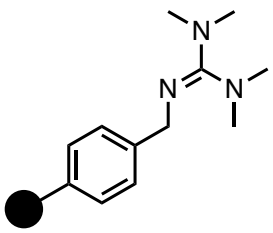

Polystyrene-supported 1,1,3,3-tetramethylguanidine (PS-TMG) C4: prepared according a reported procedure.[19] A mixture of Merrifield resin (6.5 g, 1.3 mmol g^{-1} loading, 100-200 mesh, cross-linked with 1% DVB) and dry 1,4-dioxane (50 mL) was stirred under nitrogen for 30 min at rt to swell the polymeric material. Then 1,1,3,3-tetramethylguanidine (4.28 g, 37.2 mmol) was added and the reaction was shaken for 16 h at 70 °C under nitrogen. The heterogeneous mixture was then diluted with H_2O (10 mL), filtered, and the catalyst successively washed with MeOH (3 × 20 mL), CH_2Cl_2 (3 × 20 mL) and *n*-pentane (3 ×20 mL). Finally, the beads (white color) were dried overnight under vacuum at 50 ºC. f_{exp} = 1.011 mmol/g.

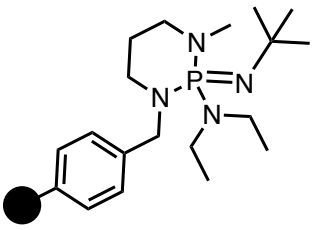

Polystyrene-supported 2-*tert*-butylimino-2-diethylamino-1,3-di-1,3-dimethylperhydro-1,3,2-diazaphosphorine, BEMP@PS, C5: was purchased from Sigma Aldrich. CAS: 536490-1G (1% DVB, 100-200 Mesh), loading 2.5 mmol/g.

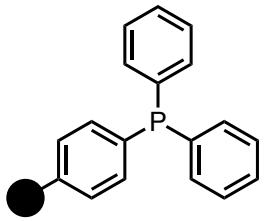

Polystyrene-bound triphenylphosphine, PPh_3@PS, C6: was purchased from Sigma Aldrich. CAS: 39319-11-4, 93094-25G, (1% DVB, 100-200 Mesh) loading 1.6 mmol/g.

4.4.4 Synthesis of formylated products

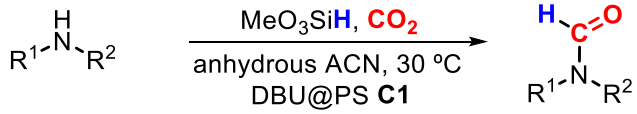

General procedure for the synthesis of compounds 2a-2p in batch mode: Catalyst **C1** (*f* = 1.91 mmol/g, 15.7 mg, 10% mol% loading) was added to a 20 mL glass vial at room temperature, then a solution of **1a** (0.3 mmol, 32.5 uL, 1 equiv) in dry acetonitrile (0.45 mL) was added. The vial was left under a CO_2 atmosphere for 10 minutes and then trimethoxysilane (1.5 mmol, 0.191 mL, 5 equiv) was added. Finally, a CO_2 balloon was connected to the reaction vessel and the reaction mixture stirred at 150 rpm for 18 h. Then, the crude product was filtered and the resin beads were extracted by EtOAc (3 × 8 mL). The organic fractions were then washed with water and the organic phase dried over $MgSO_4$. The solvent was concentrated in vacuo and the product was isolated after purification by flash column chromatography using 3:7 (v/v) cyclohexane/ethyl acetate as eluent.

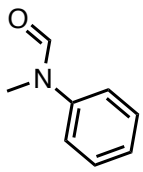

***N*-methyl-N-phenylformamide (2a)** 0.35 mmol, 0.045 g, 95 % yield transparent oil, mixture of rotamers 95:5. **^{1}H NMR** (400 MHz, $CDCl_3$) δ 8.45 (s, 1H), 8.33 (s, 1H, minor rotamer), 7.42 – 7.34 (m, 2H), 7.28 – 7.21 (m, 1H), 7.17 – 7.12 (m, 2H), 3.32 (s, 3H, minor rotamer), 3.29 (s, 3H). **^{13}C NMR** (101 MHz, $CDCl_3$) δ 162.3, 162.2, 142.2, 129.6, 129.1, 126.4, 126.3, 123.6, 122.4, 36.9, 32.0.

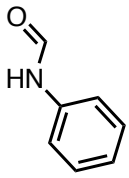

***N*-phenylformamide (2b)** 0.350 mmol, 0.041 g, 95 % yield, transparent oil, mixture of rotamers 53:47. **^{1}H NMR** (400 MHz, $CDCl_3$) δ 8.94 (bs, 1H), 8.74 – 8.67 (m, 1H), 8.37 – 8.32 (m, 1H), 8.07 (bs, 1H), 7.59 – 7.51 (m, 2H), 7.39 – 7.26 (m, 4H), 7.22 – 7.14 (m, 1H), 7.17 – 7.06 (m, 3H). **^{13}C NMR** (101 MHz, $CDCl_3$) δ 163.1, 159.6, 137.1, 136.9, 129.8, 129.1, 125.3, 124.9, 120.2, 118.9.

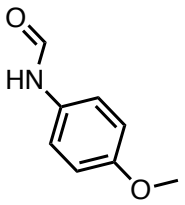

***N*-(4-methoxyphenyl)formamide (2c).**[20] 0.049 g, 93% yield, dark oil, mixture of rotamers 52:48. **^{1}H NMR** (400 MHz, $CDCl_3$) δ 8.56 – 8.45 (m, 2H, N-H and H-CO), 8.33 – 8.23 (m, 1H), 7.77 (bs, 1H), 7.49 – 7.37 (m, 2H), 7.09 – 6.99 (m, 2H), 6.92 – 6.79 (m, 4H), 3.79 (s, 3H), 3.77 (s, 3H). **^{13}C NMR** (101 MHz, $CDCl_3$) δ 163.4, 159.3, 157.7, 156.8, 130.1, 129.8, 122.0, 121.6, 115.0, 114.3, 55.6, 55.6.

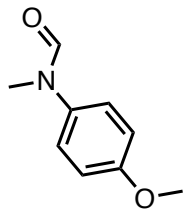

***N*-(4-methoxyphanyl)-*N*-methylformamide (2d).**[21] 0.027 g, 55% yield, transparent oil, mixture of rotamers 92:8. **^{1}H NMR** (400 MHz, $CDCl_3$) δ 8.34 (s, 1H), 8.31 (s, 1H, minor rotamer), 7.33 – 7.28 (m, 2H, minor rotamer), 7.14 – 7.06 (m, 2H), 6.96 – 6.89 (m, 2H), 3.82 (s, 3H), 3.81 (s, 3H, minor rotamer), 3.31 (s, 3H, minor rotamer), 3.27 (s, 3H). **^{13}C NMR** (101 MHz, $CDCl_3$) δ 162.59, 158.45, 135.43, 124.82, 114.92, 55.70, 32.84, 0.13.

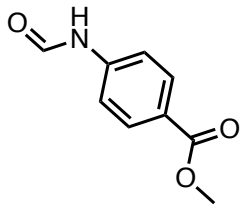

Methyl 4-formamidobenzoate (2e).[22,23] 0.051 g, 81 % yield, white solid, mixture of rotamers 57:43. **^{1}H NMR** (400 MHz, $CDCl_3$) δ 8.88 – 8.81 (m, 1H, minor rotamer), 8.55 – 8.46 (m, 1H, minor rotamer), 8.45 – 8.40 (m, 1H), 8.07 – 7.97 (m, 3H), 7.66 – 7.60 (m, 2H), 7.17 – 7.11 (m, 2H, minor rotamer), 3.91 (s, 3H, minor rotamer), 3.90 (s, 3H). **^{13}C NMR** (101 MHz, $CDCl_3$) δ 166.65, 166.44, 162.06, 159.18, 141.14, 141.06, 131.70, 131.05, 126.79, 126.32, 119.24, 117.33, 52.33, 52.24, 0.11.

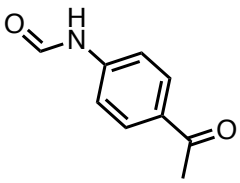

***N*-(4-Acetylphenyl)formamide (2f).**[24] 0.033 g, 67% Yield, white solid, mixture of rotamers 60:40. **^{1}H NMR** (400 MHz, $CDCl_3$) δ 8.95 – 8.82 (m, 2H, N-H and H-CO minor rotamer), 8.47 – 8.37 (m, 1H), 8.26 (bs, 1H), 8.00 – 7.87 (m, 3H), 7.71 – 7.63 (m, 2H), 7.21 – 7.14 (m, 2H, minor rotamer), 2.58 (s, 3H, minor rotamer), 2.57 (s, 3H). **^{13}C NMR** (101 MHz, $CDCl_3$) δ 197.3, 197.0, 162.2, 159.5, 141.5, 141.4, 133.8, 133.3, 130.6, 129.9, 119.4, 117.3, 26.6.

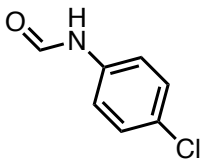

***N*-(4-chlorophenyl)formamide (2g).**[25] 0.035 g, 76% yield, white solid, mixture of rotamers 58:42. **^{1}H NMR** (400 MHz, $CDCl_3$) δ 8.71 – 8.64 (m, 1H), 8.57 (bs, 1H), 8.43 – 8.37 (m, 1H), 7.61 (bs, 1H), 7.55 – 7.49 (m, 2H), 7.38 – 7.27 (m, 4H), 7.10 – 7.03 (m, 1H). **^{13}C NMR** (101 MHz, $CDCl_3$) δ 162.7, 159.2, 135.5, 135.4, 130.9, 130.0, 120.0, 129.3, 121.4, 120.2, 29.8.

[20] B-X. Leong, Y.-C. Teo, C. Condamines, M.-C. Yang, M.-D. Su and C.-W. So, *ACS Catal*. **2020**, *10*, 14824–14833.
[21] X.-F. Liu, X.-Y. Li, C. Qiao, H.-C. Fu and L.-N. He, *Angew. Chem. Int. Ed*. **2017**, *56*, 7425-7429.
[22] M. K. W. Mackwitz, A. Hamacher, J. D. Osko, J. Held, A. Schöler, D. W. Christianson, M. U. Kassack and F. K. Hansen, *Org. Lett.* **2018**, *20*, 3255–3258.
[23] S. Kamijo, T. Jin and Y. Yamamoto, *J. Am. Chem. Soc.* **2001**, *123*, 9453-9454.
[24] M. Hosseini-Sarvari and H. Sharghi, *J. Org. Chem.* **2006**, *71*, 6652–6654.
[25] K. Mishra, H. D. Khanal and Y. R. Lee, *Eur. J. Org. Chem.* **2021**, *2021*, 4477-4484.

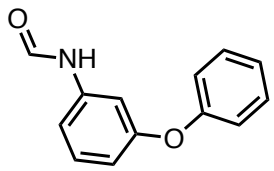

***N*-(3-phenoxyphenyl)formamide (2h).**[26] 0.050 g, 78% yield, transparent oil, mixture of rotamers 53:47. **^{1}H NMR** (400 MHz, $CDCl_3$) δ 8.79 – 8.71 (m, 1H), 8.71 – 8.65 (m, 1H), 8.36 – 8.28 (m, 1H), 7.94 (bs, 1H), 7.44 – 7.28 (m, 9H), 7.21 – 7.16 (m, 1H), 7.16 – 7.10 (m, 1H), 7.10 – 7.01 (m, 4H), 6.91 – 6.72 (m, 4H).**^{13}C NMR** (101 MHz, $CDCl_3$) δ 162.7, 159.4, 158.8, 158.0, 156.8, 156.4, 138.4, 138.4, 130.9, 130.2, 130.0, 129.9, 124.1, 123.7, 119.5, 119.3, 115.0, 114.9, 114.8, 113.1, 110.6, 108.8.

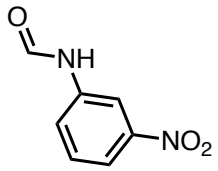

***N*-(3-nitrophenyl)formamide (2i).**[27] 0.044 g, 88% yield, white solid, mixture of rotamers 84:16. **^{1}H NMR** (400 MHz, DMSO-d_6) δ 10.65 (s, 1H), 10.51 – 10.42 (m, 1H, minor rotamer), 8.98 – 8.90 (m, 1H, minor rotamer), 8.59 (t, *J* = 2.2 Hz, 1H), 8.37 (d, *J* = 1.8 Hz, 1H), 8.02 – 7.98 (m, 1H, minor rotamer), 7.95 – 7.82 (m, 2H), 7.70 – 7.64 (m, 1H, minor rotamer), 7.59 (t, *J* = 8.1 Hz, 1H). **^{13}C NMR** (101 MHz, DMSO-d_6) δ 162.7, 160.3, 148.4, 147.9, 139.9, 139.2, 130.7, 130.3, 125.1, 123.1, 118.1, 117.8, 113.3, 111.6.

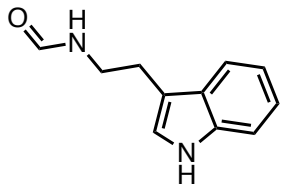

***N*-(2-(1H-indol-3-yl)ethyl)formamide (2j).**[28] 0.032 g, 56% yield, white solid, mixture of rotamers 82:18. **^{1}H NMR** (400 MHz, $CDCl_3$) δ 8.48 (bs, 1H), 8.06 – 8.01 (m, 1H), 7.86 – 7.79 (m, 1H, minor rotamer), 7.62 – 7.56 (m, 1H), 7.57 – 7.53 (m, 1H, minor rotamer), 7.39 – 7.33 (m, 1H), 7.24 – 7.18 (m, 1H), 7.16 – 7.09 (m, 1H), 7.02 – 6.97 (m, 1H), 6.95 – 6.92 (m, 1H, minor rotamer), 5.80 (bs, 1H), 3.65 – 3.57 (m, 2H), 3.49 – 3.42 (m, 2H, minor rotamer), 3.01 – 2.95 (m, 2H), 2.95 – 2.90 (m, 2H, minor rotamer). **^{13}C NMR** (101 MHz, $CDCl_3$) δ 164.8, 161.5, 136.6, 136.5, 127.3, 126.9, 122.9, 122.4, 122.3, 122.2, 119.6, 119.5, 118.7, 118.4, 112.4, 111.6, 111.5, 111.4, 42.1, 38.4, 27.4, 25.2.

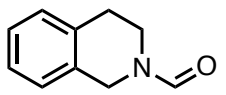

3,4-dihydroisoquinoline-2(*1*H)-carbaldehyde (2k).[29] 0.043g 89% yield, transparent oil, mixture of rotamers 63:37. **^{1}H NMR** (400 MHz, $CDCl_3$) δ 8.23 (s, 1H, minor rotamer), 8.18 (s, 1H), 7.24 – 7.05 (m, 6H), 4.67 (s, 2H), 4.52 (s, 2H, minor rotamer), 3.80 – 3.74 (m, 2H, minor rotamer), 3.67 – 3.59 (m, 2H), 2.91 – 2.87 (m, 2H), 2.87 – 2.83 (m, 2H, minor rotamer). **^{13}C NMR** (101 MHz, $CDCl_3$) δ 161.7, 161.2, 134.5, 133.6, 132.3, 131.8, 129.2, 128.9, 127.1, 126.8, 126.7, 126.5, 125.9, 47.3, 43.2, 42.3, 38.0, 29.8, 28.0.

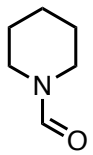

1-Piperidinecarboxaldehyde (2l). 75% ^{1}H NMR yield, transparent oil. **^{1}H NMR** (400 MHz, $CDCl_3$) δ 7.97 (s, 1H), 3.50 – 3.41 (m, 2H), 3.32 – 3.23 (m, 2H), 1.69 – 1.62 (m, 2H), 1.59 – 1.47 (m, 4H). **^{13}C NMR** (101 MHz, $CDCl_3$) δ 160.9, 46.9, 40.7, 26.7, 25.2, 24.8.

[26] E. Surmiak, C. G. Neochoritis, B. Musielak, A. Twarda-Clapa, K. Kurpiewska, G. Dubin, T. A. Holak and A. Dömling, *Eur. J. Med. Chem.* **2017**, *126*, 384-407.
[27] J. Yin, J. Zhang, C. Cai, G. Deng and H. Gong, *Org. Lett.* **2019**, *21*, 2, 387–392.
[28] C Li, M. Wang, X. Lu, L. Zhang, J. Jiang and L. Zhang, *ACS Sustain. Chem. Eng.* **2020**, *8*, 11, 4353–4361.
[29] J. Ma, F. Zhang, J. Zhang and H. Gong, *Eur. J. Org. Chem*. **2018**, 4940-4948.

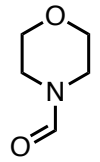

***N*-Formylmorpholine (2m)** 78% ^{1}H NMR yield, transparent oil. **^{1}H NMR** (400 MHz, $CDCl_3$) δ 8.05 (s, 1H), 3.72 – 3.62 (m, 4H), 3.59 – 3.54 (m, 2H), 3.41 – 3.36 (m, 2H). **^{13}C NMR** (101 MHz, $CDCl_3$) δ 161.0, 67.4, 66.6, 45.9, 40.8.

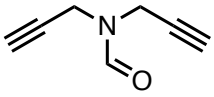

***N*,*N*-di(prop-2-yn-1-yl)formamide (2o).** 0.025 g, white solid, 69% yield, **^{1}H NMR** (400 MHz, $CDCl_3$) δ 8.09 (s, 1H), 4.26 (d, J = 2.5 Hz, 2H), 4.14 (d, J = 2.5 Hz, 2H), 2.35 (t, J = 2.5 Hz, 1H), 2.23 (t, J = 2.5 Hz, 1H). **^{13}C NMR** (101 MHz, $CDCl_3$) δ 161.46, 77.18, 76.97, 74.11, 72.72, 36.23, 30.91, 0.08. FT-IR (neat, ν in cm^{-1}): 3241, 2120, 1659. **ESI-MS** $[C_7H_8NO^+]^+$: calcd, 122.0600; found, 122.0605.

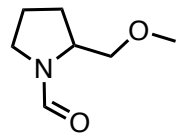

2-(Methoxymethyl)pyrrolidine-1-carbaldehyde (2p).[30] 0.039 g, white solid, 78% yield, mixture of rotamers 72:28. **^{1}H NMR** (400 MHz, $CDCl_3$) δ 8.31 (s, 1H), 8.24 (s, 1H, minor rotamer), 4.19 – 4.10 (m, 1H, minor rotamer), 3.99 – 3.89 (m, 1H), 3.62 – 3.34 (m, 5H), 3.33 (s, 3H), 3.33 (s, 3H, minor rotamer), 3.29 – 3.23 (m, 1H), 2.08 – 1.66 (m, 6H). **^{13}C NMR** (101 MHz, $CDCl_3$) δ 162.0, 161.3, 75.5, 72.5, 59.2, 59.2, 56.9, 54.8, 47.1, 43.7, 28.0, 27.9, 24.0, 22.9.

[30] D. Seebach, H. Kalinowski, B. Bastani, G. Crass, H. Daum, H. Dorr, N. P. DuPreez, V. Ehrig, W. Langer, C. Nussler, H. Oei and M. Schmidt, *Helv. Chim. Acta* **1977**, *60*, 301-325.

Chapter 5: Summary and General Conclusion

CO_2 has become a versatile reagent in synthetic organic chemistry. Its use in the preparation of heterocyclic structures is a clear testament of the successful valorization of this renewable carbon feedstock, and the versatility that it creates by expanding the chemical space in C_1 conversions. Key to these developments is the use of catalysis that enables fast-track access to organic compounds with increased complexity and commercial value.

Since a decade, there is a clear rise of alternative metal-free approaches to transform CO_2 into various organic frameworks as opposed to metal-depending protocols. As such, and particularly in those cases where toxic and/or rare metals are used, organocatalysis offers a tangible sustainable solution for the upgrade of CO_2 into compounds of interest in fine chemical, pharmaceutical and polymer chemistry. Moreover, a combination of organocatalysis and flow chemistry techniques represents a powerful synergy that may additionally contribute to offer more sustainable carbon-fixation processes while enabling their scalability. Organocatalysts can be easily covalently bound to a support and therefore applied under continuous flow operation, provided that they retain activity and stability as the result of a proper design.

At the start of this PhD work, the use of organocatalysis in flow processes in this particular field was severely underdeveloped. Therefore, the **main and most general objective of this thesis** was to advance the use of heterogeneous organocatalysis under continuous flow in the field of CO_2 reutilization. The designed flow set-ups and catalysts are essentially beneficial for a day-to-day operation but have potential for further scale-up and application in commercial laboratories providing several advantages including mild reaction conditions, being halide-free and having a modular character.

Chapter 2 shows how an effective immobilized organocatalyst can be optimized for continuous flow operation in the conversion of glycidol and CO_2 to its corresponding and commercially relevant cyclic carbonate “glycerol carbonate”. In our approach, we focused principally on the development of a stable organocatalyst that retains its activity and does not contaminate the eluting product stream. The use of a swellable polystyrene (PS) support in combination with a superbase as organocatalyst (i.e., TBD) allowed for the first time to avoid halogen contamination of the carbonate product prepared under flow conditions. Furthermore, the novel configuration of a tube-in-tube reactor with a second reactor equipped with a catalyst supported on Merrifield resin disclosed clear potential of these PS supports in reactions involving gaseous reagents. Our method tolerates the handling of rather large quantities of glycidol, and glycerol carbonate was synthesized at de decimolar scale (up to 147 mmol; 17.3 g) in 48 h. Such a quantity of product would most likely otherwise have required an autoclave and more extreme conditions. The eluting stream was essentially pure, and thus no further purification was needed.

In **Chapter 3**, a different flow setup was developed in order to ease up the scalability of the selected CO_2 transformation process. By using a 5.5 % DVB-crosslinked polystyrene we could employ mass flow controllers (MFCs) to provide the gaseous feed, and this modification allowed to achieve a more flexible setup in which pressure, temperature and flow-rates could be adjusted without being dependent of each other. Secondly, every component feed in the system can be controlled by computers facilitating the operating controls. The stability of the system could be easily assessed by checking the CO_2 flow monitored by the computer that panels the MFC, and by checking the volume collected in each fraction by the home-made auto-collector. This setup and the use of an immobilized TBD catalyst were applied to chemo-selectively prepare pharmaceutically relevant 2-substituted oxazolidinones from a range of epoxy amines and CO_2. The manifold that is involved is based on a substrate-triggered CO_2

activation approach, in which the amino group activates the CO_2 molecule forming a hemi-carbamate species that subsequently attacks the oxirane thereby forming the desired compound. A small library of oxazolidinone scaffolds could be prepared with different substitution patterns. Furthermore, these compounds possess potential biological activity (i.e., Toloxatone – an antidepressant) and hold promise as synthons in medicinal chemistry development programs.

In **Chapter 4**, the *N*-formylation of various amines with CO_2 is described, which was performed by reducing the CO_2 with trimethoxysilane in the presence of a heterogenized superbase catalyst. The process variables of the reaction were first optimized in batch mode and the reactivity further studied by preparing various formamides. Based on the collected data, a safer process was developed under continuous flow allowing to scale up the transformation. The use of a continuous flow method permits to avoid thermal/process run-aways caused by hydrogen formation, and hence the optimization of the variables (temperature, silane amount and type, catalyst) allowing to selectively run the transformation while minimizing by-products.

The **General Conclusion** from the thesis work is that the information gathered in the area of catalytic CO_2 valorization will further boost the use of this C_1 reagent under flow conditions empowered by organocatalysis. The potential of heterogeneous catalysis with gaseous reagents is surely underexploited in flow chemistry and the achievements described in this thesis provide a novel reactivity platform that can inspire the community to design and develop new transformations based on CO_2 but also with other gases including O_2, CO and F_2. The 'evolution' from purely batch processes (i.e., autoclaves operated under pressure) to continuous flow reactors of similar CO_2 transformations can create new incentives in multistep procedures to achieve more complex scaffolds with application potential in various fields. Some required developments are an improved reactivity profile of organocatalysts to achieve higher and competitive productivity, and diversification of available catalysts to explore new types of CO_2 transformations. Future efforts could also focus on the development of new methodologies that merge heterogeneous organocatalysis with photochemical and electrochemical approaches leading to amplification of the synthetic toolbox for the efficient recycling of CO_2.

UNIVERSITAT
ROVIRA i VIRGILI